CANADIAN THESES

THÈSES CANADIENNES

NOTICE

The quality of this microfiche is heavily dependent upon the quality of the original thesis submitted for microfilming. Every effort has been made to ensure the highest quality of reproduction possible.

If pages are missing, contact the university which granted the degree.

Some pages may have indistinct print especially if the original pages were typed with a poor typewriter ribbon or if the university sent us an inferior photocopy.

Previously copyrighted materials (journal articles, published tests, etc.) are not filmed.

Reproduction in full or in part of this film is governed by the Canadian Copyright Act, R.S.C. 1970, c. C-30.

AVIS

La qualité de cette microfiche dépend grandement de la qualité de la thèse soumise au microfilmage. Nous avons tout fait pour assurer une qualité supérieure de reproduction.

S'il manque des pages, veuillez communiquer avec l'université qui a conféré le grade.

La qualité d'impression de certaines pages peut laisser à désirer, surtout si les pages originales ont été dactylographiées à l'aide d'un ruban usé ou si l'université nous a fait parvenir une photocopie de qualité inférieure.

Les documents qui font déjà l'objet d'un droit d'auteur (articles de revue, examens publiés, etc.) ne sont pas microfilmés.

La reproduction, même partielle, de ce microfilm est soumise à la Loi canadienne sur le droit d'auteur, SRC 1970, c. C-30.

THIS DISSERTATION
HAS BEEN MICROFILMED
EXACTLY AS RECEIVED

LA THÈSE A ÉTÉ
MICROFILMÉE TELLE QUE
NOUS L'AVONS REÇUE

Canada

NL-339 (r. 86/06)

HYDROTREATMENT OF ATHABASCA BITUMEN DERIVED HEAVY GAS OIL OVER MODIFIED ZEOLITE SUPPORT CATALYST

by

INDERJIT SINGH SAMBI

A thesis
presented to the University of Ottawa
in fulfillment of the
thesis requirement for the degree of
DOCTOR OF PHILOSOPHY
in
Chemical Engineering Department,
University of Ottawa,

Ottawa, Ontario, 1986

ISBN 0-315-33248-4

UNIVERSITÉ D'OTTAWA
UNIVERSITY OF OTTAWA

The University of Ottawa requires the signatures of all persons using or photocopying this thesis. Please sign below, and give address and date.

ABSTRACT

Hydrotreatment of a heavy gas oil derived from the Athabasca tar sands bitumen was carried out in a trickle-bed reactor. The main objective of this study was to develop a high efficiency Ni-Mo catalyst using zeolite material as well as a composite of silica-alumina as support materials. The present information available in the literature was used as a starting point. The available literature on the hydrodynamics of trickle-bed reactors was used for design of the research reactor and statistical experimental designs were used for efficient data collection and analysis.

A catalyst support consisting of 10% by wt. silica, 25% by wt. rare-earth exchanged Y-type zeolite and 65% by wt. alumina gave the best performance for hydrodesulfurization (HDS) and hydrodenitrogenation (HDN). Kinetic study with this catalyst was carried out and the data fitted the 1.5th order model for HDS and 2nd order model for HDN. The corresponding rate constants at four temperatures (i.e., 350° C, 375° C, 400° C, and 425° C) were estimated and the activation energies for HDN and HDS were determined.

ACKNOWLEDGEMENT

The author is indebted to his research supervisor Prof. Dr. R. S. Mann for his help and encouragement at all stages of this work. Nearly all professors of the Department of Chemical Engineering, through their graduate courses, have enhanced understanding in various Chemical Engineering fields and the author expresses his sincere gratitude. The atmosphere in the department was always like that of a family and the author expresses his thanks to all the members.

Prof. Dr. V. Hornoff, the present chairman, and Prof. Dr. F. D. F. Talbot and Prof. Dr. D. D. McLean, the two ex-chairpersons of the department deserve special thanks for departmental financial support and the facilities for this work. Mr. G. Gasperetti, Mr. Daniel Lafebvre and Mr. Adriano Bonaldo, the three friendly technicians of the departmental workshop were very helpful at all times. Mr. Banito Carraro and Mr. Master Mohemed of the Department of Electrical Engineering were a great help to do modifications and repairs of some of the electronic instruments. The author acknowledges their help with gratitude.

The author also wishes to aeknowledge the help and encouragement he received from Mrs. Gurkirat Kaur Sambi (author's wife) and her

sacrifices during the time of this graduate work. Dr. K. C. Khulbe was a great help in the university as well as outside and the author feels indebted to him for his help.

NOMENCLATURE

a_s	Specific surface area of the packing material per unit bed volume $(6(1-\varepsilon)/d_p)$
A_{eff}	Ratio of wetted surface area to total surface area
bbl	Barrel (42 U.S. Gallons)
C_i	Inlet reactant concentration
C_o	Outlet reactant concentration
d_p	Diameter of particle
d_t	Diameter of reactor tube
Eö	Eötovs number = $\rho_L g d_p^2/\sigma_L$
E_z	Axial dispersion coefficient
g	Accealration due to gravity
Ga	Galileo number = $d_p^3 \rho_L (\rho_L g + \delta_{LG})/\mu_L^2$
G_L	Superficial liquid mass velocity
G_G	Superficial gas mass velocity
h_d	Dynamic liquid hold-up
h_s	Static liquid hold-up
HDN	Hydrodenitrogenation (% by wt. nitrogen removed)
HDS	Hydrodesulfurizatiion (% by wt. sulfur removed)
K	Calibration factor for elemental analysis
k_{app}	Apparent kinetic rate constant
k_v	Intrinsic kinetic rate constant
k''_m, k'_m	Intrinsic mth order kinetic rate constants
k_m	Apparent mth order kinetic rate constant

L	Reactor length
LHSV	Liquid-hourly-space-velocity (based on catalyst volume)
m	Order of the reaction
n	Number of data points
p	Number of parameters in a fitted model
Pe	Peclet number = uL_c/E_z
Re	Reynold's number
SSR	Sum of squares of residuals
u	Intersticial fluid velocity
U_o	Superficial fluid velocity based on empty bed
We	Weber number = $U_L^2 d_p \rho_L / \sigma_L$
x_i	Coded i'th variable
Y_i	Coded i'th response criterion
z_i	Coded i'th varable used in canonical form of model

GREEK LETTERS

α	Used for a particular type of Alumina
β_i	i'th Parameter estimate of a given model
γ	A lumped parameter
γ_i	i'th Parameter estimate of canonical form of a model
ε	Bed void fraction
ρ	density
δ_{LG}	Two phase fractional pressure drop
σ	Surface tension
σ_{pe}^2	Pure error variation
μ	Viscosity of fluid
η	Effectiveness factor
ψ	$=(\sigma_{wat}/\sigma_L)((\mu_L/\mu_{wat})(\rho_{wat}/\rho_L)^2)^{0.333}$

λ	$= (\rho_G \sigma_L / \rho_{wat} \sigma_{air})$

SUBSCRIPTS

c	Critical value
C	For carbon
d	Dynamic
G	For gas
H	For hydrogen
L	For liquid
N	For Nitrogen
p	For particle
t	For reactor tube

CONTENTS

Abstract v

Acknowledgement vi

NOMENCLATURE viii

Chapter I: INTRODUCTION 1

Properties of Heavy Gas Oils 3
Sulfur Compounds 4
Nitrogen Compounds 5
Oxygen Compounds 5
Metallic Impurities 6
Chemical Structure of The Heavy Oils 7
Heavy-Gas Oil Used In This Investigation 7
Hydrotreatment 9

Chapter II: LITERATURE REVIEW 12

Previous Study 12
Zeolites 14
Types of Zeolites 14
Types X and Y 16
Thermal and Hydrothermal Stability 17
Sodium Removal 17
Aluminium Removal 18
Acidity 18
Cracking Catalyst 19
Effect of Zeolite Input 20
Hydrocracking Catalyst 21
Hydrotreating Catalyst 22
Zeolite Material Used in This Study 23
Trickle-Bed Reactors 23
Advantages of Trickle-Bed Reactors 24
Disadvantages of Trickle-Bed Reactors 25
Hydrotreatment Applications 26
Dynamics of Trickle-Bed Reactors 27
Prediction of Flow Regime 28
Liquid and Gas Distribution 30
Effective Catalyst Wetting 32
Liquid Holdup 33
Axial Dispersion 35
Mathematical Models for Trickle-Bed Reactors 38

Ideal Plug-Flow Model 39
Holdup Model 40
Effective Catalyst Wetting Model 41
Choice of Reactor 43

Chapter III: OBJECTIVES 45

Chapter IV: EXPERIMENTAL EQUIPMENT 46

Hydrotreatment System 46
Liquid Feed System 48
Gas Manifold 48
The Reactor 49
Sand Bath 49
Oil Separation and Sampling System 52
Wet Test Gas Flow Meter 52
Gas Chromatograph 53
Analytical Equipment 53
Catalyst Testing 53
Chemical composition 54
Pore Volume 54
Surface Area 54
Analysis of Oil Samples 55
Density 55
Viscosity 55
Aniline Point 55
Boiling Point Distribution 55
Elemental Analysis 56

Chapter V: EXPERIMENTAL PROCEDURE (PART - I) 57

CATALYST PREPARATION 57
Gel Preparation 58
Filtration and Washing 58
Extrusion and Drying 59
Calcination 59
Size Reduction 60
Pore Volume Measurement 61
Impregnation 62
Analysis of Chemical Composition 63
BET Surface Area 65
SEM Imaging and Energy-Dispersive X-Ray Analysis 65

Chapter VI: EXPERIMENTAL PROCEDURE (PART - II) 66

CATALYTIC HYDROTREATMENT 66
Reactor Filling With Catalyst 66
Sulfiding and Activation 67
Hydrotreatment 68

Sample Withdrawal 69
Gas Analysis 69
Shut-Down 70
Analysis of Oil Samples 72
Density and Viscosity 72
Aniline Point 72
Boiling Point Distribution 73
Elemental Analysis 77

Chapter VII: RESULTS AND DISCUSSION 79

LOCATION OF OPTIMUM OPERATING POINT 81
Experimental Design 82
Operating Region 83
Randomization of the Experimental Runs 84
Analysis of Results of Experimental Design 85
Model Building 85
Fitted Model 89
Interpretation of The Fitted Models 95
Response Surfaces and their Analysis 95
Optimal Operating Conditions 96
Example Analysis For %HDS 98
Conclusions of Operating Region Study 99
Temperature Effect 101
Pressure Effect 101
Liquid Flow Rate Effect 101
Gas Flow Rate Effect 102
Optimal Operating Point 103
SEARCH FOR BEST CATALYST COMPOSITION 104
Experimental Design 105
Results of Catalyst Physical and Chemical Testing 108
Hydrotreatment Results 111
Study of Catalyst Initial Activity Decay 111
Results 113
Model Fitting 115
Model Interpretation 117
Canonical Transformation 117
Contour-Plots 124
Results of Three Repeat Runs 124
Conclusion 129
KINETIC STUDY 130
Catalyst Used for Kinetic Study 130
SEM Imaging and Energy-Dispersive X-Ray Analysis 131
X-Ray Diffraction Studies 134
Operating Conditions Used 134
Kinetic Study Results 135
Kinetic Models 138
Material Balance 145
Hydrogen Consumption 147
Reactor Performance 149
Axial Dispersion 149
Effective Catalyst Utilization 150

Mass-Transfer Effects and Effectiveness Factor 151
Heat Transfer Effects 154
Hydrotreatment Without Catalyst. 156

Chapter VIII: CONCLUSIONS 160

BIBLIOGRAPHY 163

Appendix A: COMPUTER PROGRAMS 169

Appendix B: Impregnation Solution Calcualtions 185

FIGURES

1. Sodalite Unit Depicted in Three Ways 15
2. Zeolites X and Y (Faujasite) Structure 15
3. Flow-Regime Boundaries for (a) Foaming and (b) Nonfoaming liquids 30
4. Contacting Effectiveness as Function of Liquid Loading 33
5. Correlation of Static Liquid Holdup With Eotovs Number 34
6. Schematic of Hydrotreatment System 47
7. Details of Sand Bath 51
8. Vacuum Impregnation Arrangement 63
9. Exit Gas Analysis - A typical Gas-Chromatogram 70
10. Simulated-Distillation (Standard Sample) 75
11. Boiling Point vs Retention Time 76
12. Simulated Distillation Chromatogram of Oil Sample 76
13. Simulated Distillation - Boiling Point Distribution Curve 77
14. Activity Decay During Operating Region Study 88
15. Observed vs Predicted Values of Response Variables 92

16. Residuals vs The Order of Experimental Runs 93
17. Contour Plot for Response Surface of %HDS 100
18. Pictorial Representation of Centre-Composite Design 107
19. Initial Activity Decay 112
20. Contour Plots for Nitrogen Concentration 119
21. Contour Plots for Sulfur Concentration 120
22. Contour Plots for Density 121
23. Contour Plots for Viscosity 122
24. Contour Plots for Mid-Boiling-Point 123
28. Nitrogen Results of Sixteen Design Catalysts 126
29. Sulfur Results of Sixteen Design Catalysts 127
30. Density Results of Sixteen Design Catalysts 127
31. Viscosity Results of Sixteen Design Catalysts 128
32. Mid-Boiling-Point Results of Sixteen Design Catalysts 128
33. SEM Image for Aluminium 131
34. SEM Image for Silicon 132
35. SEM Image for Nickel 132
36. SEM Image for Molybdenum 133
37. SEM Image for Lanthanum 133

TABLES

1. Sulfur Distribution in Petroleum Fractions 4
2. Properties of Great Canadian Tar Sands Bitumen 8
3. Distillation Analysis of Bitumen 8
4. Properties of Heavy Gas Oil 10
5. Details of Zeolite Material 23

6. Comparison of silica-alumina-zeolite and alumina-zeolite support. 80

7. Coding of The Operating Variables. 83

8. Results of 3-Level Fractional Factorial Design. 87

9. Results of The Full Fitted Model 90

10. Results of The Reduced Models 91

11. Summary of Optimal Operating Conditions and Surface Characteristics 97

12. Central Composite Design 106

13. Physical Properties and Chemical Composition of Catalysts (For 8 Replicate Runs) 109

14. Physical Properties and Chemical Composition of Catalysts (For 8 Design Runs) 110

15. Results Obtained With Sixteen Design Catalysts 114

16. The Estimated Parameters of Fitted Model 116

17. Canonical Transformation Parameters 118

18. Results of Three Repeat Catalysts 125

19. Results Obtained With Catalyst No.20 129

20. Physical Properties and Chemical Composition of Catalyst Used for Kinetic Study 131

21. Results of Kinetic Runs (I) 136

22. Results of Kinetic Runs (II) 137

23. Rate constants, COD and Prob>F for Sulfur Data (Order 1 to 1.4) 140

24. Rate Constants, COD and Prob>F for Sulfur Data (Order 1.5 to 2) 141

25. Rate Constants, COD and Prob>F for Nitrogen Data (Order 1 to 1.4) 142

26. Rate Constants, COD and Prob>F for Nitrogen Data (Order 1.5 to 2) 143

27. Final Rate Constants for HDS and HDN 143

28. Activation Energies for HDN and HDS 144

29. Material Balance 146
30. Hydrogen Consumption 148
31. Effectiveness Factors 152
32. Results Obtained With Catalyst Number 31 154
33. Results of Hydrotreatment Without Catalyst (I) 157
34. Results of Hydrotreatment Without Catalyst (II) 158

Chapter I

INTRODUCTION

Petroleum plays an important role in the energy scene of Canada and most other countries. Self sufficiency in this major source of energy has always been envisaged as the necessary ingredient of the formula to get a stable and steady economic growth. The development of Canadian tar sands is a step in the right direction, to achieve such objectives.

Canada has an estimated 250 billion bbl of heavy crude oil reserves as tar sands [72]. In fact the estimated recoverable reserves of 550 billion bbl in Canada and Venezuela are comparable in size to the world's total recoverable reserves of conventional crudes which have been estimated at 670 billion bbl. It is because of this reason that Canada, more than any other country, needs to give more emphasis on the development of technology to tap this vast source of energy.

The operation of a modern oil refinery is very complex. With the present day demands on the product streams and always changing quality of the feed-stocks, a modern refinery has to be quite flexible in its operations. Given an economic environment, oil companies have to meet market demands as well as product standards. Several process steps are involved for each of the products and the whole operation is carried out within the frame work of maximization of profits.

Therefore, processes with better efficiencies are continuously sought and the research work in the field of catalysis used in oil the industry is an important part of this evolution.

The world market of crude oil supply has been slowly shifting towards heavier crudes. Quality of crude is expected to decline further as the high API gravity, low sulfur crudes are depleted. Also more and more heavy crude is becoming available from the tar sands of Canada, Mexico and Venezuela. These heavy crudes give rise to increased amounts of heavy oils and residuals. Inherently, the heavy crudes contain higher levels of sulfur, nitrogen and metallic impurities (especially V and Ni). During the processing these impurities concentrate in the heavier fractions. This makes further processing of the heavy oils and the residuals even more difficult.

The processing of petroleum crudes and/or the tar sands bitumen always leads to substantial fractions of heavy oils and residual oils for which there is very little market. This makes it necessary that such heavy oils be further processed to more salable lighter fractions. Further processing of these heavier fractions involve a series of process steps. Choice of a particular processing scheme for any of the heavy fractions, would obviously depend upon the quality of the fraction. Generally the vacuum residues are processed in delayed cokers or visbreakers (depending on the severity of cracking required). The coker oils as well as the virgin vacuum gas oils may be processed using catalytic cracking or hydrocracking.

The heteroatoms and the metallic impurities present in the heavy fractions are very harmful for the catalyst used in cracking, hydrocracking or the reforming processes. Also the environmental standards make removal of such objectionable elements from the finished products an absolute essential. This removal of harmful impurities from the heavier fractions as well as some of the finished low boiling products is carried out using a hydrotreating process.

Hydrotreating plays a very important role in the further processing of heavy oils. Various aspects of hydrotreatment and properties of heavy oils that affect the hydrotreatment process were discussed in my M.A.Sc. thesis [57]. However, a short review is presented here.

1.1 Properties of Heavy Gas Oils

The term 'heavy gas oil' is quite arbitrary. It is generally applied to petroleum fractions boiling between 320°C (610°F) and about 427°C (800°F). These are viscous liquids with API gravity values generally less than 20. They contain the objectionable heteroatoms such as sulfur (up to 10%) and nitrogen (up to 2%) which pose the difficulties in further processing. In addition, these heavy gas oils generally have metallic impurities in the form of metallic complexes. These are mainly vanadium (V), nickel (Ni) and iron (Fe), and the total amount of these may be as high as 3000 ppm.

The presence of heteroatoms (particularly N) and metallic impurities in feed-stocks is harmful for the processing catalysts. The heteroatoms like S and N in the final products, not only pose problems of environmental pollution and corrosion of user machinery but are very detrimental to product stability. The metallic impurities (particularly V) in the final products, lead to ash formation which can be dangerously harmful to the user machinery like generators, oil-fired gas turbines and furnace refractory linings.

1.1.1 Sulfur Compounds

Sulfur is present in the heavy oils mostly in the forms of thiophenes and their derivatives. Other forms like sulfides, sulfates, mercaptans, thiols and their derivatives are also present. The degree of difficulty in the sulfur removal in the hydrotreatment process is generally proportional to the complexity of sulfur containing molecules which increases in the order paraffins, naphthenes, aromatics. A typical distribution of sulfur originally present in crude and in its fractions in a typical distillation process is shown in Table 1.

Table 1: Sulfur Distribution in Petroleum Fractions

Sulfur content of crude oil(wt%)	Sulfur in product (% of original sulfur in oil)			
	Naphtha (Gasoline)	Kerosene	Gas oil	Residuum
0.15 to 2.45	0.05 to 1.8	0.55 to 4.2	6.60 to 38.6	57.50 to 92.8

Generally it can be seen that the portion of sulfur will increase with the boiling point of the fraction as in the above table, but if distillation is allowed to proceed at too high a temperature, thermal decomposition of the high molecular weight sulfur compounds will ensue and, hence, the middle fractions will contain more sulfur than the higher boiling fractions.

1.1.2 Nitrogen Compounds

Nitrogen in petroleum is classified in to two arbitrary classes; 'basic' and 'nonbasic' depending upon whether they can be titrated with perchloric acid in a 50/50 solution of glacial acetic acid and benzene. The basic nitrogen compounds are composed of mainly pyridine homologs and occur throughout the boiling ranges and have a tendency to exist in the higher boiling fractions and residua. The nonbasic compounds are of pyrrole, indole and carbazole type also occur mainly in higher boiling fractions. The amounts of nitrogen in a crude is generally found to be related to its carbon residue. The higher the carbon residue (or the asphaltenes) the higher would be the nitrogen amount in a crude.

1.1.3 Oxygen Compounds

Oxygen in petroleum is mainly due to exposure of the oil to atmosphere. A wide variety of oxygen compounds are generally found in petroleum. Alcohols, ethers acids, anhydrides, acetates, ketones and furans are all found to be the constituents of the oxygen content. Oxygen too is

mainly present in high molecular weight compounds and thus gives rise to higher amounts of oxygen in heavy fractions.

The presence of oxygen in the finished products generally aids the product deterioration which may be due to the presence of other objectionable elements. Some acidic forms of oxygen compounds could pose corrosion problems. Oxygen also promotes the gum formation in the finished products.

1.1.4 Metallic Impurities

The presence of even the trace amounts of metallic impurities like iron, copper and especially nickel and vanadium, in the feed stocks for catalytic cracking adversely affects the activity of the catalyst resulting in increased gas and coke formation. These metallic impurities are mainly present in the form of metallic complexes. Distillation process tends to concentrate these metallic constituents in the heavier fractions and residua.

Most of the vanadium, nickel, iron and copper (the four main metallic impurities) in the heavy fractions may be precipitated along with asphaltenes using pentane. This can reduce the concentration of especially vanadium by up to 95%, with substantial reductions in the amounts of nickel, iron, copper and other metallic impurities as well.

1.1.5 Chemical Structure of The Heavy Oils

Heavy oils are a complex mixture of several different types of heavy molecules and therefore, can not be described in terms of simple structures. For better understanding of the structure of the heavy oils, they are separated into different fractions by using different types of solvents. These solvents separate out one type of molecule from the other. There is no universally accepted method for doing this separation. An example of such a separation method is presented below:

1. Asphaltenes, precipitated by n-pentane.
2. Resins, precipitated with propane, can be further divided into:
   a. Soft Resins, soluble in aniline;
   b. Hard Resins, precipitated with aniline.
3. Wax, precipitated with methyl-isobutyl ketone.
4. Oils, the remaining fraction. This could be further subdivided into:
   a. Paraffinic oils, precipitated with acetone at -23°C
   b. Naphthenic oils (remaining material)

1.2 Heavy Gas Oil Used In This Investigation

The oil used in this study was a 345°C (650°F) to 524°C (975°F) heavy gas oil fraction derived from hydrocracking Athabasca tar sands bitumen. The bitumen contains 51.5 wt.% pitch (material boiling above 524°C) and about 0.6 wt.% of ash. Other properties of the bitumen are given in Table 2 [36].

Table 2: Properties of Great Canadian Tar Sands Bitumen

Specific gravity (60/60°F)	1.010
Sulfur (wt.%)	4.73
Ash (wt.%)	0.56
Viscosity (cst. at 210°F)	175.8
Conradson carbon residue (wt.%)	13.7
Pentane insoluble (wt.%)	15.6
Benzene insoluble (wt.%)	0.57
Nickel (ppm)	68
Vanadium (ppm)	211

The distillation analysis of the bitumen is given in Table 3. The process of bitumen hydrotcracking is quite complex and exact details are not available. However, from the available information, it is known that bitumen is hydrocracked at temperature of up to 450°C with hydrogen pressure of up to 2000 psig and a liquid hourly space velocity (LHSV) of the order of 1.0.

Table 3: Distillation Analysis of Bitumen

Equivalent distillation range at 1 atms. Temp. °C (°F)	Fraction (wt.%)	Cumulative (wt.%)	Sp.Gr. of fraction	Sulfur wt.% in fraction
IBP2200(IBP-392)	1.4	1.4	0.816	1.52
200-250(392-482)	2.2	3.6	0.856	1.02
250-333(482-632)	9.7	13.3	0.904	1.78
333-418(632-785)	17.7	31.0	0.955	2.98
418-524(785-975)	17.5	48.5	0.989	3.8
+524(-975)	51.5	100.0	1.073	6.39

There is substantial reduction in concentrations of sulfur, nitrogen, as well as the metallic impurities during thermal hydrocracking of bitumen. The heavy gas oil derived from this process constitutes about 35% of the total liquid products. The heavy oil was tested for its physical properties, elemental analysis and ASTM D-2887 distillation. The results are shown in Table 4.

1.3 - Hydrotreatment

Hydrotreatment is a process to catalytically stabilize petroleum products and/or remove objectionable elements from products or feed-stocks by reacting them with hydrogen [24]. This mainly involves removal of the objectionable elements like sulfur, nitrogen, oxygen and metallic impurities, as well as hydrogenation of olefins and gum-forming unstable diolefins to paraffins. It could be applied to a wide variety of feed-stocks ranging from naphtha to reduced crude.

The process involves contacting hydrogen and oil mixtures with a suitable hydrotreatment catalyst. Most hydrotreating reactions are carried out at temperatures below 425°C (800°F) to minimize cracking and coke formation. Fixed bed reactors are used for such operations. Pressures of between 100 psig to 3000 psig has been used for various feed-stocks. Liquid flow rates in terms of liquid hourly space velocity (LHSV in short) between 1.0 to 8.0 have commonly been employed.

Table 4: Properties of Heavy Gas Oil

Specific gravity	(60/60°F)	0.9803
API gravity	(°API)	12.8
Viscosity (at 25°C)		
Centipoise	(cp)	241.5
Centistokes	(cst)	246.4
Equivalent Saybolt Universal vis. (100°F)	(sec)	1140.0
Asphaltenes	(wt.%)	1.0
Aniline point	(°C)	52.7

Elemental Analysis :-

	(wt.%)
C	88.8
H	10.4
N	0.4831
S	3.05
C/H Atomic Ratio	0.71

ASTM-2887 Distillation :-

Temperature (°C)	322	340	373	392	411	429	452	477	504
Volume (%)	5	10	20	30	40	50	60	70	80

Hydrogen is consumed in the conversion of sulfur to hydrogen sulfide, nitrogen to ammonia, oxygen to water vapor and for the hydrogenation of the cracked or the unsaturated components. Consumption rates of between 200 to 800 scf/bbl of oil are quite common. However, an excess of hydrogen is always passed through the reactor for hydrotreating applications. These rates could be anywhere from 2000 to 10,000 scf/bbl of oil. Catalysts used in hydrotreatment include oxides of Co-Mo, Ni-Mo, and Ni-W on gamma-alumina which are generally presulfided prior to use. These three catalysts were used in a

previous study [57]. Some of the conclusions of that study and a review of the literature on catalysis aspects as well as various important factors influencing the operation of trickle-bed reactors are discussed in next chapter.

Chapter II

LITERATURE REVIEW

The present study was limited to the catalysis aspect of hydrotreatment and therefore, the literature survey was confined to this particular aspect. Commercially hydrotreatment is mostly carried out in trickle-bed reactors. A similar laboratory scale reactor was used for this study and the published information on the performance of trickle-bed reactors is also reviewed in this chapter. A thorough survey of the literature pertaining to this field was presented in an earlier work (M.A.Sc. Thesis [57]). This includes the published literature up to 1981. The work of Wittington et.al., [81], Green et.al. [25], Furimsky [23], Parsons and Ternan [53], Frost et. al. [22], Eberline et. al. [18], Mirza et. al. [46], Ahuja et. al. [2], and Hass [27] were discussed in this literature survey.

2.1 Previous Study

The above mentioned literature review was the basis of the research work that formed a part of the M.A.Sc. thesis. The objectives of this study were two fold:

1. to establish a scheme of experimental and analytical procedures, and

2. to test the most commonly used commercial catalysts (oxides of Co-Mo, Ni-Mo, and Ni-W on alumina).

The objectives set forth previously were successfully achieved. Some of the aspects highlighted by this study are the following:

1. A higher level of hydrodenitrogenation (HDN) and hydrodesulfurization (HDS) was possible if the catalyst hydrogenolysis properties could be improved.
2. Temperatures higher than 400°C give rise to higher hydrogenolysis activity at the cost of more coke formation and high gas yields.
3. Nitrogen removal was more difficult than sulfur removal for the given heavy gas oil. Ni-Mo combination performed the best HDN.

The nitrogen removal was found to be more difficult for this heavy gas oil and thereby needed particular attention. Therefore, the search for ideas to develop more efficient catalysts led to the hypothesis that some zeolite materials could be tried to enhance the hydrogenolysis activity of the hydrotreatment catalysts. The following text is presented as a brief description of zeolites and the literature survey that led to the above hypothesis.

2.2 Zeolites

Zeolites are best described as crystalline, hydrated aluminosilicates of group I and II elements (Jacobs [35]). Structurally these are infinitely extending three dimensional network of SiO_4 and AlO_4 tetrahedra linked together through common oxygen atoms. Their chemical formula can be written as :

$$M_{2/n}O \cdot Al_2O_3 \cdot x\,SiO_2 \cdot z\,H_2O.$$

where M is the compensating cation of valency n for net negative charge that is the result of isomorphic substitution of Si by Al. A unit cell of zeolite can be structurally represented as :

$$M_{x/n}[(AlO_2)_x\,(SiO_2)_y] \cdot z\,H_2O$$

2.2.1 Types of Zeolites

There are many types of natural and synthetic zeolites and some of the important types are briefly described here. The framework structure of zeolites are composed of arrangements of tetrahedra building units going from ring structure to polyhedra. Zeolites A, X and Y consists of linked cubooctahedra (β-cages or 24-hedra) - which is also called a sodalite unit (Figure 1).

Types X and Y are structurally and topologically related to mineral faujasite and are frequently referred to as faujasite-type zeolites (shown in Figure 2). The interconnection of cancrinite, or ε-units

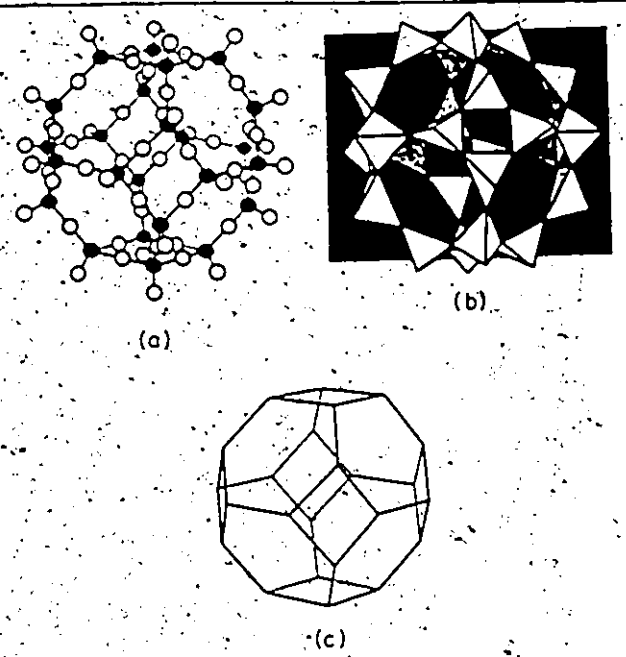

Figure 1: Sodalite Unit Depicted in Three Ways. (Taken from [68])

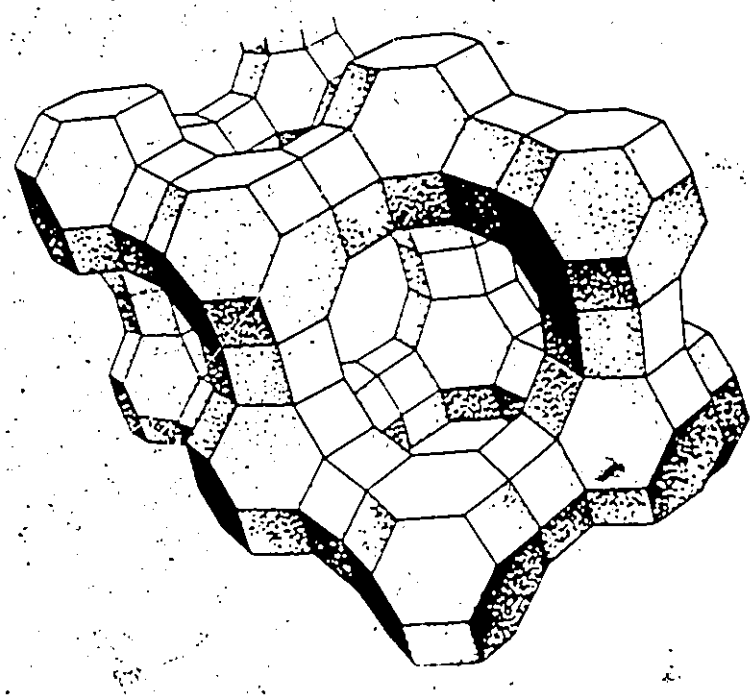

Figure 2: Zeolites X and Y (Faujasite) Structure. (Taken from [63])

generate the zeolites offretite, erionite, zeolite T and L. In zeolite Z or mordenite, the basic building unit consists of a ring of linked tetrahedra. The structure consists of chains of these building units cross linked by the sharing of neighboring oxygen atoms.

These different types of zeolites have different size of voids or cages interconnected by channels. These channels and the interconnected voids are occupied by the cations and water molecules. The cations are generally mobile and can be replaced, to a varying degree, by exchange with other cations. Removal of water molecules, constricts the interconnecting channels thereby giving rise to higher diffusion resistance to molecular movement in and out of the zeolite structure. The complete dehydration, in case of some of the zeolites, results in partial collapse of the structure. For process applications only the structurally stable zeolites are of real interest.

2.2.2 Types X and Y

Faujasite type X and Y zeolites have among the largest minimum aperture restrictions of any zeolite, and the highest void fractions. These consist of an array of cavities (also called supercages) having internal diameters about 1.2 nm. Access to each cavity is through six equispaced necks having a diameter of about 0.74 nm. Because of these bigger size channels and cavities, these are extensively used in hydrocarbon conversion applications. Y type zeolites are thermally more stable than X types because of their higher silica/alumina ratio.

2.2.3 Thermal and Hydrothermal Stability

Most synthetic zeolites are crystallized in the monovalent alkali metal form (generally Na) and have little or no catalytic activity for so called acid-catalyzed reactions. Also they are not very stable to high temperature conditions encountered in process applications. Therefore, these are modified by exchanging the alkali metal ions with higher valency ions to make them catalytically active as well as thermally and hydrothermally more stable.

2.2.3.1 Sodium Removal

The structural stability of less stable zeolites is increased by exchanging the Na ions with rare earth ions for catalytic cracking applications. Commercially, a mixed rare earth salt containing principally cerium (Ce), lanthanum (La), neodymium (Nd), and preseodymium (Pr) is used. These ions are incorporated into zeolite material replacing from 80 to more than 97% of equivalent Na. Catalyst activity and selectivity in cracking are independent of the rare earth ratio of Ce, La or Nd in the zeolite content of the catalyst. However, zeolite stability is directly proportional to lanthanum or neodymium content and inversely proportional to cerium content (Magee and Blazek [39]).

The catalytic activity of these materials depend upon the alkali metal content and so a significant increase in catalytic activity is brought about by removal of the residual Na. This is generally achieved by multiple ion-exchanges with intermediate calcinations. This treatment

causes the sodium cations to migrate to positions accessible by ion-exchange solutions. It is possible to reduce the residual sodium content from 2-3% to less than 0.2%.

2.2.3.2 Aluminium Removal

The thermal stability of zeolites is also increased after gradually leaching out the aluminium atoms and thereby increasing the SiO_2/Al_2O_3 ratio. Such structures also become more resistant to mineral acids. This aluminium extraction is carried out by leaching with strong acid solutions. For example, mordenite as synthesized, has a SiO_2/Al_2O_3 ratio of approximately 10. After, refluxing with 6N HCl for periods up-to 8 hr., this ratio can be increased to between 14 to 100. Too much de-aluminization may not always be advantageous for the catalytic activities and therefore, an optimum level can be determined experimentally for a particular application.

2.2.4 Acidity

Zeolites have highly acidic structures. Both Bronsted and Lewis type of acid sites are present in zeolite structures. Protons (i.e. Bronsted type of acid sites) are introduced in to the zeolites either by thermal decomposition of NH_4-exchanged form, hydrolysis of water of hydration of cations or by reduction of cations to a lower valency state, whereas, dehydration of these structures results in dehydroxylation and thereby formation of Lewis type of acidic sites. Acidity of rare-earth exchanged Y type zeolites is attributed to the dehydroxylation of the hydroxyl groups associated with rare-earth ions (Bolton [8]).

2.3 Cracking Catalyst

High acidity of the catalyst is one of the main requirements of a cracking catalyst and therefore, zeolites have been extensively used for such applications. Pure zeolite materials are not suited for cracking applications because of their fine pores. For example Haynes et.al. [28] have found a critical molecular size of 0.9 nm (size of pyrene molecule) for a Y-type zeolite in their hydrocracking experiments. Their catalyst was ineffective in processing of molecules bigger than the critical size. Therefore, these materials are generally mixed with other amorphous support materials for catalysis applications.

A cracking catalyst of silica-alumina matrix containing 15% of Y-type zeolite was first introduced in 1962 [63]. Such catalyst were found to give not only higher catalytic activity because of the high acidity of the catalyst, but also higher yields of the high octane gasoline were obtained. Miale et.al. [42], from their work on cracking of n-hexane on zeolite materials found that such materials are at least 10^4 times as active as amorphous silica-alumina. However, the concentration of acid sites on zeolites is only 10 to 100 times greater than that on the silica-alumina. This alone did not provide a satisfactory explanation for the high activity of the zeolite materials. It has been suggested that in the vicinity of unshielded cations within the small pores, high electrostatic fields are created that may enhance the catalyst activity. This was observed by NMR studies of adsorbed xenon molecules on zeolite materials by Fraissard [21].

2.3.1 Effect of Zeolite Input

Magee and Blazek [39] have summarized the following effects of the amount of Y-type zeolite rare earth exchanged (REY-type in short) on the activity and selectivity of cracking catalysts:

1. At constant conversions, lower coke, lower dry gas yields and higher yields of gasoline and cycle oils are obtained with increase in zeolite content.
2. Aromatics and olefins decrease in gasoline fractions at low zeolite levels with corresponding decrease in motor and research octane numbers. Above 9% zeolite, however, aromatic content increase probably from cracking of aromatic compounds in the light cycle oil into gasoline range.
3. At high zeolite inputs C_3 and C_4 olefins disappear faster than would be expected as a result of acid activity only. They may be undergoing a type of conjunct polymerization to form saturates and aromatics in the light cycle oil range and coke.
4. Residence time plays a more important role than acid activity in catalyst of very high acid activity. Thus at high zeolite inputs, high yields of light cycle oil cannot be obtained since the long contact time required to convert heavy oil to lighter hydrocarbons inevitably lead to overcracking of light cycle oil to gas fractions and to a lesser degree to gasoline fractions.

2.4 Hydrocracking Catalyst

As mentioned earlier in 'Introduction', catalytic cracking and hydrocracking are both very important parts of a modern refinery. These two processes supplement each other. Virgin gas oils are generally used in catalytic cracking whereas refractive gas oils that are derived from cracking and coking operations are processed in hydrocracking. Operating conditions in hydrocracking are more severe than in catalytic cracking and a high pressure of hydrogen is required to reduce the coke formation as well as to convert the refractive materials to oils.

Bolton [7] has described in great details the use of zeolites in hydrocracking. A good hydrocracking catalyst should have highly acidic cracking component along with a noble metal or a combination of non-noble metals as the hydrogenation component. Heinmann [29], indicated that rare earth exchanged Y-zeolite (faujasite) dispersed in matrix of silica-alumina, synthetic clays or natural clays are most commonly used as cracking catalysts. However, he pointed out that the use of such catalysts in hydrocracking is still quite limited. Heinemann further narrows down the choice of zeolite for hydrocracking purposes to large pore ultrastable zeolite-Y and hydrogenation components such as platinum or palladium in relatively small quantities (0.5%) or nickel, tungsten, or molybdenum oxided or sulfided in larger amounts (3-8%).

Two of the recent books namely 'Zeolite Technology and Applications' [82] and 'Hydroprocessing Catalysts for Heavy Oil and

Coal' [34] give information available from U.S. patent literature from 1974 to 1981. This information is also indicative of the same conclusions as made by Heinemann. No more information is available in this field beyond the range of compositions of catalysts.

2.5 Hydrotreating Catalyst

Catalytic hydrotreatment is a hydrogenation process used mainly to achieve high degrees of impurity removal, whereas in catalytic hydrocracking, a feed stock is mainly cracked along with active hydrogenation of cracked products. Some degree of hydrotreatment is achieved in hydrocracking , and similarly, feed stocks do get cracked to a certain extent in a hydrotreating process depending upon the operating conditions. This is generally desireable if the feed stocks are heavy. Hydrotreatment of some of the final lighter products is carried out at very mild conditions so as to maintain the product quality.

The heavy gas oil used in the present study contains about 1% of the refractive material (asphaltenes in Table 4) and in this case mild cracking is considered desirable. Also as indicated by our previous study [57], higher levels of HDS and HDN could be achieved with higher degree of hydrogenolysis. Therefore, in the development of an efficient hydrotreatment catalyst for this oil, the above mentioned review of the catalysts used in the catalytic cracking as well as hydrocracking forms a good starting point.

Table 5: Details of Zeolite Material

Description	:	Type Y, molecular sieve rare-earth exchanged	
Composition	:	SiO_2	- 65%
		Al_2O_3	- 23%
		Na_2O	- 2%
		Rare Earth	- 11%
Form	:	Powder	(38μm to 53μ)
Surface Area	:	Approx.	550 m^2/g.
Catalogue No.	:	14-8910 (powder) of Sterm Chemicals, USA.	

2.5.1 Zeolite Material Used in This Study

According to the above literature review, rare-earth exchanged Y-type zeolite is the best suited material for hydroprocessing applications. Preparations and testing of such materials is quite involved and the required facilities were not available. Therefore, it was decided to use the material available from a commercial source. Some details of the zeolite material used in this study are listed in Table 5.

2.6 Trickle-Bed Reactors

The types of industrial gas-liquid-solid reactors can be divided in two categories, i.e., one where the solids are fixed and the other where solids are in a suspended state (e.g. fluidized or ebullated bed reactors). The fixed bed reactors can be operated in three ways. The

gas and liquid can both flow concurrently upwards or downwards or a countercurrent operation in which liquid flows downwards.

One of the most widely used three-phase reactors is the trickle-bed reactor (Shah Y.T. [67]). This type of reactor is particularly favoured by the hydroprocessing industry. In a trickle-bed reactor, the liquid flows down over the packings in the form of a thin liquid film and the continuous gas phase flows in between the packings either concurrently or counter-currently. Concurrent gas flow is generally preferred to avoid flooding problems.

Tubular reactors offer ease of operation, simple equipment format and better heat transfer compared to stirred bed batch reactors (Smith [69]). However, in the case of trickle-bed reactors, fluid flow patterns, liquid hold-up, catalyst wetting and axial dispersion effects play important roles. A lot of work has been done to understand the hydrodynamics of trickle-bed reactors and various models are available for prediction of various flow regimes. A recent review of Smith et. al. [70] has discussed most of such available literature.

2.6.1 Advantages of Trickle-Bed Reactors

Some of the advantages of trickle-bed reactors are as follows:

1. Flow is close to plug flow, allowing high conversion to be achieved in a single reactor.

2. Liquid-to-solid ratio is small, minimizing the homogeneous side reactions.

3. Liquid flows in the form of a thin film on the solid packing thus offering a small resistance to the gas diffusing to the solid surface.

4. Flooding is not a problem and pressure drop is less than in the concurrent up-flow and countercurrent flow reactors. This results in essentially uniform partial pressure of reactants across the length of the reactor.

5. As compared to fluidized or ebullated bed reactors, the trickle-bed reactor systems have simple equipment format and operation and maintenance is easy.

2.6.2 Disadvantages of Trickle-Bed Reactors

Along with above mentioned advantages of the trickle-bed reactors, there are some inherent disadvantages of such a reactor system. At low liquid flow rates maldistribution of liquid such as channeling, bypassing and incomplete catalyst wetting can occur in trickle-bed reactors. Catalyst particle size cannot be too small as this could give rise to higher pressure drops as well as it increases the chances of bed plugging. Therefore, the catalyst particle are of larger size in such reactor systems as compared to fluidized bed or ebullated bed systems, and so the intra-particle diffusional effects are more pronounced.

In large scale trickle-bed reactors, a major disadvantage could be the poor radial mixing of heat. This could cause excessive localized

heating resulting in rapid catalyst deactivation and/or increase in undesireable reactions. This problem becomes important for the reaction systems involving high heat effects and can be solved to some extent by addition of one or more streams of quench fluids at different points along the reactor length.

2.6.3 Hydrotreatment Applications

Trickle-bed reactors are particularly suited for the hydrotreatment type of reactions because of the above mentioned advantages. Low liquid hold-ups in the reactor minimize the undesireable homogeneous reactions. Predominantly plug-flow type of behaviour of fluids in trickle-bed reactors makes high degree of conversions possible in a single reactor. The above mentioned disadvantage concerning the heat effects do not seriously affect the hydrotreatment reactions because the heat effects in such reactions are quite moderate.

For better distribution of liquid, distributers are used at the top of reactor as well as along the length of the reactor (if so desired). In commercial applications, high liquid flow rates are used which minimizes the maldistribution problems. Intra-particle mass transfer effects have to be considered for the design of such reactors as this disadvantage can not be circumvented. This makes it important to evolve catalyst of high efficiencies.

2.7 Dynamics of Trickle-Bed Reactors

For concurrent gas-liquid down-flow in a packed bed, various flow regimes can be obtained depending upon the gas and liquid flow rates, the nature and size of packing, and the nature and properties of liquid as well as gas. These are:

1. TRICKLE-FLOW REGIME

   In this flow regime, the liquid trickles down over the packing in the form of discontinuous film or rivulets. The liquid flow is mainly laminar and the gas flows around the wetted particles in a gas continuous fashion. The gas flow could be laminar or turbulent.

2. SPRAY-FLOW REGIME

   With the increase in gas flow, the drag force on the liquid film increases and the liquid flow around the particles also become turbulent. At certain flow conditions, small droplets of liquid start to separate from the liquid film and flow along the gas in the gas continuous region in the form of a liquid spray. This flow regime is also called the 'transition regime' or 'rippling flow'.

3. PULSE-FLOW REGIME

   If the gas flow rate is further increased, for suitable liquid flow rates, the amount of liquid drops or slugs in the gas continuous phase become sufficient to momentarily block a part of the flow channels between the packings. This causes increased flow in other part of the packed bed and, thus, increasing the chance

of separation and blocking in parallel channels. This disturbance tend to accelerate towards the lower part of the reactor and gives rise to pulses or waves in the outlet stream.

4. BUBBLE-FLOW REGIME

This is quite an undesireable situation in the trickle-bed reactors which can occur at high liquid flow rates. In this flow regime the liquid flows down in a continuous phase whereas the gas bubbles are dispersed in the liquid phase. Such a situation can occur at very low gas flow rates and liquid flow rates sufficient to form a liquid continuous phase. The liquid entraps some gas bubbles before it forms a liquid continuous phase somewhere along the length of the reactor.

2.7.1 Prediction of Flow Regime

A lot of work has been reported in the recent past. For air-water systems, Sato et.al. [60] presented a summary of flow pattern boundaries. Charpentier and coworkers [12] [13] [14] have done a lot of work in this area and have proposed generalized diagrams for prediction of flow regimes for foaming as well as nonfoaming systems. Baldi and coworkers [4] are also active in this field and they denote the trickle-flow regime or the gas-continuous regime as a "low-interaction regime" and pulsed flow or the spray flow regime as "high-interaction regime". Results of Baldi et.al. agree quite well with those of Charpentier et.al. for the nonfoaming systems whereas, for the foaming systems there is some discrepancy between the two. Recently Tosun [26] has reported his results of studies of the generalized flow maps.

His data were in quite good agreement with the generalized flow map proposed by Charpentier et.al.. Shah [67] has presented the generalized flow map of Charpentier et.al. in his recent book. The same is shown in Figure 3. The symbols in Figure 3 have the following meaning:

G_L = superficial liquid mass velocity (kg/m^2 s)

G_G = superficial gas mass velocity (kg/m^2 s)

The symbols ρ, μ, and σ represent density, viscosity and the surface tension and their subscripts are G for gas, L for liquid, 'air' for air and 'wat' for water.

As can be seen from the generalized flow regime chart, the values of the densities, viscosities and the surface tension are required for making any prediction. At present such information for the complex systems such as the hydrotreatment of heavy gas oils, is not available. Therefore, it is possible to have some understanding of the flow regimes in a hydrotreatment process only through the actual experimental studies.

For the present study, it was decided to study the effects of both gas and liquid flow rates, within the nominal range of flow rates, so as to get some insight into the flow regimes present in the experimental reactor.

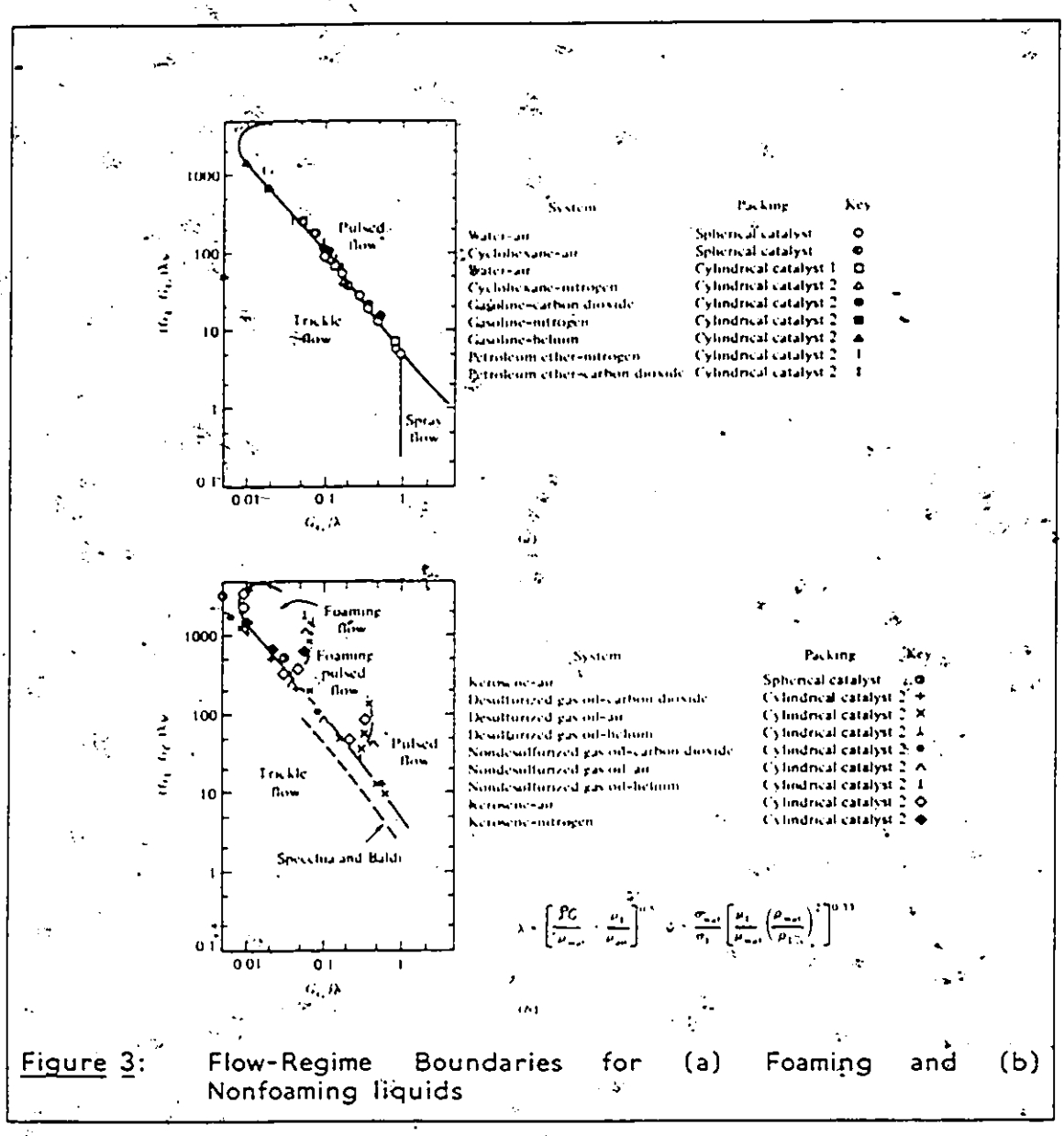

Figure 3: Flow-Regime Boundaries for (a) Foaming and (b) Nonfoaming liquids

2.7.2 Liquid and Gas Distribution

The distribution of liquid and gas in the trickle-bed reactors is another important factor to be considered. In hydrotreatment applications, the limiting reactants are in the liquid phase and so the distribution of liquid is quite important whereas gas distribution is generally very good. Depending upon the ratio of reactor tube diameter to particle

diameter (d_t/d_p), it has been found that liquid has a tendency to channel towards the walls of the reactor. In the low interaction regime (superficial liquid velocity $u_L < 0.9X10^{-3}$ m/s) liquid distribution has been found to be uniform (Specchia et.al. [73], Sylvester and Pitayagulsarn [75], and Herskowitz and Smith [31]). Sylvester and Pitayagulsarn found the liquid distribution to be unstable when the liquid superficial velocity was higher than 0.01 m/s and the gas superficial velocity was lower than 0.033 m/s. A significant increase in the liquid flow rate at the centre of the column was observed by these authors, at the onset of the pulsing flow regime.

Prchlik et.al. [54] reported that for $d_t/d_p > 25$, the wall flow was less than 10% of the total flow. Herskowitz and Smith [32] found that for $d_t/d_p > 18$, the wall flow is negligible, and granular particles cause less wall flow than spherical or cylindrical particles. As the distribution of liquid in the reactor will depend upon many physical factors concerned with the fluids and the packing, the available information can only be used as speculation. However, increasing the ratio (d_t/d_p) does have a positive effect on the uniformity of the liquid distribution in trickle-bed reactors as was indicated by these studies. No single value of this ratio will be good for all the physical situations, but these studies tend to indicate that at $d_t/d_p > 20$, the chances of a uniform liquid distribution are very good.

2.7.3 Effective Catalyst Wetting

In the hydrotreatment processes, the reactions occur in the liquid film on the catalyst particles as well as the liquid inside the pores of these particles, it is very important that they be wetted by liquid in order to use the catalytic sites effectively. Mears [40], Paraskos at.al. [52], Montagna and Shah [47], and Montagna et.al. [48], have recently shown that some of the data on trickle-bed reactors can be better correlated assuming incomplete catalyst wetting. At present very little is known on how liquid-solid contact efficiency depends upon the gas and liquid flow rates, however, it is believed that higher gas and liquid loadings and higher dynamic liquid holdups can improve the catalyst efficiencies.

Satterfield [64] defined the contacting effectiveness in chemical reactors in terms of the apparent kinetic constant (k_{app}) obtained in a trickle-bed reactor and the actual kinetic constant (k_v) obtained in the continuously-stirred-tank reactor. Based on the experimental data, Satterfield proposed a graphical correlation which is shown in Figure 4.

Recently, Mills and Dudukovic [45], obtained additional data by using tracer methods. For a small particle size (0.72 mm) the wetting efficiency was found to be close to unity over the range of liquid flow rates : 0.15 to 3.5 kg/m² s., whereas, from Satterfield's correlation the predicted values are much lower. There are many similar correlations proposed by Schulman [65], Kranze and Serwinski [38], Onda et.al.

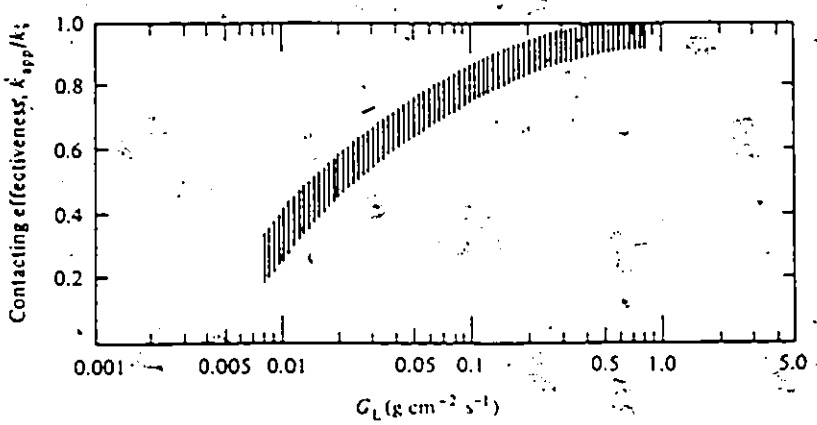

Figure 4: Contacting Effectiveness as Function of Liquid Loading

[50], Puranik and Vogelpohl [55] and others, some of which are listed by Shah [67]. Since there is large degree of discrepancy between the predictions of various correlations, it is best to rely on the experimentally determined values for a particular trickle-bed operation.

2.7.4 Liquid Holdup

Liquid holdup is the amount of liquid present in the packed bed at steady state conditions. This is further divided in to two categories; dynamic and static holdup. The dynamic holdup is considered to be the amount of liquid at a steady state condition that will drain out of the packed bed if the inflow of liquid is stopped. The difference in the total liquid holdup and the dynamic holdup is considered as the static holdup.

It was first proposed by Henery and Gilbert [30] that the departure of trickle-bed reactor behaviour from an ideal plug-flow could be explained by the liquid holdup. They proposed a model based on liquid holdup to correlate some of their own data as well as data available from other authors. This model will be described in section (2.8.2).

The static liquid holdup is correlated by the Eötovs number ($Eö = \rho_L g d_p^2/\sigma_L$, where d_p is the nominal particle diameter and g is the gravitational acceleration). Figure 5 shows a correlation given by Swaaij et.al [78] for the static liquid holdup.

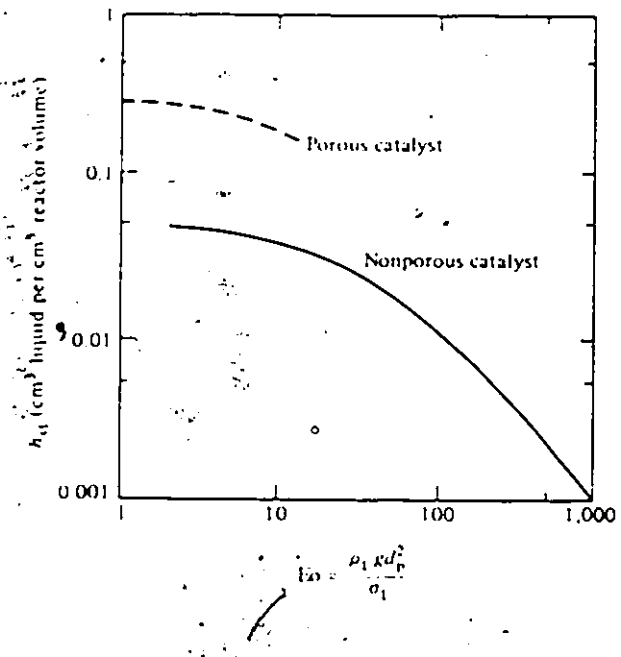

Figure 5: Correlation of Static Liquid Holdup With Eötovs Number

There are several correlations available for dynamic holdup (h_d), some of which have been discussed by Shah [67]. He recommends the use of two correlations by Specchia and Baldi [74]. These are:

$$h_d = 3.86\ (Re_L)^{0.545}\ (Ga_L^*)^{-0.42}\ (a_s\ d_p/\varepsilon)^{0.65}, \qquad (1)$$

for poor-interaction regime, where Re_L is defined in terms of superficial liquid velocity, and Ga_L^* is a modified Galileo number defined as

$Ga_L^* = d_p^3 \rho_L (\rho_L g * \delta_{LG})/\mu_L^2$, where δ_{LG} is the two phase fractional pressure drop between liquid and gas. For the high-interaction regime, they obtained the following relation:

$$h_d = p[Z/\psi^{1.1}]^q (a_s d_p/\varepsilon)^{0.65}, \qquad (2)$$

where the constants

$p = 0.0125$, $q = -0.312$ for nonfoaming liquids,

$p = 0.0616$, $q = -0.172$ for foaming liquids, and

$Z = Re_G^{1.167}/Re_L^{0.767}$, and the parameter ψ is as defined in Figure 3.

2.7.5 Axial Dispersion

In trickle-bed reactors, axial dispersion of the gas and liquid reactants can occur to varying degrees depending upon the physical properties of the fluids and the characteristics of the packings. This makes the behaviour of trickle-bed reactors deviate from the ideal plug-flow regime, and as a result, longer reactors would be required to get the desired conversions.

Axial dispersions are generally estimated from residence-time-distribution (RTD) studies with the help of suitable tracers. Single-parameter axial dispersion models characterize the axial dispersion (or back mixing) using a simple one dimensional Fick's law type diffusion equation. The constant of proportionality is called the axial dispersion coefficient (E_z) and is expressed in dimensionless form as the Peclet number ($Pe = uL_c/E_z$), which is also sometimes referred to as the Bodenstein number. Here u is the superficial velocity of fluid, and L_c is generally the size (diameter) of the packing. Value of this number Pe, denotes the degree of backmixing. If Pe = 0, backmixing is complete, and if Pe = ∞, then ideal plug-flow prevails.

Various models have been proposed by different authors whereby the Peclet number has been correlated to the Reynolds number and the Galileo number of the liquid. The gas phase flow Reynold numbers generally have no effect on these correlations. One such correlation given by Michell and Furzer [44] is:

$$Pe_L = 1.00\ Re_L^{0.70} Ga_L^{-0.32}, \qquad (3)$$

where, $Pe_L = u_L d_p/E_{zL}$, $Re_L = d_p \rho_L u_L/\mu_L$, $Ga_L = d_p^3 g \rho_L^2/\mu_L^2$, u_L is the interstitial liquid velocity and E_{zL} is the liquid phase axial dispersion coefficient.

A similar relation is proposed by Elenkov and Kolev [19] in which they have defined the dimensionless groups in a different manner:

$$U_{0L}/a_s E_{zL} = 0.068(4U_{0L}/a_s \nu_L)^{0.78}(g/a_s^3 \nu_L^2)^{-0.33}, \qquad (4)$$

Here, a_s is the total surface area of packing per unit volume of column, and U_{0_L} is the superficial liquid velocity based on single-phase flow in an unpacked reactor column.

Hochman and Effron [33], on the basis of their data, proposed that the Peclet number can be successfully correlated with only the Reynolds number as:

$$Pe_L = 0.042\ Re_L^{0.5} \qquad (5)$$

where Reynolds number is defined using bed porosity (ε) as $Re_L = U_{0_L} \rho_L d_p / \mu_L (1-\varepsilon)$

A correlation similar to the one by Michell and Furzer [44] is also proposed by Kobayashi et.al. [37] which is presented by Mordechay and Smith in their review [70]. In this correlation the dimensionless numbers are defined in a different way and the reviewers recommend the use of this equation.

Once again, use of the available equations for predictions in the case of a real hydrotreatment situation is questionable as these correlations are based on simple air-water (or similar) systems. Mears [40] and [41], has developed a criterion for judging the significance of backmixing in trickle-bed reactors. This has been commonly used by most of the authors working with such reactor systems. As per this criterion, if axial dispersion effects are to increase reactor length by less than 5% over the minimum length required with ideal plug-flow assumption, then the criterion to be met is:

$$\frac{L}{d_p} > \frac{20m}{Pe} \ln\frac{C_i}{C_o} \qquad (6)$$

where, $Pe = U_o d_p / E_z$, U_o is the superficial velocity of fluids based on empty bed, d_p is the particle size, E_z is the axial dispersion coefficient, m is the order of the reaction, C_i and C_o are the inlet and outlet concentrations of reacting component and u is the order of reaction.

For various gas oils, Mears estimated Pe value of 0.2 for Reynolds numbers of about 10. Taking a first order reaction, for 95% conversion, the right hand side of the above criterion comes to about 300. Therefore, as a 'rule of thumb' most of the authors have used a ratio of $L/d_p > 350$ for assuming ideal plug-flow conditions in trickle-bed reactors. This criterion is quite conservative and has been varified by Mears [40] and [41], Montagna and Shah [48] and many other authors. van Klinken and van Dongen [77] have recently shown with their RTD studies that for small particles and diluted bed laboratory reactors, the criterion of Mears is in fact very conservative.

2.8 Mathematical Models for Trickle-Bed Reactors

Trickle-bed type of columns are used for a variety of applications in the chemical industry and each application requires a different type of mathematical treatment which results in models suitable for only those particular applications. For this work, models mainly associated with the hydrotreatment type of applications will be discussed here.

2.8.1 Ideal Plug-Flow Model

For hydrotreating applications, a simple plug-flow model can be assumed if the following conditions are satisfied:

1. No significant axial dispersion.
2. Catalyst completely wetted by liquid.
3. Reaction occurs only at the liquid-solid interface.
4. Negligible mass transfer resistance (both gas-liquid as well as the liquid-solid).
5. Heat effects are negligible and operation is isothermal.
6. No vaporization of liquid or condensation of vapours occur.

For such an ideal case, a differential mass balance of one of the reacting species will give a simple plug flow equation of the type shown below:

$$\frac{dC}{dz} = -\frac{k''_m(1-\varepsilon)\,\eta}{(LHSV)}[C]^m = -\frac{k'_m\,\eta}{(LHSV)}[C]^m, \qquad 0 < z \leq 1, \qquad (7)$$

where C is the concentration of the reactant, k''_m the intrinsic rate of reaction and m is the order of reaction, z is a dimensionless length parameter, ε is the void fraction of the catalyst bed, LHSV is liquid-hourly-space-velocity which is generally taken as the volumetric hourly flow rate of liquid divided by the catalyst volume. η is the catalyst effectiveness factor and k'_m is the m'th order reaction rate constant based on the total volume of catalyst. This rate constant can be defined in many ways. It could be defined on the basis of unit catalyst area, or unit catalyst mass as well and accordingly, the above equation will be modified. The definition based on the total volume of the catalyst is

most often used. Integration of the above equation over the entire length of the reactor yields:

$$\ln\frac{C_i}{C_o} = \frac{k_1 \cdot \eta}{(LHSV)}, \qquad (8)$$

while k_1 is the first order rate constant for a first order reaction, for second order reaction, (m=2), the integration yields:

$$\frac{1}{C_o} - \frac{1}{C_i} = \frac{k_2 \eta}{(LHSV)}, \qquad (9)$$

where subscripts i and o indicate the inlet and outlet concentrations of the reactant. Mostly the concentrations are expressed in terms of percentage by weight rather than in terms of the moles.

2.8.2 Holdup Model

Henry and Gilbert [30] proposed that the dependence of catalyst effectiveness on the liquid flow rate in a pilot scale and other smaller reactor systems was due to insufficient liquid holdup in the reactor. Therefore, they included the liquid holdup term in the ideal plug-flow equation. for a first order reaction, the modified equation is:

$$\ln\frac{C_i}{C_o} = \frac{k_1 \eta h_L}{(LHSV)}, \qquad (10)$$

where h_L is the liquid holdup. They used the liquid holdup correlation of Satterfield et.al. [61], which is:

$$h_L = \beta[d_p \rho_L u_L / \mu_L]^{0.333} [d_p^3 g \rho_L^2 / \mu_L^2]^{-0.333}, \quad (11)$$

where β is a constant and other symbols has the usual meaning. Using this value of the liquid holdup, they derived the model equation in the following form:

$$\ln \frac{C_i}{C_o} = (L)^{0.333} (LHSV)^{-0.667} (d_p)^{-0.667} (\nu_L)^{0.333}, \quad (12)$$

where η is taken as unity, L is the length of the catalyst bed and ν_L is the kinematic viscosity of the liquid. The above relation is valid for $10 < Re_L < 600$.

2.8.3 Effective Catalyst Wetting Model

Mears [40] did not agree with the model proposed by Henry and Gilbert (Holdup Model). He suggested that dependence of reactor performance on the velocity of liquid in pilot-scale reactors is due to incomplete catalyst wetting at low flow rates. Therefore, for a first order reaction, he modified the ideal plug-flow equation as:

$$\frac{dC}{dz} = -\frac{k_1 \eta C A_{eff}}{(LHSV)}, \quad (13)$$

where, A_{eff} is the ratio of wetted to actual surface area of the catalyst. Mears used the following correlation given by Puranik and Vogelpohl [55] for A_{eff} :

$$A_{eff} = 1.05 \, (Re_L)^{0.047} \, (We_L)^{0.135} \, [\sigma_c / \sigma_L]^{0.206}, \quad (14)$$

where $We_L = U_L^2 d_p \rho_L / \sigma_L$ is the Weber number; σ_L is the surface tension of liquid and, σ_c is the critical value of the surface tension for a given combination of liquid and catalyst. Below this value of the critical surface tension, the contact angle is zero and the liquid completely wets the the catalyst. Using this equation for the value of A_{eff}, Mears derived the following equation for his model based on the effective catalyst wetting:

$$\ln \frac{C_i}{C_o} = (L)^{0.32}(LHSV)^{-0.68}(d_p)^{-0.18}(\nu_L)^{-0.05}[\sigma_c/\sigma_L]^{0.21}\eta(d_p), \qquad (15)$$

This model is similar to the one given by Henry and Gilbert in predicting the dependence of $\ln(C_i/C_o)$ on L and LHSV. However, it differs from the holdup model of Henry and Gilbert, in predicting the affect of particle size, surface tension and viscosity on the performance of the trickle-bed reactors.

The correlation for the effective wetting by Puranik and Vogelpohl does not provide a good prediction for commercial trickle-bed reactors where higher liquid flow rates are used and the effective catalyst wetting is generally close to one. Mears suggested using the correlation given by Onda et.al. [51] for the reactors using liquid mass velocities of more than 500 g/h cm^2 . Their correlation for effective wetting is:

$$A_{eff} = 1-\exp[-1.36Ga_L^{0.05}We_L^{0.2}(\sigma_c/\sigma_L)^{0.75}], \qquad (16)$$

Using this equation for the first order model, the model equation of the following form results:

$$\ln\frac{C_i}{C_o} = \frac{k_1 \eta}{(LHSV)}[1-\exp(-\gamma(L)^{0.4}(LHSV)^{0.4})], \qquad (17)$$

In this equation the viscosity, surface tension, density and particle diameter terms have been combined in one parameter γ .

2.9 Choice of Reactor

Unfortunately the available data on hydrodynamics of trickle-bed reactors is based on simple air-water or similar systems at normal temperature and pressure conditions. Therefore, the application of such data to a complex system such as heavy gas oil at hydrotreatment conditions is quite questionable. Moreover, the accurate estimates of the physical properties of the heavy gas oil and hydrogen system at the operating conditions are very essential for using the available models for predicting the hydrodynamic conditions inside the reactor. Such estimates are not yet available in the published literature.

Inspite of the above mentioned limitations some useful hints were quite handy in the design of the trickle-bed reactor. This information was used in the earlier work, [57] and quite good results were obtained. The reactor used in the earlier study was 40 cm long with 17.5 mm inside diameter. 40 cc of catalyst was required for each filling.

In the present study the catalyst was made in the laboratory and our trials indicated that to make a batch of about 100 cc catalyst, quite big reaction and mixing vessels, filtering and washing facilities are required. Therefore it was decided to use a smaller reactor for this work. Based on this limitation and the available literature on trickle-bed hydrodynamics, a 1 m long, 0.52 cm inside diameter tube was used for this study. Average size of catalyst particles was 0.2 mm (70 to 80 mesh size) Poor catalyst wetting or any adverse axial dispersion effects were not expected with this design as per the available literature. A similar system was also used by Satterfield and Yang [62] for their HDN and HDO study of heavy gas oils.

Chapter III

OBJECTIVES

The outcome of the literature survey and the first hand information obtained in this field from the earlier work, was to develop and test more efficient catalysts for hydrotreatment of the heavy gas oil derived from Canadian Athabasca bitumen. Some of the main features of the present research were as follows :

1. To study the operating region and find out an optimum operating point for performing catalyst testing.
2. To evolve a catalyst preparation scheme and test its reproduciblity.
3. To make and test catalysts of different compositions with respect to the silica and zeolite concentrations.
4. Find an optimum composition of catalyst support material from the above mentioned tests.
5. Study kinetics of the reactions over catalyst prepared with the optimum composition and to evaluate rate constants and activation energies for both sulfur and nitrogen removal from the heavy gas oil.

Chapter IV

EXPERIMENTAL EQUIPMENT

The equipment needed for the catalyst preparation were items such as laboratory glass ware, stirrers, crushing and screening facilities, ovens, extrusion facilities, muffle furnace, etc.. A short description of this equipment is given in the catalyst preparation section (5.1). Since most of the equipment were standard laboratory items, no detailed description is considered necessary. The equipment used for the testing of catalysts in the hydrotreatment of heavy oil is described below.

4.1 Hydrotreatment System

The schematic of the hydrotreatment system is shown in Figure 6. The equipment mainly consisted of the trickle-bed reactor kept in a sand bath. The oil and gas were fed from the top. The product stream was removed from the bottom of the reactor through a back pressure regulator. The product stream was either run through two one litre liquid separators when no sample was to be withdrawn, or the exit stream was connected to a weighed sample bottle where the liquid was separated from the gases. The exit gases were analyzed by an online gas chromatograph system. The exit gases were scrubbed in a hydrogen sulfide scrubber before they were vented to the atmosphere.

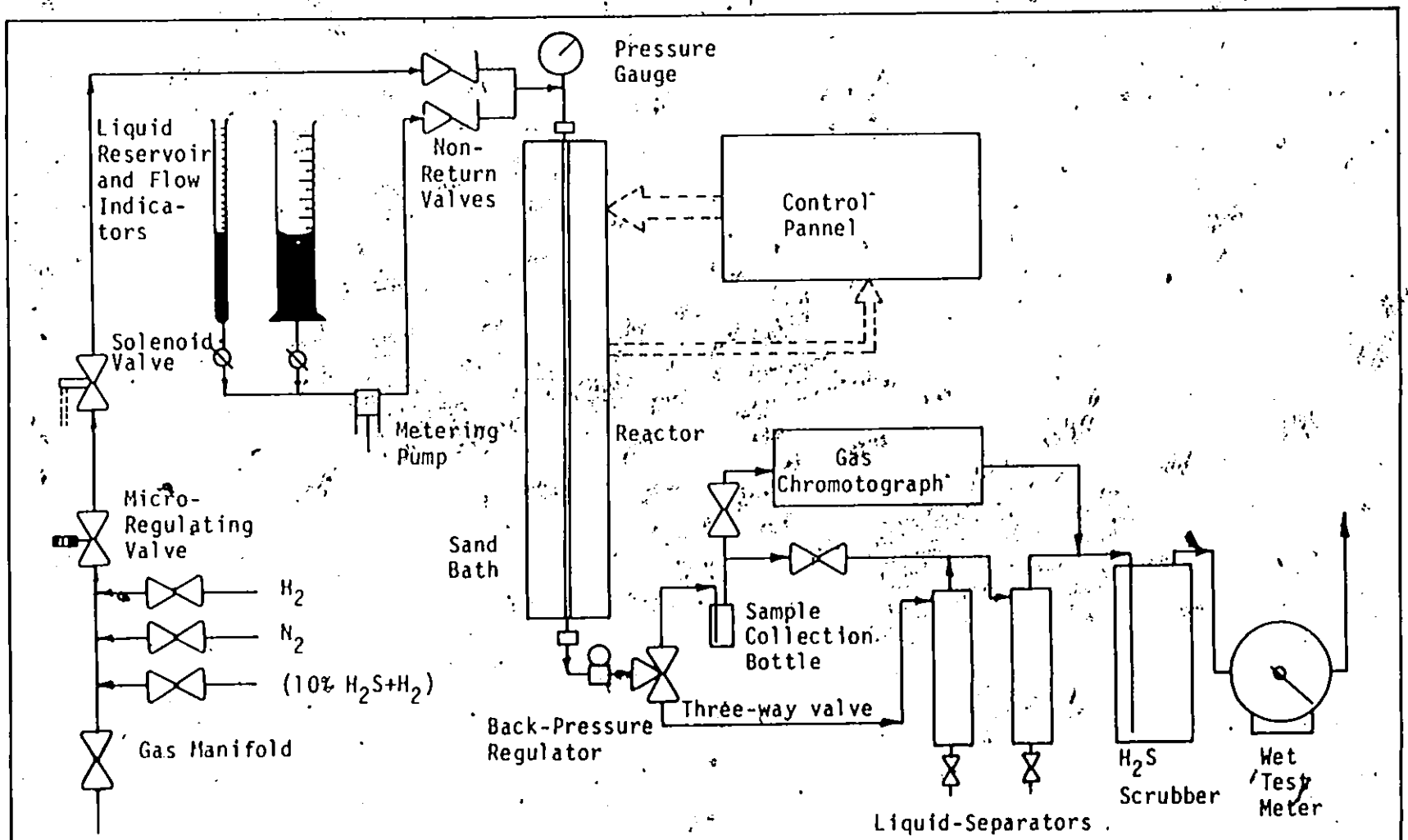

Figure 6: Schematic of the Hydrotreatment System

Except for the gas manifold system and the gas chromatograph, all the experimental setup was installed inside a fume hood to avoid the exit gases going into the building ventilation system. Also this was a safety precaution to avoid the hydrogen concentrations in the room atmosphere reaching dangerous proportions. While the fume hood fan was continuously run during the experimental runs, a fume hood air flow sensor was used to monitor the air draft. In case of failure of the fume hood fan, this sensor would send a signal to the main control panel to shut off the gas supply as well as to shut off power to all units.

4.1.1 Liquid Feed System

The heavy gas oil was pumped in to the reactor by a high pressure metering pump (Milton Roy Company, Model No. 396-31). The pump was calibrated before use. A one litre measuring cylinder was used as the main oil reservoir along with a 50 cc burette for measuring the instantaneous flow rate of oil. All feed lines were 3 mm O.D.- 20 BWG, SS-316 tubes. A non-return valve was used to prevent any possibility of back flow of gas in to the oil pump. The power supply to the pump was obtained from the main control panel which was designed to cut off power to the pump in case of any emergency situation.

4.1.2 Gas Manifold

A gas manifold was constructed outside the fume hood for connecting gas cylinders of hydrogen, nitrogen and a 10% by volume mixture of

hydrogen sulfide in hydrogen. Only one gas was passed to the tube going to the reactor top at any time depending on the need. The gas line to the reactor had a micro-regulating high pressure valve to control the gas flow, a power-to-open solenoid valve, a pressure gauge and a non-return valve. The solenoid valve was used to cut off the gas flow in the event of power failure or in case of the fume hood failure. The non-return valve was used to avoid the possibility of any oil going back in the gas line as the pressure gauge and the micro-regulating valve were quite sensitive to the presense of oil in the gas stream.

4.1.3 The Reactor

The reactor was a 1 m long, 0.516 cm ID and 0.953 cm O.D. SS-316 tube (internal volume = 20.9 ml), and had high pressure end fittings. The bottom had a 3 mm outlet whereas a 6 mm tube was connected to the reactor top. Both top and bottom end tubes were provided with the high pressure quick-connectors to facilitate the frequent removal of the reactor assembly. The bottom end tube size was chosen to be 3 mm to make the size of the quick-connect fitting small enough to pass through the narrow tube in the bottom of the sand bath.

4.1.4 Sand Bath

The detailed construction of the sand bath is shown in Figure 7. It was fabricated out of a 50 mm nominal size pipe. At the top a conical hopper was welded to facilitate the filling of sand as well as to keep the sand from being blown away by sudden increase in the air flows. At

the bottom of the pipe a heater filled with Kiselguhr was added to preheat the air. Three separate heaters were used for this sand bath. The one at the bottom was for the air heater, followed by a heater for the middle of the reactor sand bath and then one for the top. These three heaters were individually controlled by the three Honeywell temperature controllers. While the thermocouples for the top two heaters were placed at the middle of of each heater length inside the sand bath, the thermocouple for the bottom air heater was placed above the porous plate.

The semi-circular heater elements were kept in their proper positions by tightening them with the metal clamps around the sand bath. The sand bath was insulated with about 40 mm of ceramic wool followed by about 25 mm of glass wool. The sand bath was designed by the author and was fabricated at the University machine shop facilities. The sand used in this sand bath was screened between 35 and 50 mesh screens. A drain was provided just above the porous plate for the sand removal.

The sand bath was tested several times for checking the uniformity of temperature inside the entire bath. After the temperature controllers were tuned to the required loads the sand bath was able to give a steady state temperatures of within 2°C inside the entire bath. The temperatures were measured with by a digital thermometer. The thermocouple probe was moved along the entire length at different radial positions.

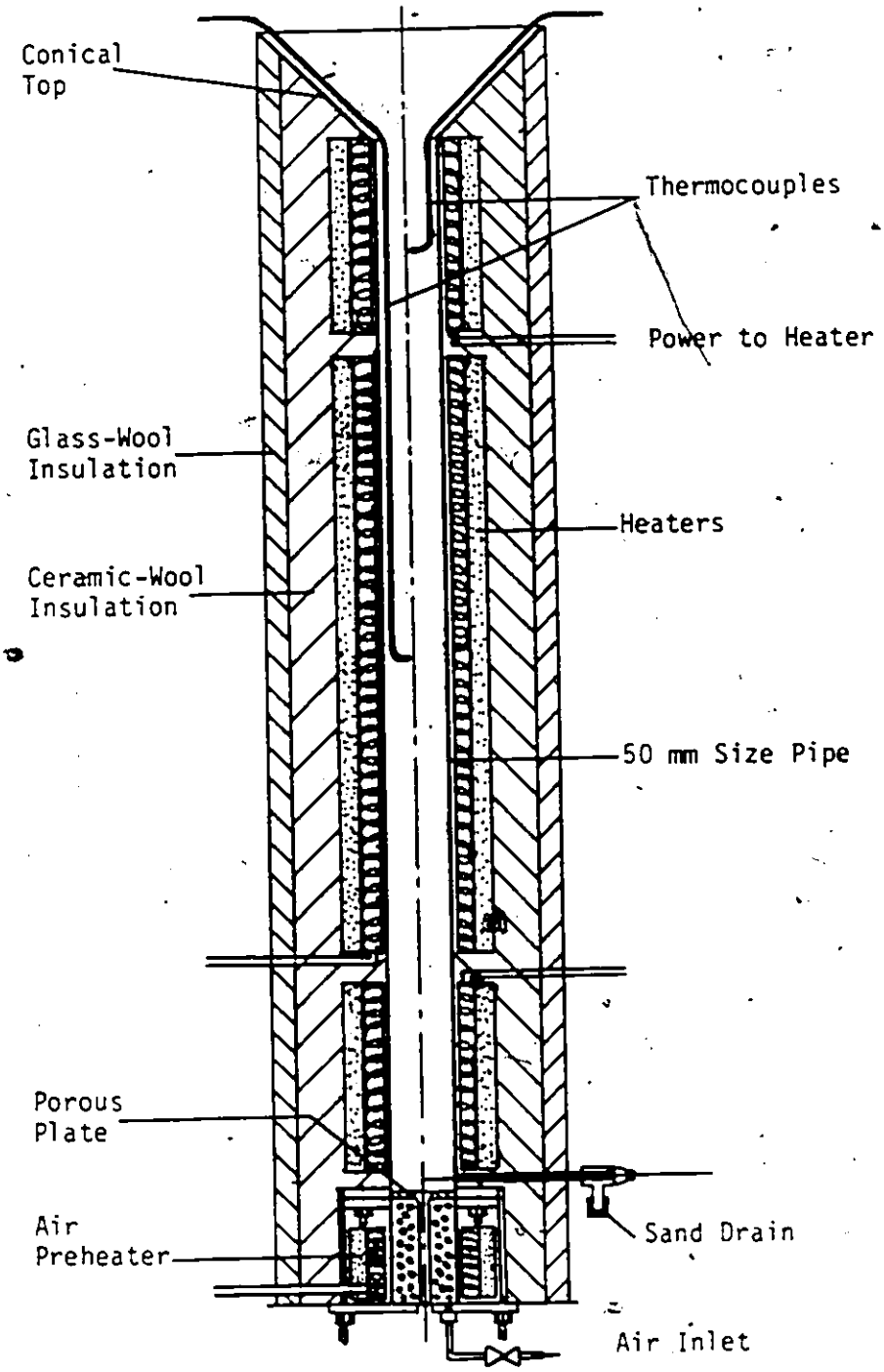

Figure 7: Details of Sand Bath

4.1.5 Oil Separation and Sampling System

The product oil and gas mixture coming from the reactor bottom was released through the back-pressure regulator into the oil separation and sampling system. This section mainly consisted of two one litre volume stainless steel separators connected in series. When samples were not being drawn, the exit stream was passed through these separators to remove the oil from outgoing gases. While the oil could then be removed from the separator bottom valve, the exit gases would pass to the hydrogen sulfide scrubber. For sample withdrawals, the first separator was bypassed and the oil was separated from the out going gases in a weighed 200 cc glass bottle. The exit gases at the time of sample withdrawals were analyzed by passing a part of the exit gas through the gas chromatograph sample loop. The exit gases returning from the gas chromatograph as well as the gases going out from the second separator were scrubbed in the hydrogen sulfide scrubber before the gas flow meter. A three way ball valve was used to shift the flow of the exit product stream between the separators and the sample bottle. This valve and the sample collection bottle were kept very close to the back pressure regulator to minimize the dead volume between the reactor exit and the sample bottle.

4.1.6 Wet Test Gas Flow Meter

A Precision Scientific wet test gas flow meter (catalogue no. 63115) was used to monitor the exit gas flow continuously. A Hewlett Packard integrator (model no.3373B) was modified and was used as a timer to get the time for each complete rotation of the wet test gas flow meter needle.

4.1.7 Gas Chromatograph

The exit gases were analyzed with a Hewlett Packard gas chromatograph (model no. 5700A) attached to an integrator (model no. 3380A). A 0.5 cc heated sample loop was used to inject the gas. 23% SP-1700 on 80/100 Chromosorb PAW packed in 1/8 inch OD stainless steel tube 30 feet long column of the Supelco company was employed. A 6 feet long 1/8 inch OD Chromosil 310 column was added in series to the above column for better separation of the hydrogen sulfide peak from the peak for normal butane. Columns were kept at an isothermal temperature of 70°C. A thermal conductivity detector at 100°C with a current of 200 mA was used. The sample loop was also kept at a constant temperature of 100°C and the carrier gas (helium) flow was 25 cc/minute. The chromatograph was calibrated using the standard gas mixtures of known compositions.

4.2 Analytical Equipment

The equipment used for the testing of the catalyst as well as the product oil samples is described very briefly in this section. Most of the equipment was of standard nature and therefore does not require any detailed description.

4.2.1 Catalyst Testing

The final catalyst particles were tested for their chemical composition, pore volume and the nitrogen adsorption surface area.

4.2.1.1 Chemical composition

The catalyst particles were ground to a fine powder (< 150 mesh size). 0.1 g of this powder was then fused with about 0.5 g of lithium metaborate powder in graphite crucible at 1000°C for ten minutes. The melt was then dissolved in 1N nitric acid. This solution was then analyzed for the amounts of silicon, aluminium, molybdenum and nickel with the help of Direct Current Argon Plasma Atomic Emission Spectrophotometery (Beckman Spectraspan-V). The gravimetric method for silicon and aluminium testing (as per Vogel's [80] text book) were also used to check the accuracy of the Atomic Emission spectrophotometeric method.

4.2.1.2 Pore Volume

Pore volume of the particles of the support material (before impregnation), and the final catalyst was measured using the carbon tetrachloride adsorption method (Benesi, Bounar and Lee [5]).

4.2.1.3 Surface Area

Nitrogen adsorption surface area was measured using a standard BET [6] method. A glass apparatus was assembled as per the details given in the Technical Bulletin [20] of the Mellon Institute of Industrial Research.

4.2.2 Analysis of Oil Samples

The original oil and the product oil samples were tested for their density, viscosity, aniline point, boiling point distribution and elemental analysis (C, N, H and S) using the methods mentioned below.

4.2.2.1 Density

Density of oil samples at 25°C was measured using a 2 cc specific-gravity bottle.

4.2.2.2 Viscosity

The kinematic viscosity at 25°C was measured using a calibrated Cannon-Fenske Routine viscometer tube No. 400.

4.2.2.3 Aniline Point

Aniline point of the oil samples was measured using the standard procedure and the equipment as per ASTM D-611.

4.2.2.4 Boiling Point Distribution

Simulated Distillation of the oil samples was carried out accordding to ASTM D-2887. A Hewlett Packard gas chromatograph model 5730A was used with a flame-ionization detector. An integrator model 3373B was modified to give the area under the chromatogram after every 2.5 minutes. For the oil samples analyzed in this work, this method was found to be sufficiently accurate. A chart recorder model 7127A was

used to get a chromatogram. 1.5% V-101 on 100/120 mesh chromosorb-G packed in 1/8 inch SS 5 feet column was used with oven temperature programming of 0°C (0 min.) - 16°C/min. - 350°C (16 min.). The temperature of the injection port and the FID detector was kept at 350°C. 1 micro litre sample was injected each time. Calibration sample No. 5080-8716 of Hewlett Packard containing normal paraffins from C_5 to C_{40} was used to get the retention times for different carbon numbers.

4.2.2.5 Elemental Analysis

Elemental analysis for C, N and H was carried out with the Elemental Analyzer model No. 240B of Perkin Elmer. Sulfur analysis was carried out by an outside laboratory using micro-analytical techniques.

Chapter V

EXPERIMENTAL PROCEDURE (PART - I)

The experimental procedure is divided in two parts. In the first part the procedure for the catalyst preparation and testing is discussed and in the second part actual testing of the prepared catalyst in the hydrotreatment trickle-bed reactor as well as the methods for the product oil sample analysis is presented.

5.1 CATALYST PREPARATION

All the catalysts used in this study were prepared by first making silica-alumina gel and mixing it with powdered zeolite material. That gel-zeolite mix was then filtered, washed and extruded through a 3/8 inch round opening. These extrusions were then dried, calcined, crushed and screened to the right size. The catalyst support particles were then tested for the pore volume and required concentration of nickel and molybdenum in the impregnation solution were calculated. An impregnation solution was prepared and the support particles were impregnated using a vacuum impregnation technique. The impregnated catalyst particles were then dried and calcined.

The catalyst particles were tested for silicon, aluminium, nickel and molybdenum concentrations and nitrogen adsorption surface area. After

getting satisfactory results from the above tests, the catalyst particles were then tested in the trickle-bed reactor. Some of the relevant details of the catalyst preparation method as well as the testing methods are described below.

5.1.1 Gel Preparation

The required amount of aluminium nitrate was dissolved in distilled water in a 4 litre beaker fitted with a stirrer and a pH meter. The appropriate amount of sodium silicate was weighed and slowly added to the aluminium nitrate solution. Ammonium hydroxide was then added from a burette to the well stirred contents of the beaker to bring the pH to a neutral level. Silicon and aluminium, thus precipitate out as respective hydroxides in form of a white gel. The beaker was filled to the top with distilled water. The gel was left to settle as well as to age for a period of about one day.

The clear liquid above the settled gel was decanted and the required amount of Zeolite powder (Type-Y Zeolite, rare earth exchanged, 38 to 53 micron size powder supplied by Sterm Chemical company) was added to the gel. The contents of the beaker were stirred thoroughly to disperse the powder uniformly.

5.1.2 Filtration and Washing

The above gel-powder mixture was filtered in two 18.5 cm vacuum-filter funnels. The gel-powder mixture was equally divided in the two funnels

and the resulting filter cake was washed three times with a 2% by weight solution of ammonium acetate. About 1.3 litre of solution was used for each washing. Care was taken not to let the filter cakes dry during filtration and washing. After three successive washes, the filter cake was allowed to stay in the funnels letting the air run through the cakes. This was continued until no more water drops were coming down from the filtration funnels.

5.1.3 Extrusion and Drying

The filter cakes from both the filtration funnels were removed and placed on a plate and were mixed by a stainless steel spatula to make a uniform extrudeable paste. The paste was then pressed through a 3/8 inch round hole dye of an extruder and the extrusions were spread over glass plates for drying. The extrusions were dried for a period of one day in air and then dried in an oven at 60°C for a period of 3 to 6 hours depending on the water contents of the extrusions.

5.1.4 Calcination

Partially dried extrusions were then transferred to a crucible and kept in a muffle furnace at 700°C. This calcination was carried out for a period of 5 to 6 hours. The calcined extrusions were cooled and stored in a glass desiccator.

5.1.5 Size Reduction

The calcined extrusions had good mechanical strength and were crushed using a 160 mm O.D. size porcelain mortar and pestle. The extrusions were not crushed to the desired size at one time. The crushing was carried out in stages. The desired size of the particles was between 70 and 80 mesh. Therefore, the screens were stacked starting with a 18 mesh at the top followed by 50, 60, 70, and then 80 mesh screen at the bottom. Initially, the crushed material was put on the top (18 mesh) screen and the screening was done for a period of 15 minutes. After this the material left on the top screen was taken out, further crushed and was put back on same screen. Again the screens were shaken for 15 minutes. This process was repeated till no material was left on the top screen. The top screen was then removed and the material on the next screen was crushed and screened in the same manner. This was done until no material was left on that screen.

The crushing and screening sequence was continued until almost no material was left on the 70 mesh screen. The crushed particles retained on the 80 mesh screen were then collected and stored in glass bottles for pore volume measurements and vacuum impregnation. This technique of crushing and screening sequence was found to be most efficient in getting the maximum amounts of the desired size particles.

5.1.6 Pore Volume Measurement

The pore volume of the catalyst support particles was measured using the carbon tetrachloride adsorption technique of Benesi et.al. [5]. In a 16 cm diameter glass desiccator 27.5cc of n-hexadecane and 182.5cc of carbon tetrachloride was added and was thoroughly mixed. About 1 to 2 g of the dry catalyst support particles were weighed in a 5 cc narrow neck measuring bottle with a hexagonal base. It was kept in the desiccator and was then evacuated using a vacuum pump. An ice trap was used for condensing carbon tetrachloride vapors. The pump was run till about 10 cc of carbon tetrachloride was collected in the cold trap. The desiccator was then isolated and left for a period of at least 4 hours for an equilibrium to be reached. Subsequently the desiccater was opened and the bottle containing the catalyst support particles was immediately closed with a stopper. The bottle was then weighed. The difference in weights gave the amount of carbon tetrachloride condensed in the catalyst pores and on the bottle walls.

The above procedure was repeated with the empty bottle to find the amount of carbon tetrachloride adsorbed on the sides of the sample bottle. Appropriate amounts of carbon tetrachloride were added to the desiccater to keep the concentration of the two components at initial levels. The concentration of the mixture in the desiccater was checked by measuring the refractive index. The weight of carbon tetrachloride adsorbed in the catalyst pores was then divided by its density and the weight of dry sample to get the pore volume per unit weight of the support particles.

5.1.7 Impregnation

The concentrations of nickel nitrate and ammonium molybdate required to get the desired amounts of these compounds into the pores of a support material of known pore volume was estimated. Sufficient quantity of impregnation solution to immerse the entire amount of the support particles was prepared (details in Appendix).

A special twin flask was made from two 500 ml conical flasks to quickly drop the entire amount of the catalyst support particles in the impregnation solution under vacuum. That special flask was supported on a stand that allowed rotation of the flask in such a way that the evacuated catalyst particles could be dropped from one section of the flask to the other. Figure 8 shows the details of the arrangement.

The catalyst support particles dried at 110°C for at least 3 hours were taken in the part A of the impregnation flask. The flask was then connected to a vacuum pump and the catalyst support particles were evacuated to a vacuum of 0.2 mm Hg to remove all the gas from the pores. The vacuum valve was then closed and the impregnation solution was slowly introduced in part B of the flask taking care not to let any air in or to splash the solution on to the catalyst support particles. The flask was then turned to drop all the catalyst support particles into the impregnation solution. Once all the particles were immersed in the solution air was slowly introduced into the flask to bring it to the atmospheric pressure. The particles were then allowed to reach equilibrium for about 15 minutes. The particles and the solution

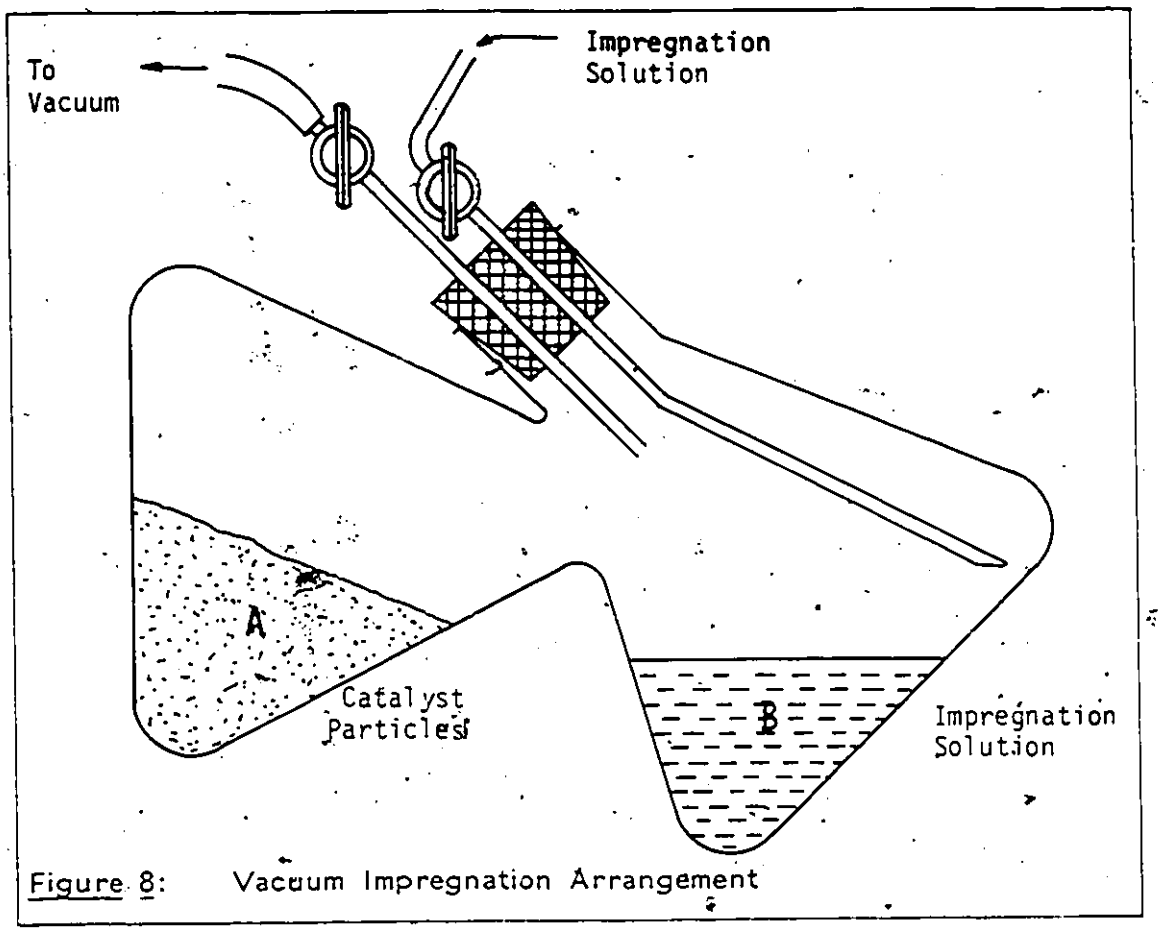

Figure 8: Vacuum Impregnation Arrangement

slurry was then transferred to a coarse sintered glass filter funnel and the solution separated from the particles. The impregnated particles were dried and calcined at 700°C for about six hours.

5.1.8 Analysis of Chemical Composition

The concentrations of silicon, aluminium, nickel and molybdenum were analyzed using the D.C. Argon Plasma Atomic Emission Spectrophotometer. Approximately 0.1 g of the powdered catalyst was weighed in a graphite crucible and about 0.5 g of lithium metaborate was added to it. The crucible was covered with a graphite lid and was then kept in a muffle furnace at 1000°C for about 10 minutes. 75 ml of

1N-nitric acid was placed in a 400 ml beaker kept on a magnetic stirrer. The red hot crucible was taken out from the furnace and the lid was removed. The melted bead of the fused mass was carefully dropped into the nitric acid. The content of the beaker were kept well stirred till all the melt was dissolved. That solution was then transferred to a 100 ml measuring flask and the volume was made up to the graduation mark. The solution was stored in a plastic bottle.

A Beckman Spectraspan-V was used to analyze the solution prepared above. Standard solutions were prepared in 1N-nitric acid using the available standards for the four elements to be analyzed for the calibration of the equipment. Blank solutions were prepared by fusing 0.5 g of the lithium metaborate with no catalyst powder. These blank solutions gave zero reading of emission levels for each of the elements. Three readings were taken for each element and an average was obtained. The weight of each element was calculated from the volume of solution and the weight of the catalyst powder used. The % by wt. of silica, alumina, nickel oxide and molybdenum oxide were then determined.

The concentrations of silicon and aluminium were also checked using the gravimetric method given in Vogel's [80] book. The catalyst particles were fused in sodium hydroxide in a nickel crucible and then dissolved in distilled water. The same solution was used for both the tests. The agreement between gravimetric methods and the Atomic Emission Spectrophotometery method was quite good. Therefore the gravimetric methods were used only for the first few catalysts.

5.1.9 BET Surface Area

The glass equipment for the measurement of surface area was assembled as described in the 'Technical Bulletin' [20] of the Mellon Institute. The surface area measurements were carried out as described in that bulletin.

After checking and correcting for all vacuum leaks the volumes of the glass burets were calibrated by weighing the amount of mercury required to fill the glass bulbs. Bulb factors were then calculated. 1 to 2 g of the catalyst particles were taken in the sample tube and degassed at 200°C for about three hours. Dead space factor was calculated by using helium gas. Three to five points were obtained on the nitrogen adsorption isotherm up to a nitrogen pressure of about 0.4 atmosphere.

A computer program was written using least-squares method for fitting a straight line through the points of the adsorption data. The program is given in the Appendix. The values of the slope and the intercept of the straight line was calculated from which the surface area was determined. The results were found to be quite reproducible.

5.1.10 SEM Imaging and Energy-Dispersive X-Ray Analysis

Catalyst samples for scanning-electron microscope x-ray dot maps were mounted in epoxy-resin and were polished in oil.

Chapter VI

EXPERIMENTAL PROCEDURE (PART - II)

6.1 CATALYTIC HYDROTREATMENT

After various characteristics of the catalyst were satisfactory, it was placed in the reactor to determine its performance. In this section, catalyst filling in the trickle-bed reactor, sulfiding and activation, hydrotreatment and sample withdrawal are described. This is followed by the gas analysis of the reactor exit gases and the analysis of the oil samples.

6.1.1 Reactor Filling With Catalyst

The reactor was 1 m in length and had a volume of 20.9 ml. The volume of catalyst used for each test was 8 ml. The catalyst particles were between 70 and 80 mesh size. The catalyst was diluted with equal volume of α-alumina of the same size. Catalyst volume was measured by packing it to the 8 ml mark in a 10 ml glass measuring cylinder. The cylinder was kept on a vibrator to get the maximum packing. The packed cylinder was also weighed to get the bulk density of the catalyst. The volume of α-alumina was also measured in the same way. The catalyst particles and the alfa-alumina particles were thoroughly mixed in a 200 ml glass bottle to get a uniform mixture.

The reactor was also packed using a vibrator. A 5 cm long, very tightly rolled roll of 60 mesh stainless steel screen was first inserted in the reactor tube at the bottom. This was found to be quite adequate to prevent the catalyst particles from being carried away with the reactor effluent. The tube was then held vertically in a stand. A vibrator was attached at the bottom. The catalyst-alumina mixture was slowly poured in to the top end of the tube. 16 ml of the mixture filled 76.9 cm of the reactor tube. The top portion of the tube was then filled with the same size α-alumina. A 1 cm long plug of a quartz wool was then placed at the top end of the reactor tube. The reactor high-pressure end fittings were then secured at the ends and the reactor was lowered into the sand bath.

6.1.2 Sulfiding and Activation

After connecting the reactor at the top and bottom to the quick-connectors, the complete system was pressurized to 1500 psig with nitrogen to check for leaks. The gas was then released and the reactor system was brought to atmospheric pressure. The flow of 10 mole % mixture of hydrogen sulfide in hydrogen (of Matheson Co.) was started through the reactor at a pressure of 50 psig. The sand bath was filled with sand and heating was started. The temperature was set at 350° C for sulfiding. The temperature reached the set value in about one hour period and sulfiding of the catalyst was carried at those conditions for 4 hours. Hydrogen was then passed through the reactor at the same conditions for 30 minutes.

6.1.3 Hydrotreatment

After the sulfiding was completed, the sand was taken out of the sand bath and the reactor was allowed to cool to a temperature below 150°C as it was not advisable to pass the oil on hot dry catalyst. The pump was then started and the feed oil was pumped into the reactor. Hydrogen continued flowing through the reactor.

Pumping of oil was then started. 10 ml of the oil was passed through the reactor before setting the actual operating conditions. This was found sufficient to wet all the catalyst particles. The back-pressure regulator was pressurized to the desired hydrotreatment pressure and the pressure of the hydrogen cylinder regulator was also adjusted accordingly. The flow of the hydrogen was adjusted with the micro-regulating valve. The sand was put back into the sand bath and heating was resumed. The hydrotreatment temperature was set at the desired value.

It took about 90 minutes for the reactor system to reach a steady state. During normal runs the reactor effluent was passed through the first one litre separator. The exit gases were scrubbed in the hydrogen sulfide scrubber and later passed through the wet-test-flow meter. The integrator, connected to the wet-test-flow meter, gave a continuous record of the gas flow rates. The gas flow rates remained fairly constant over the entire run although slight decrease in the gas flow rate was observed.

6.1.4 Sample Withdrawal

A 200 ml glass bottle was weighed and attached at the sample collection point. The reactor effluent flow was shifted to the sample bottle using the three-way valve for withdrawing the oil sample. The oil was separated from the gases in the sample bottle and a part of the gas stream was sent to the gas chromatograph for analysis. The rest of the gas stream along with the return gas from the gas chromatograph was then scrubbed in the hydrogen sulfide scrubber containing a 20 wt.% solution of KOH. The gas flow of the effluent gases was continuously monitored by the wet-test-flow meter. The sample collection and the gas analysis was continued till the required amount (e.g. amount sufficient for further oil analysis) of oil was collected.

6.1.5 Gas Analysis

The details of the gas chromatograph and accessories used to analyze the reactor effluent gases has already been described in the previous chapter. A portion of the gas going out of the sample bottle was continuously passed through a heated 0.5 cc sample volume. When the gas was to be analyzed, the gas was injected into the gas chromatograph by flipping the sample valve. A typical chromatogram obtained during the analysis is shown in Figure 9. Areas under various peaks were given by the integrator. These areas were then converted to the number of moles of the corresponding pure gas components using the calibration curves for each gas. Hydrogen was calculated by difference. Subsequently the molar % of each of the component was estimated.

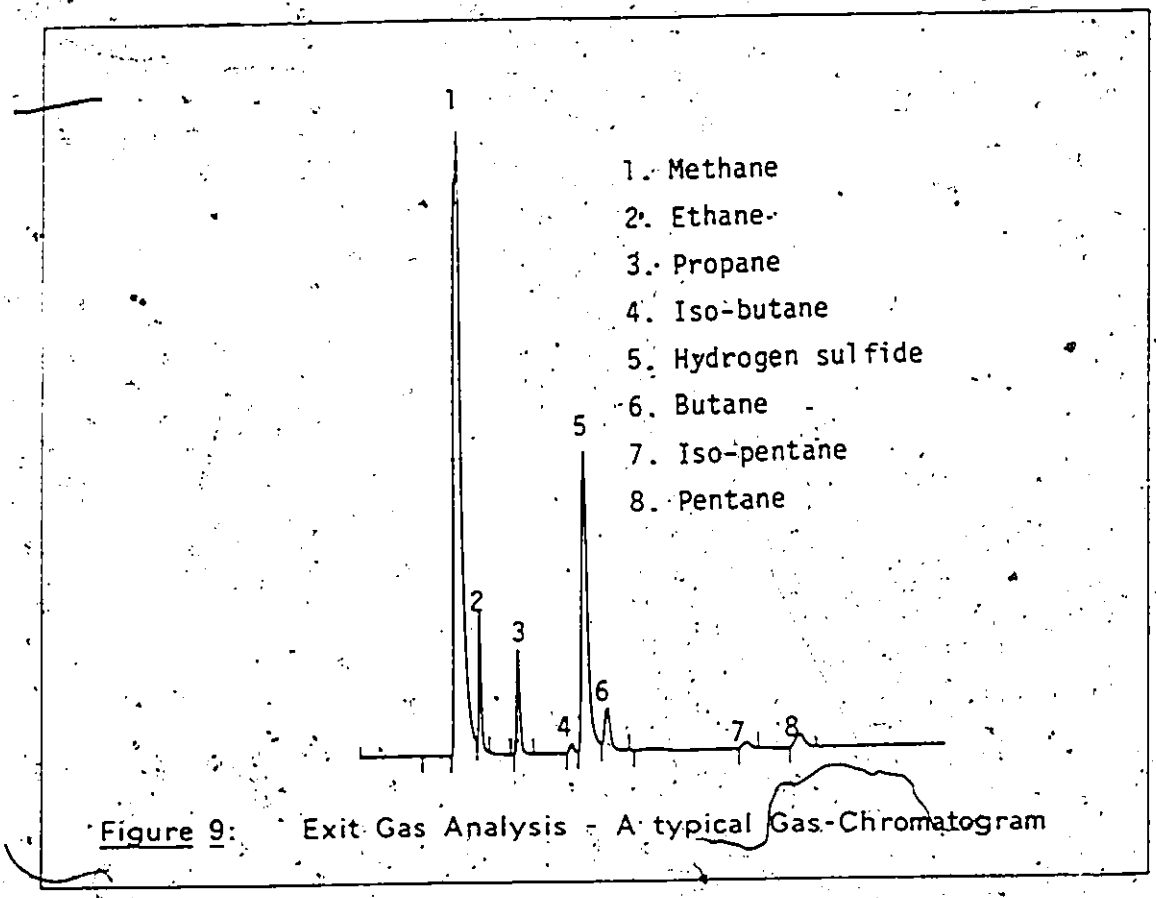

Figure 9: Exit Gas Analysis - A typical Gas-Chromatogram

The gas chromatograph was calibrated using a standard mixture of known composition and three different sizes of the sample loops (i.e. 0.125 cc, 0.5 cc and 1.0 cc). Areas under the different peaks were plotted against the absolute amounts of the gas components and the points were connected by the straight lines. These were used for analysis of exit gas.

6.1.6 Shut-Down

During the shut-down of the hydrotreatment system, care was taken not to let the catalyst run dry under hot conditions. This was to prevent any excess formation of coke on the catalyst. The excess coke formation

during the start-up periods would have resulted in the premature deactivation of the catalyst. The purpose of avoiding the excess coke build-up during the shut-down was to get accurate data on the coking property of the catalyst.

The heating was first stopped and all the sand was withdrawn from the sand bath. Air was blown into the sand bath to facilitate cooling of the sand-bath. The oil pump as well as the hydrogen flow through the reactor were not interrupted until the temperature inside the reactor was less than 100°C. At that time the pump was stopped and the reactor was depressurized slowly by reducing the pressure on the back-pressure-regulator and the hydrogen pressure regulator simultaneously. The hydrogen gas cylinder valve was then closed and nitrogen valve was opened. This was done to flush out all hydrogen from the reactor system before taking the reactor apart.

A mixture of 25% by volume of benzene and acetone was used as a cleaning solution to remove all the oil from inside of the reactor. This solution was passed through the catalyst bed several times till clear liquid was seen coming out of the reactor. Nitrogen was purged through the reactor to dry out the catalyst. The reactor was then taken out of the sand-bath, opened and the catalyst and α-alumina particles were removed and collected.

6.1.7 Analysis of Oil Samples

Physical properties (i.e. density and viscosity), Aniline point, Boiling-Point distribution, and elemental analysis (i.e. N, C, H and S) of the original oil and oil samples from hydrotreatment experiment were determined.

6.1.7.1 Density and Viscosity

Density of the oil samples was measured by a 2 ml specific-gravity bottle. The oil sample at 25°C was introduced into the bottle and the bottle was wiped clean from the outside. The bottle was weighed and the density was determined from the weight of the oil in the bottle.

Viscosity was measured using the Cannon-Fenske type calibrated viscometer tube No. 400. A constant temperature bath was used to keep the viscometer tube at 25°C. 6.7 ml of the oil was placed in the viscometer tube and was allowed to attain the temperature of the bath. The oil was then sucked to just above the upper etched mark on the tube and the time was noted for the oil level to pass through the two etched markings on the viscometer tube. The measurement was repeated four times and the average value of the viscosity was calculated.

6.1.7.2 Aniline Point

The aniline-point of the oil was determined according to ASTM D-611. The aniline was first contacted with sodium hydroxide pellets in a glass

bottle and kept overnight to remove the moisture. Aniline was then distilled under vacuum in a rotary evaporator. The first 10% of the distillate was discarded. The distillation was stopped when last 10% of the aniline remained in the distillation flask. The distillate was stored in an opaque glass bottle under nitrogen atmosphere.

The aniline-point apparatus was assembled as per ASTM D-611. 10 ml of the oil and 10 ml of the aniline were used for each measurement. Both aniline and oil were poured into the inner test-tube and the contents were kept well stirred. Heating was started and the temperature was noted when a clear liquid appeared in the test-tube. The test tube was cooled and the above procedure was repeated till three reproducible readings were obtained. This temperature was the aniline-point for the oil sample.

6.1.7.3 Boiling Point Distribution

The Simulated Distillation technique as per ASTM D-2887 was used to determine the boiling-point distribution of the oil samples. The equipment used for this has been described in the chapter "EXPERIMENTAL EQUIPMENT". The gas-chromatographic column was conditioned at 350°C overnight. The injection-port and the detector temperatures were kept at 350°C and the Flame-Ionization Detector (FID) was lit. The oven temperature programming was set for 0°C (0 min.) - 16°C/min. - 350°C (16 min.). A blank run was taken to check if the column performance was satisfactory. 1 micro-litre of the standard sample (Hewlett-Packard No. 5080-8716, containing C_5 to

C_{40} normal paraffins) was injected and the retention times for various carbon-numbers were noted. A typical chromatogram obtained with the standard sample is shown in Figure 10.

In Figure 11 a smooth curve is drawn through the points obtained from the standard sample. 1 µl of each sample was injected, the chromatogram (as shown in Figure 12) and the area under the curve at every 2.5 minute time interval was measured. This area was correlated with the boiling-points at various retention times. The boiling-point distribution curve was generated. A computer program was written for these repetitive calculations and is given in the appendix. A typical boiling-point distribution curve is shown in Figure 13.

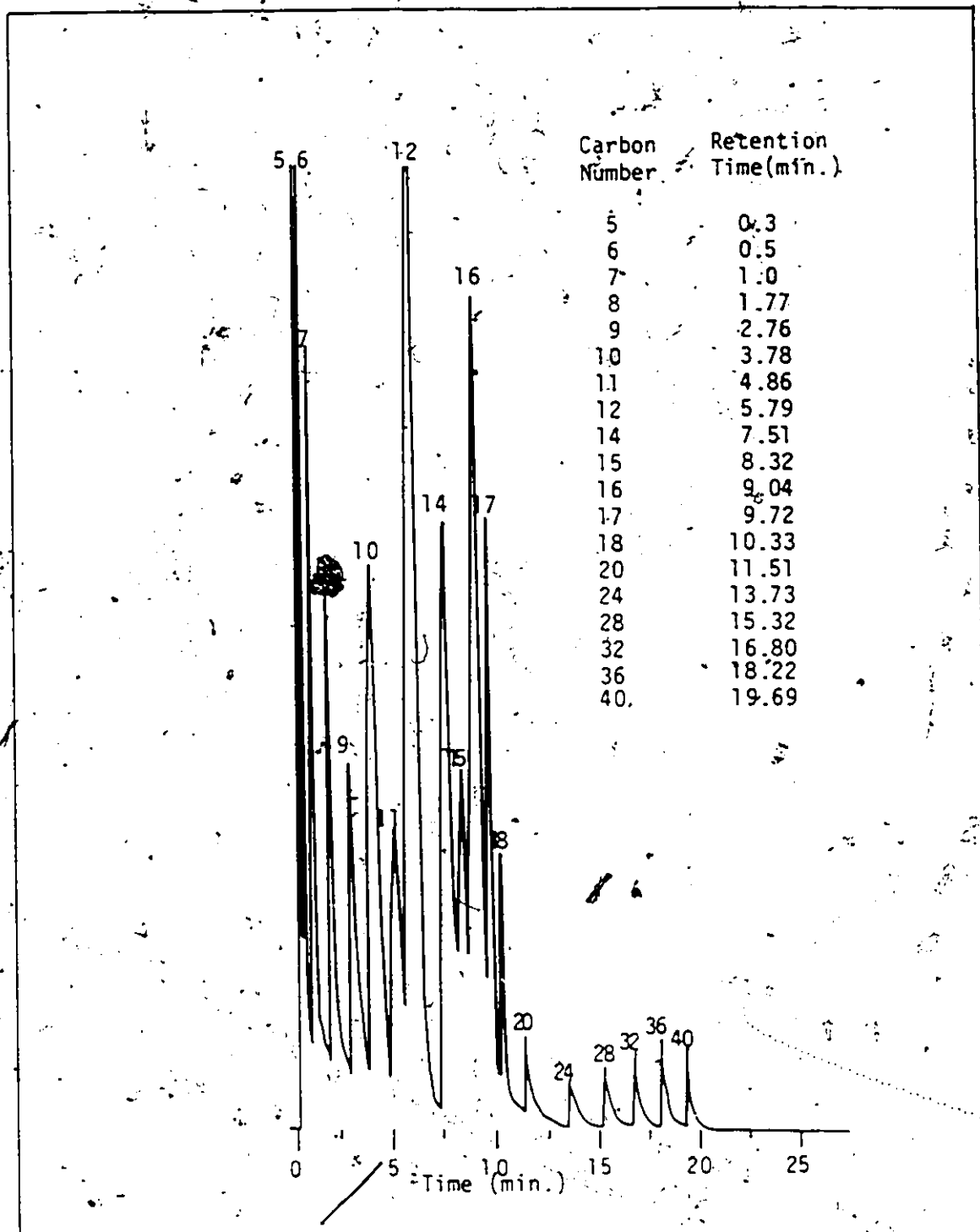

Figure 10: Simulated-Distillation (Standard Sample) This Figure shows the retention times for different carbon-numbers.

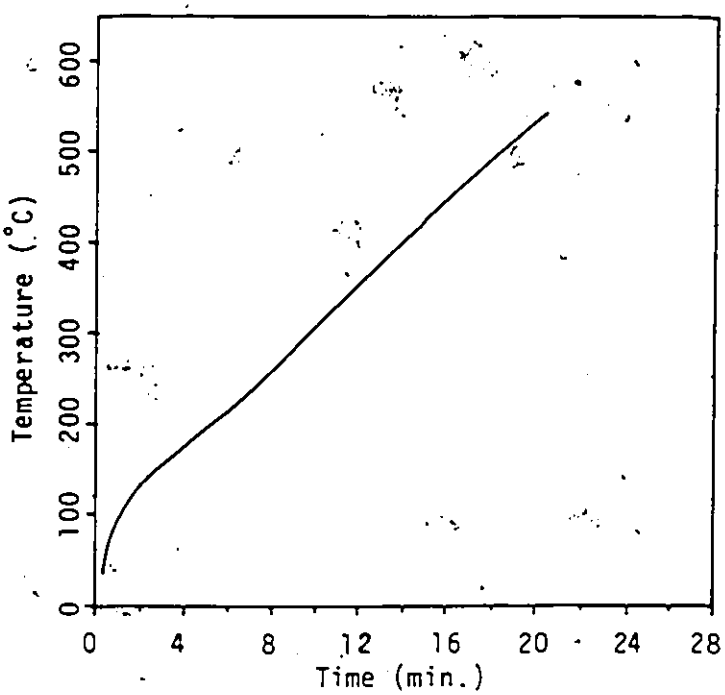

Figure 11: Boiling Point vs Retention Time

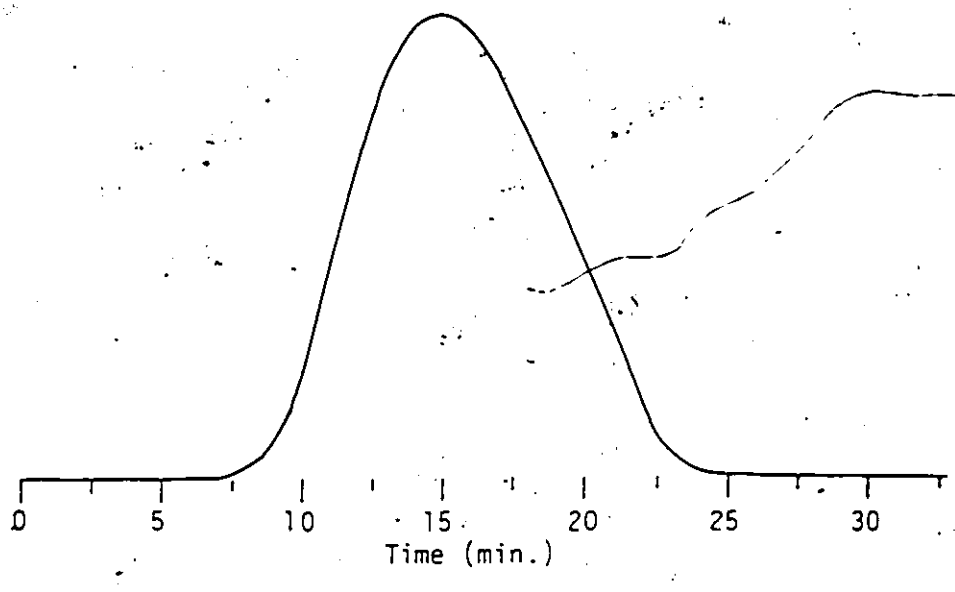

Figure 12: Simulated Distillation Chromatogram of Oil SAmple

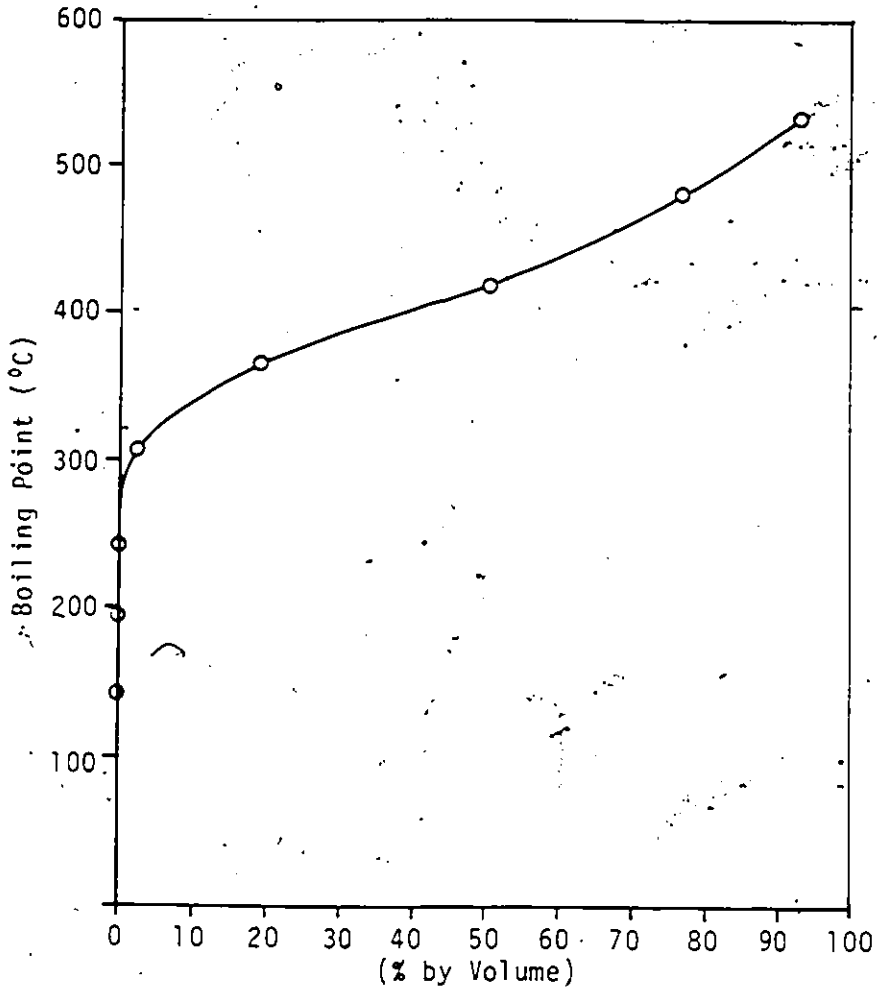

Figure 13: Simulated Distillation - Boiling Point Distribution Curve

6.1.7.4 Elemental Analysis

The analysis of oil samples for the determination of amounts of carbon, nitrogen and hydrogen was carried out with a Perkin Elmer Elemental Analyzer Model No. 240B. Since maximum nitrogen in the oil samples

was only 0.49% (by wt.) there was a need to make a standard for calibration of the nitrogen factor K_N. Since no pure compound was available with such a low Nitrogen concentration, appropriate amount of diphenylamine was dissolved in benzene. It was then dissolved in the desired amount of squalane ($C_{30}H_{62}$). The amounts of the three components were adjusted to get a final mixture containing 0.5 % (by wt.) of nitrogen. This was used as a standard to find the nitrogen factor for the machine. The carbon and hydrogen factors (i.e. K_C and K_H) were evaluated using acetanilide as a standard.

After the K-factors were determined, the oil samples were analyzed by weighing about 1.3 µl of oil in an aluminium capsule. The capsule was sealed, kept in a nickel shell and was then loaded on the combustion ladel. The ladel was inserted in to the combustion tube of the machine and the program was started. The analysis of the sample from this point onwards was automatic except for pushing the ladel into the combustion zone and bringing it back. The magnitude of the signals from the three detectors were recorded with a chart recorder. The values were read form the chart and corresponding amounts of the three elements were calculated using the K-factors. Three tests were made for each sample and the mean value was reported. The sulfur analysis was performed at an outside laboratory.

Chapter VII

RESULTS AND DISCUSSION

Ample evidence is available in the literature concerning the use of zeolite mixed with amorphous silica-alumina supports for cracking applications. There are not much data available on its use for hydrotreating applications. Therefore, before carrying out any detailed experimental work it was thought fit to evaluate the potential of such a mixed support material in the hydrotreating of the heavy gas oil. The following three catalysts were prepared.

1. Cat. No. 1-1 : 14.5% zeolite and 85.5% alumina with no active metal:
2. Cat. No. 1-2 : 14.5% zeolite plus equal parts of silica and alumina (i.e. 42.2% silica and 42.2% alumina) with no active metal.
3. Cat. No. 1-3 : zeolite, silica and alumina as in Cat. No. 1-2 but impregnated with 4.7% MoO_3 and 1.65% NiO.

These three catalysts were first tested to determine their performance for the removal of nitrogen and sulfur from the heavy gas oil. The results obtained and the test conditions are given in Table 6.

Table 6: Comparison of silica-alumina-zeolite and alumina-zeolite support.

Operating conditions were: Temperature = 425°C, Pressure = 1000 psig; LHSV = 1.5; and H_2 flow = 0.36 st.l/ml (2000scf/bbl)

Catalyst No.	%HDS	%HDN	Mid-Boiling Point(°C)
1-1	62.2	40.0	392.5
1-2	78.0	48.3	379.3
1-3	91.1	59.0	390.5
Ni-Mo[1]	86.2	61.4	307.0
Ni-Mo[2]	70.0	35.0	

As can be seen from Table 6, catalyst 1-3 gave the best performance. The best commercial catalyst was Ni-Mo[1,2] on gamma-alumina. A comparison of the catalyst performance of Cat. No. 1-1 and 1-2 confirmed the positive effect of the presence of silica in the support material. Based on these preliminary results there was no doubt that a catalyst much superior to the commercial hydrotreating catalyst could be prepared by using zeolite powder along with a suitable mixture of silica-alumina base.

Catalysts of different compositions were prepared by changing the silica and the zeolite concentrations. The compositions were varied as per a central-composite design [10] to get maximum information with the minimum number of trials. Analysis of the data obtained led to an optimum composition for the catalyst.

[1] Tested at 450°C, 1000 psig pressure and LHSV = 1.25 in the previous work [57].

[2] Data interpolated at 425°C, 1000 psig pressure and LHSV = 1.5.

In the last part of this study, a kinetic study of the catalyst prepared with the optimum composition was taken up. In the presentation that follows, the results are presented in the same sequence.

7.1 LOCATION OF OPTIMUM OPERATING POINT

The choice of an operating point is very crucial for testing a hydrotreatment catalyst. Four operating variables are important, namely, temperature, pressure, liquid and gas flow rates. The criteria on which the performance of a given catalyst could be judged are also numerous. Some of these criteria could be hydrodesulfurization (HDS), hydrodenitrogenation (HDN), hydrodeoxygenation (HDO), removal of metallic impurities, density, viscosity, aniline-point, cetane-index, diesel-index, mid-boiling-point, C/H ratio etc... etc.... A desired criteria could be any of the ones listed above or a combination of two or more individual performance criteria depending upon the final product requirements.

A given catalyst may give best results for one of the above criteria but it may not be as good in other aspects. Similarly the choice of a particular set of operating conditions is not expected to give the best results for all criteria for a given catalyst. Therefore, in our study the next step was to evaluate the operating region for finding an optimum operating point for testing different catalysts.

The operating region for hydrotreatment (as described in section 7.1.1.1) is quite large and to explore the entire region with a standard method of grid search would have involved very large number of experiments. Therefore, modern statistical experimental designs were used to explore the entire operating region to get response surfaces for different performance criterion, i.e. a mathematical representation of a performance criterion within the defined region.

7.1.1 Experimental Design

An adequate description of all the response surfaces by simple first order models was not expected and thus only experimental designs with at least three levels of each operating variable were considered. A full 3-level factorial design with four operating variables requiring 81 experiments was judged excessive and wasteful with respect to experimental effort. However, an incomplete 3-level factorial design [9] which involves only 27 runs yields enough information of interest and was therefore employed in this work. The application and analysis of such an experimental design are exemplified particularly well by Bacon [3]. The information of interest was specifically the set of estimates of the parameters in the following second degree polynomial representation of each response surface :

$$E(y_i) = \beta_0+\beta_1x_1+\beta_2x_2+\beta_3x_3+\beta_4x_4+ \beta_{12}x_1x_2+\beta_{13}x_1x_3+\beta_{14}x_1x_4+\beta_{23}x_2x_3+\beta_{24}x_2x_4+ \beta_{34}x_3x_4+\beta_{11}x_1^2+\beta_{22}x_2^2+\beta_{33}x_3^2+\beta_{44}x_4^2 \quad (18)$$

where $i = 1, 2, 3, \ldots$ indicate a particular performance criterion, $E(y_i)$ is the expected value of the i'th performance criterion (e.g. nitrogen removal) and x_1, x_2, x_3 and x_4 are the four operating variables in the appropriate coded forms. The coding used for this study is given in Table 7.

7.1.1.1 Operating Region

The boundaries of the operating region for this type of work are very well defined ([24], [34] and other hydroprocessing literature). The particular heavy gas oil used in this study was the same as used earlier (Sambi [57]). The results of this study formed the basis of choosing the appropriate set of conditions for the above experimental design.

Table 7: Coding of The Operating Variables.

x_1 = [Temperature (°C) - 375]/50

x_2 = [Pressure (psig)-1000]/500

x_3 = [(LHSV) - 2.0]/1.0

x_4 = [Gas Flow Rate (st. l/hr.) - 150]/100

3-Levels of Operating Variables :-

Coded Value	Temperature (°C)	Pressure (psig)	Liquid-Flow (LHSV)	Gas-Flow (St.l/hr)
-1	325	500	1.0	50
0	375	1000	2.0	150
1	425	1500	3.0	250

The empirical models of the type given in Eqn. (1) are generally valid only within or very close to the operating region. The choice of too small a region will limit the range of applicability and therefore the usefulness of the model. It can also lead to difficulties in detecting the effects of the operating variables relative to the experimental errors. On the other hand, use of too large an operating region may lead to inadequate and thus unreliable description of the system within the operating region. Considering the above mentioned factors, the choice of the operating region was made. The operating region was a hypercube defined by the following limits :

$$325°C \leq \text{Temperature} \leq 425°C$$

$$500 \text{ psig} \leq \text{Pressure} \leq 1500 \text{ psig}$$

$$1.0 \leq \text{Liquid Hourly Space Velocity (LHSV)} \leq 3.0$$

$$50 \text{ st. l/hr.} \leq \text{Gas Flow Rate} \leq 250 \text{ st. l/hr.}$$

7.1.1.2 Randomization of the Experimental Runs

The order of execution of the runs should ideally be randomized in order to ensure the valid interpretation of the experimental results and the model. One attempts to spread the effect of any extraneous source of variation equally over all the results by randomization, thereby avoiding the confounding of the operating variables of interest with these extraneous variables. However, complete randomization was not experimentally expedient for this work. Especially changing the temperature of hydrotreatment was very time consuming and so all the

runs at each temperature were generally carried out in succession. The order of execution within each block was randomized. The three replicate runs at the centre of the operating region were purposely executed at the beginning, middle and end of the experimental program so as to evaluate any possible time effects (e.g. catalyst deactivation).

7.1.2 Analysis of Results of Experimental Design

The results obtained from the experiments are given in Table 8. It should be noted that the 27-run Box-Behnken design was augmented by one additional run at the centre point to allow for more complete checking of the catalyst decay.

7.1.2.1 Model Building

The models described by Eqn. (1) were fitted to the experimental results by linear least squares technique. The fitted models were examined for lack of fit by means of residual plots and internal lack of fit test as given in Draper and Smith [16]. In general, not all the terms in a full second degree polynomial were required to provide an adequate description of the data (as indicated by the 95% confidence intervals for the parameter estimates) and some simplification of the model form was desirable. Because of the partial orthogonality of this design, the significance of any of the individual terms involving β_1, β_2, β_3, β_4, β_{12}, β_{13}, β_{14}, β_{23}, β_{24}, or β_{34} may be judged independently and deletion of any of these will leave other parameter estimates unchanged. Deletion of any of the terms

involving β_0, β_{11}, β_{22}, β_{33} or β_{44} may be carried more carefully and will result in changes in the remaining parameters in this group since they are correlated with one another. The extent of these correlations were small and the confidence intervals still provided useful guidelines as to the significance of these terms.

Normalization of Response Variables: For this analysis and for the subsequent modelling, the observed catalyst performance criteria were scaled to have values in the range -1.0 to 1.0 using the following linear relationship :

$$Y_i = (2.y_i - \text{range})/(\text{range}) \quad \text{where,}$$

range = Maximum value of y_i - Minimum value of y_i

This allowed for easier comparison of the effects of catalyst decay relative to the effects of the operating variables. Also, this facilitated the comparison of the effects of the operating variables from one criterion to another.

Activity Decay During Experimentation:

Plots of the scaled performance criteria for the repeated runs are shown in Figure 14 as a function of time on stream. These results demonstrated that over the period of this experimentation the effect of catalyst decay on various performance criteria were small relative to the effects of the operating conditions. Therefore, catalyst decay was neglected in the subsequent analysis of the response surfaces. Results for Cetane Index and Diesel Index were not plotted since they are already reflected in the Density, Aniline Point and Mid-Boiling Point

Table 8: Results of 3-Level Fractional Factorial Design

x_1	x_2	x_3	x_4	Run Number	Density (g/cm^3)	Viscosity (cp)	Mid-Boiling Point (°C)	Aniline Point (°C)	C/H Ratio	Sulfur Removed (wt%)	Nitrogen Removed (wt%)	Cetane Index	Diesel Index
-1	-1	0	0	18	0.978	206	422	47.0	0.65	20.8	45.3	39.0	15.4
1	-1	0	0	33	0.944	68	380	51.2	0.66	78.5	49.6	41.6	22.9
-1	1	0	0	14	0.973	178	422	48.2	0.64	34.9	40.7	40.5	16.5
1	1	0	0	23	0.934	56	400	55.2	0.62	86.2	63.6	48.6	26.3
0	0	-1	-1	4	0.945	72	408	53.6	0.63	74.9	53.4	46.5	23.5
0	0	1	-1	5	0.963	133	418	52.1	0.64	41.0	46.3	42.6	19.4
0	0	-1	1	6	0.949	90	409	51.0	0.63	73.7	51.2	45.5	21.9
0	0	1	1	7	0.959	119	412	50.4	0.64	60.2	46.4	42.9	19.8
-1	0	0	1	22	0.974	206	424	47.1	0.65	22.6	41.8	40.4	16.1
1	0	0	-1	24	0.938	54	397	55.2	0.62	82.0	58.9	46.6	25.4
-1	0	0	1	21	0.973	189	423	47.9	0.65	27.2	38.9	40.6	16.5
1	0	0	1	25	0.936	57	392	52.9	0.62	89.0	55.2	46.6	25.1
0	-1	-1	0	16	0.956	105	409	51.4	0.64	66.4	43.5	34.4	20.7
0	1	-1	0	12	0.944	83	402	54.7	0.62	80.4	53.3	45.8	24.1
0	-1	1	0	17	0.967	152	415	49.2	0.64	44.7	43.0	41.1	17.9
0	1	1	0	13	0.959	128	416	51.4	0.63	54.4	42.0	43.6	20.1
1	0	-1	0	19	0.964	171	421	48.6	0.65	37.3	39.8	42.8	18.2
1	0	-1	0	26	0.926	36	384	53.3	0.61	92.1	66.3	48.0	27.2
-1	0	1	0	20	0.972	208	427	47.2	0.65	21.4	39.4	41.5	16.5
1	0	1	0	31	0.942	69	397	52.5	0.66	80.1	54.9	45.4	23.7
0	-1	0	-1	9	0.966	142	418	50.1	0.64	44.7	41.5	41.7	18.3
0	1	0	-1	11	0.954	110	408	52.1	0.63	61.5	47.6	43.6	21.1
0	-1	0	1	8	0.962	124	416	50.1	0.64	54.4	40.9	42.7	19.1
0	1	0	1	10	0.959	112	408	51.9	0.63	65.8	47.1	43.5	20.9
0	0	0	0	3	0.955	111	415	52.1	0.64	61.5	46.5	44.6	20.9
0	0	0	0	15	0.957	113	408	51.9	0.63	62.1	49.8	42.7	20.5
0	0	0	0	34	0.958	122	413	50.6	0.67	33.3	39.4	43.5	20.0
0	0	0	0	35	0.954	134	415	50.7	0.67	57.2	45.2	45.0	20.8

x_1 = (Temperature (°C) - 375)/50 x_3 = (Liquid Flow (cm^3/hr) - 80)/40

x_2 = (Pressure (psig) - 1000)/500 x_4 = (Gas Flow (L/hr) - 150)/100 (at STP)

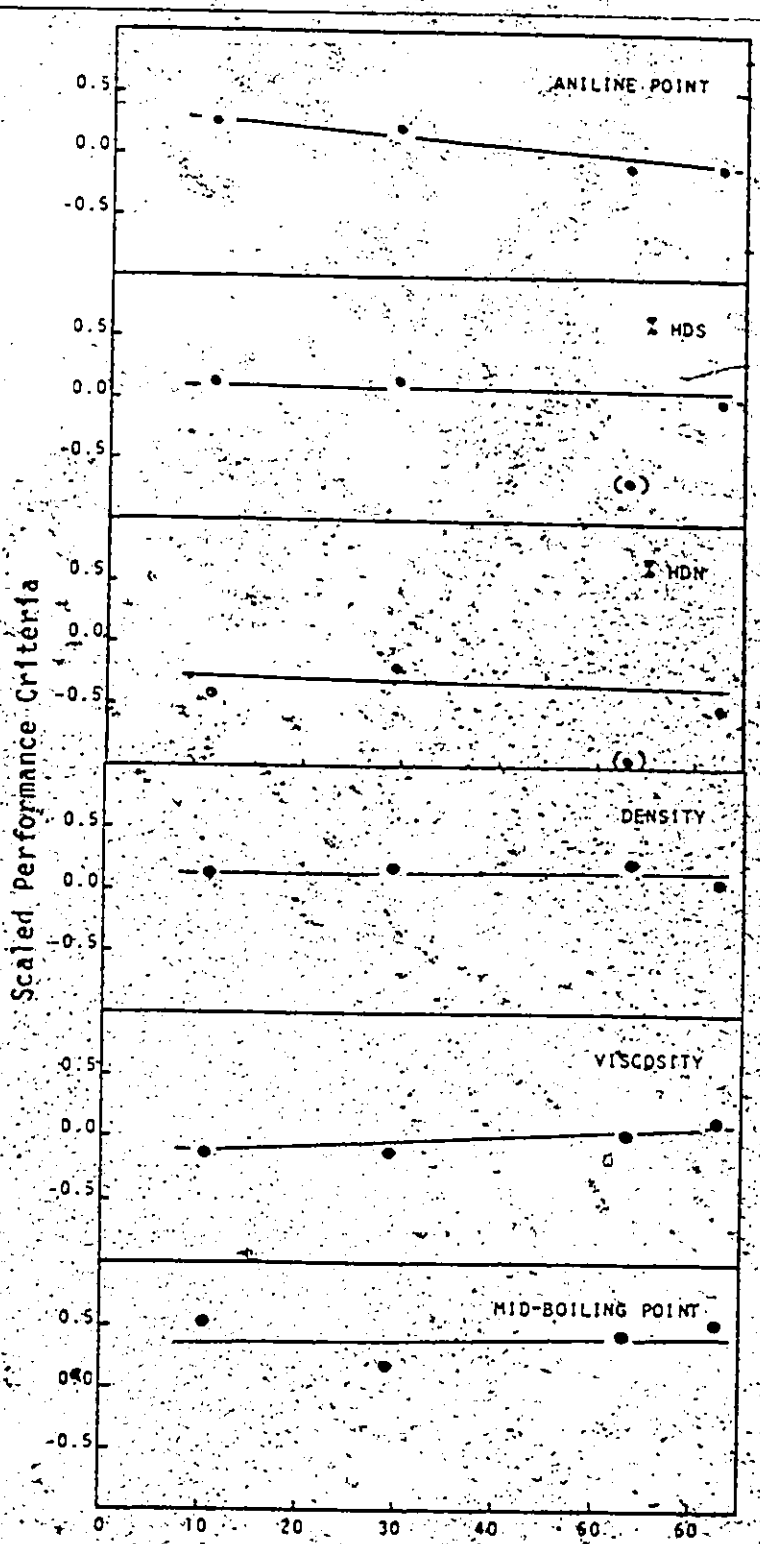

Figure 14: Activity Decay During Operating Region Study. (Operating conditions : Centre point)

data. Results of the C/H ratio were not considered reliable as a result of suspected analytical errors in the runs at 53.5 and 62.5 hours.

7.1.2.2 Fitted Model

The results of fitting a second degree polynomial model of the form given by Eqn. (1), in terms of the coded response and operating variables are given in Table 9. In this table, σ_{pe}^2, the estimate of pure error variance obtained from the repeated runs at the centre of the operating region, SSR/(n-p), the sum of squares of residuals divided by its degrees of freedom, the lack of fit test ratio as defined by Draper and Smith [16], and the abscissa values of the F-distributions having n-p-3 and 3 degrees of freedom for the numerator and denominator respectively, for a probability level of $\alpha = 0.05$, are listed beneath the parameter estimates and their 95% confidence limits.

Values of lack of fit test ratio greater than the corresponding F-value are indicative of significant lack of fit. The results in this table indicate that none of the fitted models show any significant lack of fit. All test ratios were much less than the $F_{10,3,0.05}$ value of 8.8. The adequacy of the fitted models was further verified by residual plots.

Table 9: Results of The Full Fitted Models

Parameter Estimate	Density	Viscosity (cp)	Mid-Boiling Point	Aniline Point	C/H Ratio (28 runs)	% HHS (28 runs)	% HDH	Cetane Index	Diesel Index
β_0	0.15±0.06*	-0.02±0.10	0.41±0.21	0.06±0.21	0.43±0.47	-0.08±0.22	-0.54±0.24	0.35±0.28	-0.13±0.07
β_1	-0.69±0.03	-0.79±0.06	-0.66±0.12	0.70±0.12	-0.32±0.27	0.80±0.13	0.62±0.14	0.38±0.16	0.73±0.04
β_2	-0.17±0.03	-0.13±0.06	-0.01±0.12	0.30±0.12	-0.34±0.27	0.17±0.13	0.19±0.14	0.30±0.16	0.21±0.04
β_3	0.25±0.03	0.24±0.06	0.18±0.12	-0.20±0.12	0.30±0.27	-0.29±0.13	-0.22±0.14	-0.07±0.16	-0.26±0.04
β_4	-0.03±0.03	-0.02±0.06	-0.04±0.12	-0.12±0.12	-0.01±0.27	0.10±0.13	-0.06±0.14	0.00±0.16	-0.01±0.04
β_{12}	-0.05±0.06	0.05±0.10	0.22±0.21	0.17±0.21	-0.32±0.47	-0.05±0.22	0.34±0.24	0.20±0.28	0.10±0.07
β_{13}	0.08±0.06	-0.01±0.10	0.07±0.21	0.04±0.21	0.42±0.47	0.03±0.22	-0.20±0.24	-0.05±0.28	-0.08±0.07
β_{14}	-0.01±0.06	0.06±0.10	-0.04±0.21	-0.19±0.21	0.00±0.47	0.02±0.22	-0.01±0.24	-0.01±0.28	0.03±0.07
β_{23}	0.04±0.06	-0.01±0.10	0.08±0.21	-0.07±0.21	0.12±0.47	-0.03±0.22	-0.20±0.24	-0.31±0.28	-0.05±0.07
β_{24}	0.05±0.06	0.06±0.10	0.03±0.21	-0.01±0.21	0.02±0.47	-0.04±0.22	0.00±0.24	-0.04±0.28	-0.05±0.07
β_{34}	-0.08±0.06	-0.09±0.10	-0.08±0.21	0.06±0.21	-0.08±0.47	0.14±0.22	0.04±0.24	0.05±0.28	0.09±0.07
β_{11}	-0.06±0.05	0.09±0.08	-0.21±0.17	-0.22±0.18	-0.04±0.38	-0.02±0.18	0.27±0.20	0.01±0.23	0.04±0.06
β_{22}	0.11 0.05	0.04±0.08	-0.06±0.17	-0.03±0.18	-0.21±0.38	0.05±0.18	-0.06±0.20	-0.27±0.23	-0.10±0.06
β_{33}	-0.11±0.05	-0.10±0.08	-0.05±0.17	0.06±0.18	-0.28±0.38	0.17±0.18	0.14±0.20	-0.01±0.23	0.11±0.06
β_{44}	0.03±0.05	-0.04±0.08	0.03±0.17	0.03±0.18	-0.39±0.38	0.06±0.18	0.04±0.20	0.04±0.23	-0.01±0.06
$\sigma^2_{pe}(\nu_{pe})$	0.0042(3)	0.015(3)	0.021(3)	0.037(3)	0.438(3)	0.147(3)	0.101(3)	0.021(3)	0.04(3)
SSR/(n-p)	0.027	0.0080	0.036	0.039	0.189	0.040	0.050	0.068	0.004
Test Ratio	0.5	0.4	1.9	1.1	0.3	0.1	0.3	3.8	0.9
F-value	8.8	8.8	8.8	8.8	8.8	8.8	8.8	8.8	8.8

* 95% confidence intervals are listed for each parameter.

Table 10: Results of the Reduced Models

Parameter Estimate	Density	Viscosity (cp)	Mid-Boiling Point	Aniline Point	C/H Ratio (20 runs)	C/H Ratio (24 runs)	% HDS (20 runs)	% HDS (27 runs)	% HDN	Cetane Index	Diesel Index
β_0	0.17±0.05*	-	0.37±0.09	-	-	0.11±0.06	-	-	-0.48±0.12	0.37±0.12	-0.11±0.05
β_1	-0.69±0.04	-0.79±0.06	-0.66±0.10	0.70±0.13	-0.32±0.27	-0.72±0.09	0.80±0.12	0.80±0.06	0.62±0.14	0.38±0.13	0.73±0.04
β_2	-0.17±0.04	-0.13±0.06	-	0.30±0.13	-0.34±0.27	-0.29±0.08	0.17±0.12	0.17±0.06	0.19±0.14	0.30±0.13	0.21±0.04
β_3	0.25±0.04	0.24±0.06	0.18±0.10	-0.20±0.13	0.30±0.27	0.24±0.08	-0.29±0.12	-0.28±0.06	-0.22±0.14	-	-0.26±0.04
β_4	-	-	-	-	-	-	-	0.10±0.06	-	-	-
β_{12}	-	-	0.22±0.17	-	-	-	-	-	0.34±0.24	-	0.10±0.07
β_{13}	0.08±0.07	-	-	-	-	-	-	-	-	-	-0.08±0.07
β_{14}	-	-	-	-	-	-	-	-	-	-	-
β_{23}	-	-	-	-	-	0.15±0.14	-	-	-	-0.31±0.23	-
β_{24}	-	-	-	-	-	-	-	-	-	-	-
β_{34}	-0.08±0.07	-	-	-	-	-	-	0.14±0.10	-	-	0.09±0.07
β_{11}	-0.07±0.05	0.07±0.06	-0.20±0.13	-0.14±0.13	-	-	-	-	0.25±0.18	-	-
β_{22}	0.11±0.05	-	-	-	-	-	-	-	-	-0.27±0.17	-0.10±0.06
β_{33}	-0.12±0.05	-0.12±0.06	-	-	-	-	-	0.12±0.06	-	-	0.10±0.06
β_{44}	-	-	-	-	-	-	-	-	-	-	-
$\hat{\sigma}^2_{pe}(\nu_{pe})$	0.0042(3)	0.0150(3)	0.0213(3)	0.0366(3)	0.438(3)	0.0258(1)	0.1464(3)	0.0056(2)	0.101(3)	0.0213(3)	0.0043(3)
SSR/(n-p)	0.0038	0.0093	0.0270	0.0477	0.198	0.0167	0.0392	0.0091	0.054	0.0491	0.0049
Tgt Ratio	0.9	0.2	1.3	1.3	0.4	0.4	0.2	1.7	0.5	2.5	1.1
F-value	8.7	8.7	8.7	8.7	8.7	248	8.7	19.4	8.7	8.7	8.7

* 95% confidence intervals are listed for each parameter.

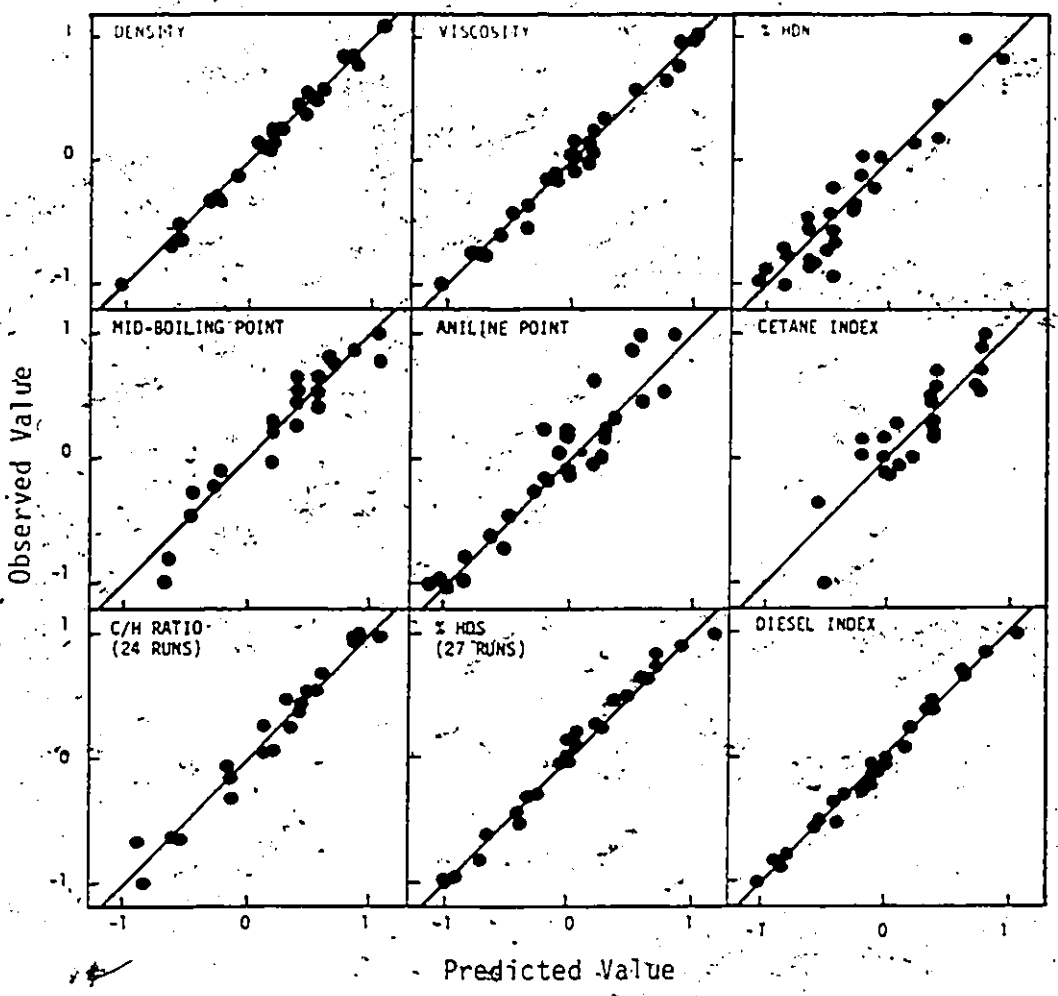

Figure 15: Observed vs Predicted Values of Response Variables

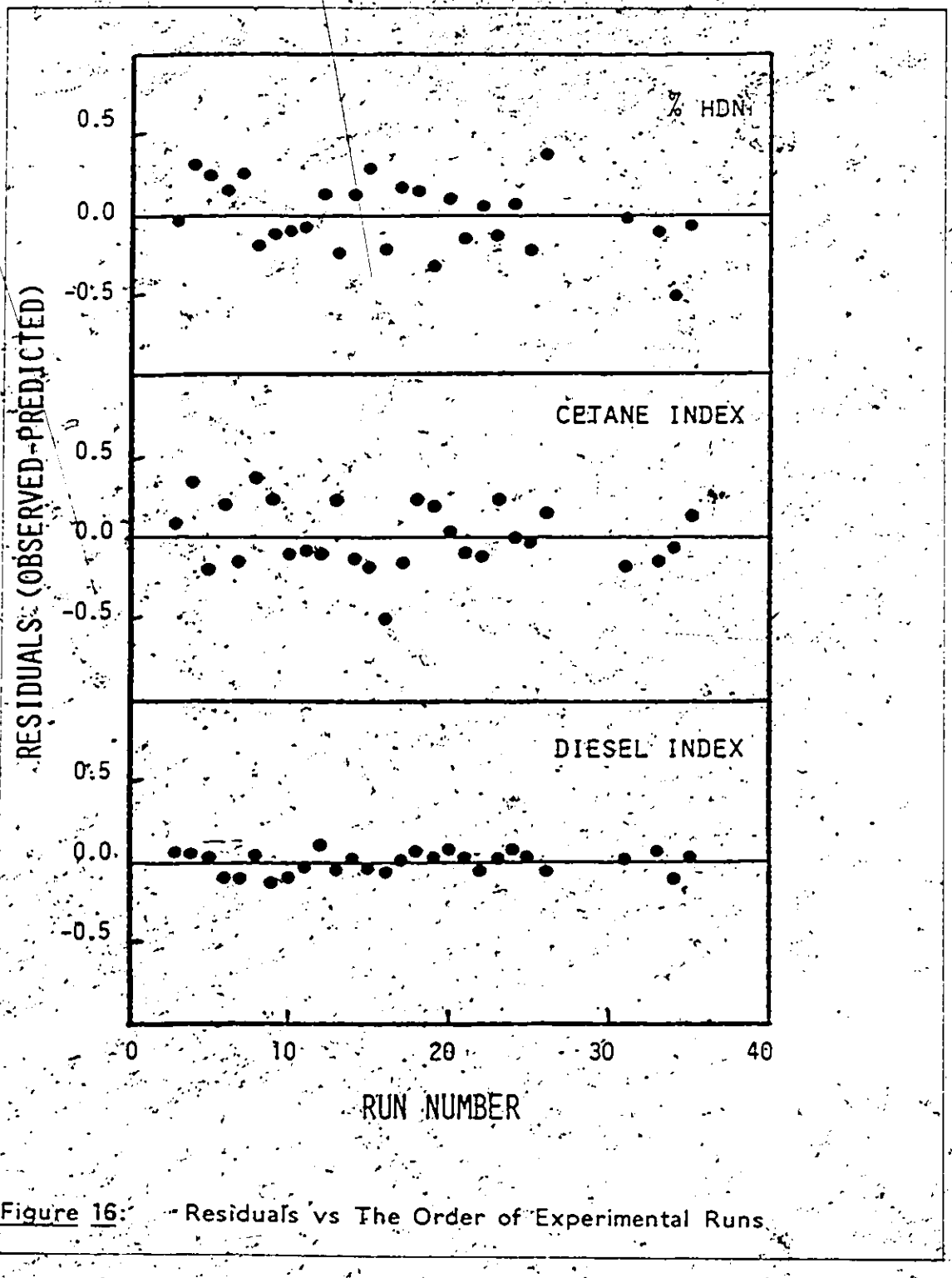

Figure 16: Residuals vs The Order of Experimental Runs

Reduced Models: Examination of the confidence limits for the parameters, however, revealed that in all models some terms did not have an important effect on the predictive ability of the model. The parameters of concern have been underlined. These terms were dropped from the model. The remaining parameters were re-estimated and the reduced models were again checked for the adequacy tests as well as lack of fit tests. The results of the reduced models are shown in Table 10. Neither the lack of fit test ratios nor the residual plots revealed any significant lack of fit. Plots of observed versus predicted values of the performance criteria are given in Figure 15. These too indicate no significant lack of fit.

Plots of the residuals also provided information concerning the extent of any catalyst aging and the occurrence of any inconsistent data. When plotted as a function of the order of execution of the runs (Figure 16) no trends were observed, confirming the conclusions drawn from the centre-point experiments discussed earlier. Examination of the plots in Figure 16 reveals, however, some suspicious values (outliers) in the C/H Ratio and %HDS data. Since the corresponding results for the other performance criteria showed no sign of any inconsistencies it was speculated that there was likely some error in the elemental analysis for C, H and S for these runs. As a result they were omitted from any subsequent analysis. This also explains the absence of a centre-point test for catalyst decay for the C/H Ratio discussed previously.

7.1.3 Interpretation of The Fitted Models

Considerable information can be obtained from the fitted models. This information is related to the precision of both observed and predicted values of the performance criteria, the location of the optimal operating conditions for each performance criterion and the nature of their response surfaces.

The precision or reproducibility of the observed response values is indicated by the quantity SSR/(n-p) for an adequate model. Alternatively, the plot of the amount of scatter in the residual or observed versus predicted values gives a qualitative picture of precision. Examination of the SSR/(n-p) values in Table 10, Figure 15 and Figure 16 reveals that density, viscosity, %HDS and Diesel Index were most precisely measured while Aniline Point and C/H Ratio determinations had relatively poor precision.

7.1.3.1 Response Surfaces and their Analysis

Examination of the parameter estimates for each fitted model provided a preliminary feeling for the sensitivities of each performance criterion to operating variables. It is seen from Table 10 that temperature (x_1) had the greatest effect on all criteria, pressure (x_2) and the liquid flow rate (x_3) had a lesser effect on all criteria and the gas flow rate (x_4) had an insignificant effect on nearly all criteria, Density, %HDS and Diesel Index being the exceptions. A more detailed analysis of these sensitivities was provided by a thorough examination of various response surfaces.

The fitted models were transformed into their canonical forms (Bacon [3]), given by

$$y_i = y_{i_s} + \lambda_1 z_1^2 + \lambda_2 z_2^2 + \lambda_3 z_3^2 + \lambda_4 z_4^2 \qquad (19)$$

The signs of the new coefficients, λ_i, identify the nature of the stationary point. If the signs of the λ's are positive then the stationary point is a minimum and if the signs are positive and negative mixed then the stationary point is a saddle point. The location of the stationary point is defined by the equations $z_1 = 0$, $z_2 = 0$, $z_3 = 0$ and $z_4 = 0$ and the value of the response at the stationary point is given by y_s. The sensitivity of the response is indicated by the magnitudes of the λ_i's.

7.1.3.2 Optimal Operating Conditions

The optimal operating conditions for each individual performance criterion was determined within the bounds of the operating region using the fitted models and a constrained optimization procedure (Ray and Szekely [56]). The results are summarized in Table 11. These reveal a number of features.

Although the predicted optimal conditions were the same (i.e. $x_1 = 1$, $x_2 = 1$, $x_3 = -1$, x_4 = any value) for most of the individual criteria, it was different for the two of them, namely for the Density and Mid-Boiling point. The difference for these being the level of pressure (x_2). The predicted optimal locations were found to be at a corner or vertex of the operating region except for Density whose optimum was on an edge.

Table 11: Summary of Optimal Operating Conditions and Surface Characteristics

Performance Criterion	Optimal Condition (x_1,x_2,x_3,x_4)	Stationary Point (x_1,x_2,x_3,x_4)	Type of Stationary Point
min (DENSITY)	(1,0.77,-1,-1)	(-4.9,0.8,0,-1.8)	Saddle Point
min (VISCOSITY)	(1,1,-1,-)	(5.6,*,1,-)	Saddle Point in x_1-x_3
min (MID-BOILING POINT)	(1,-1,-1,-)	(0,3,*,-)	Saddle Point in x_1-x_2
max (ANILINE POINT)	(1,1,-1,-)	(2.5,*,*,-)	Maximum in x_1
min (C/H RATIO)	(1,1,-1,-)	(*,-1.6,1.9,-)	Saddle Point in x_2-x_3
max (%HDS)	(1,1,-1,-1)	(*,*,-0.7,3.2)	Saddle Point in x_3-x_4
max (%HDN)	(1,1,-1,-)	(-0.6,-1,*,-)	Saddle Point in x_1-x_2
max (CETANE INDEX)	(1,1,-1,-)	(*,0,1,-)	Saddle Point in x_2-x_3
max (DIESEL INDEX)	(1,1,-1,-1)	(-16.7,-7.3,0,-1.1)	Saddle Point

The actual nature of the response surfaces were determined, to obtain information regarding the sensitivities of the performance criteria to the operating variables, using either a canonical transformation of the fitted model or by simply generating two-dimensional contour plots for the response surfaces. It was generally found difficult to interpret the canonical form in four dimensions especially when the stationary point was usually found to be well outside the operating region. On the other hand, although two-dimensional contour plotting is also a difficult to interpret procedure for a four dimensional system, the occurrence of the optimal locations at a vertex or along an edge of the operating region greatly reduced the number of such plots required to develop a picture of the response surface around the optimum.

7.1.3.3 Example Analysis For %HDS

The hydrodesulfurization (%HDS) response surface will be considered to illustrate the interpretation of the response surface by the above mentioned methods. The model is seen to be linear in temperature and pressure and quadratic in liquid flow rate and gas flow rate (Table 10). Thus the canonical analysis reduces to a two-dimensional analysis in x_3 and x_4, the response surface simply increases in a linear fashion in the x_1 and x_2 directions. The canonical form with respect to x_3 and x_4 is given by :

$$y = 0.26 + 0.80x_1 + 0.17x_2 + 0.15z_1^2 - 0.03z_2^2$$

where $z_1 = 0.91(x_3+0.71) + 0.41(x_4-3.2)$

and $z_2 = 0.41(x_3+0.71) - 0.91(x_4-3.2)$.

This represents a saddle-point at $x_3 = -0.71$ and $x_4 = 3.2$ with major axes defined by $z_1 = 0$ and $z_2 = 0$. The response (i.e. %HDS) decreases along $\pm z_2$ directions and increases along $\pm z_1$ directions with response being much more sensitive to changes along the z_1 axis. A contour plot of the response surface in the $x_3 - x_4$ plane shown in Figure 17 reveals these characteristics and the optimum at (1,1,-1,-1).

7.1.4 Conclusions of Operating Region Study

The above study of the operating region gave good mathematical representation of the effect of the four operating variables on some of the important properties of the hydrotreated heavy oil. Although, the conclusions of this study were not anything new but were the confirmation of what would normally be expected with the existing knowledge of the hydrotreatment process, this study provided the same facts with scientific precision and took the guess work out. The available information on hydrotreatment does leave a margin of uncertainty and this part of the present study fills in those gaps. Especially, the effect of the liquid and gas flow rates, which are difficult to predict with the existing knowledge, are the important outcome of this study. Also this study indicates some strong interactions between the operating variables which could not have been possible with any other type of study.

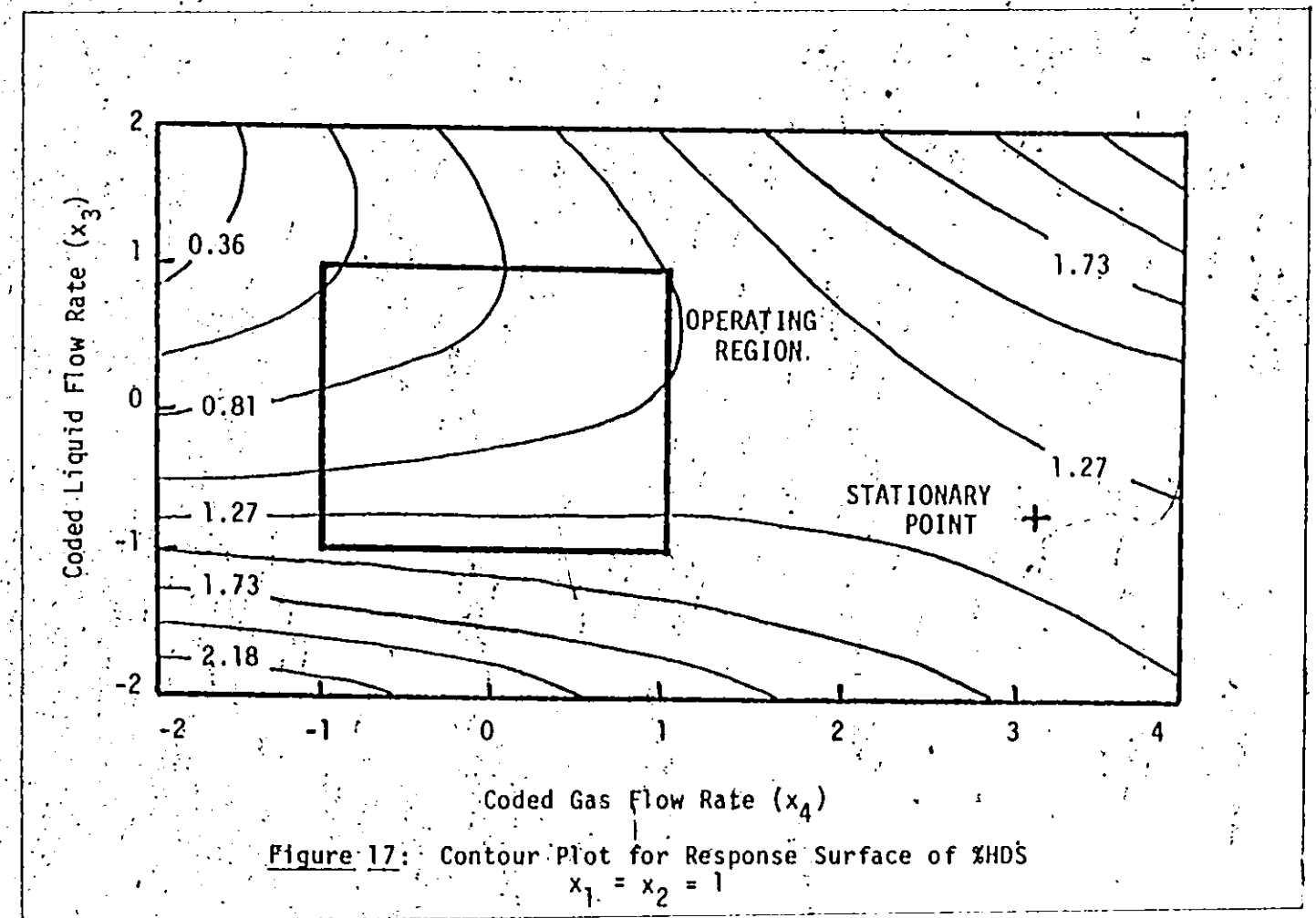

Figure 17: Contour Plot for Response Surface of %HDS
$x_1 = x_2 = 1$

7.1.4.1 Temperature Effect

As was expected, the temperature was a major factor effecting all the properties. Increase in temperature improved the properties of the product oil. The optimum for the temperature was well outside the operating region towards the high temperature range. Temperature had strong interaction with pressure terms for two of the performance criteria, namely mid-boiling point (β_{12} = 0.22) and %HDN (β_{12} = 0.34). This indicates that the combination of pressure and temperature enhances %HDN, whereas the mid-boiling point of the product would increase (because of the positive sign of β_{12} values). It is generally desirable to get a high yield of lower boiling products without affecting the quality of the product. Therefore, the above mentioned interaction also becomes an important factor to be considered.

7.1.4.2 Pressure Effect

Pressure of hydrotreatment also had a positive effect on all the performance criteria except the mid-boiling point (as indicated by β_2 values of Table 10). Pressure term appears only in the interaction term for the mid-boiling point. This is the interaction with the temperature as discussed above.

7.1.4.3 Liquid Flow Rate Effect

Increase in flow rate decreases the residence time inside the reactor and so it affects the hydrotreatment. As can be seen from the Table 10 the flow rate had the expected effect on all the performance criteria.

7.1.4.4 Gas Flow Rate Effect

This is the most interesting outcome of the study of the operating region. The gas flow rate did not indicate any substantial effect on the properties of the product oil and that was not what was expected from the available literature information on trickle-bed reactors.

As suggested in the recent literature on the flow regimes in trickle-bed reactors (Gurav, Tosun [26], Smith [70], Mordechay [49], Dudukovic [17], Charpentier [14], Shah [66], Mears [40], Hochman [33], and numerous other references) a very strong interaction should be expected between the gas and the liquid flow in trickle-bed reactors. The gas flow rates were chosen so as to get both high-interaction flow regime as well as the low-interaction flow regime.

As most of the available literature on the hydrodynamics of trickle-bed reactors is based on simple systems such as air-water generally at ambient or mild conditions, the predictive abilities of models developed with such systems are questionable. The present system is quite complex. The data for the accurate physical properties of such a system is also not available. A study of the hydrodynamics of such systems is a good project in itself. The present study was only limited to the catalysis aspect and therefore no further investigation was done in this regard. However, for the present study the effect of the gas flow rate on the catalyst performance was found to be insignificant (as is indicated above).

7.1.5 Optimal Operating Point

The above study of the operating region did not lead to any particular single set of operating conditions which could be called as optimum point for hydrotreatment of the given heavy oil. Therefore, the choice of appropriate operating point for the catalyst screening test was made considering the outcome of above study as well as various other practical aspects.

A temperature of 375°C was selected. Hydrotreatment temperatures higher than this lead to higher levels of coke formation on the catalysts and the lower liquid yields. Pressure of 1000 psig was thought appropriate as an increase in pressure did not give remarkable improvement in any of the product properties. It is also known that higher levels of pressure give higher degrees of hydrogenation, which may not be always desireable. Also higher pressure increases the capital and operating cost of plant and machinery in a real refining situation. As discussed in the above analysis the pressure term had a strong interaction with the temperature term for the mid-boiling point. For temperatures greater than 375°C (i.e. x_1 positive), pressures greater than 1000 psig (i.e. x_2 positive) tends to increase the mid-boiling point of the product oils. Therefore, considering all these factors the above choice for pressure is quite appropriate.

LHSV of 1.0 to 3.0 is quite common in the hydrotreatment of heavy oils. Hence, this was the range used in the above study. For further catalyst testing purposes a LHSV of 1.5 is selected. This liquid flow

rate was thought to be appropriate taking into consideration our past experience with the same heavy oil. The gas flow rate had very insignificant effect on nearly all the performance criteria. Excess of hydrogen gas flow is kept in trickle-bed hydrotreatment operations mainly because of the mass transfer and hydrodynamic considerations. A flow rate of 5000 scf/bbl of oil (i.e 0.89 st. l/ml of oil) is quite commonly used. Therefore, this gas flow rate was used for further catalyst screening.

7.2 SEARCH FOR BEST CATALYST COMPOSITION

It has been already discussed in the literature survey that the present knowledge of the efficient hydrotreatment catalyst is only limited. Most of the published literature indicates the results obtained by use of the available commercial catalysts. These commercial catalysts are generally available in only a few standard compositions. Therefore, in the present study it was thought necessary to make our own catalysts for a systematic study.

It was also known that the method of preparation and the various steps involved in the catalyst making have quite a significant effect on the properties of the final catalyst. Therefore, the reproduciblity was a major criterion when the method of preparation was selected. The present study was limited to variations in the compositions of silica and zeolite in a silica-alumina-zeolite based catalyst. The standard method for preparing such catalysts is by making a silica-alumina gel and then mixing it with the zeolite powder.

The exact details of the process of co-precipitation of gel were not available and therefore many trials had to be done to understand the art of making the catalysts. Many catalysts were made and tested for their chemical compositions and physical properties. On the basis of those trials a catalyst preparation scheme was finalized which has already been presented in the 'Experimental Procedure'. That scheme was reliable and gave good reproduciblity as is confirmed by the results that will follow.

7.2.1 Experimental Design

The nominal range of the compositions of silica and zeolite was selected on the basis of information available in the literature. Accordingly, the selected range for silica was from 10% to 50% by wt., and for zeolite it was 10% to 40% by wt. Again it was thought best to use some of the modern statistical experimental design techniques for carrying out a search for optimum composition within the defined region.

Nothing was known about the outcome of these experiments in terms of effects of silica and zeolite concentrations on the properties and performance of the catalysts. Therefore, it was appropriate to try at least a second degree model rather than just a simple linear one. Accordingly, a second degree polynomial type of model was considered to define the response surface:

$$E(y_i) = \beta_0+\beta_1x_1+\beta_2x_2+\beta_{11}x_1^2+\beta_{22}x_2^2+\beta_{12}x_1x_2, \qquad (20)$$

where i = 1, and 2 indicate a particular performance criterion, $E(y_i)$ is the expected value of the i'th performance criterion (e.g. - nitrogen or sulfur concentration, density, viscosity etc.,) and x_1, and x_2 are the two design variables in the appropriate coded forms. The coding used is given in Table 12.

In order to estimate the coefficients of the squared terms in the above model, at least three values of each variable must be tested. Three level factorial design similar to the one used in the study of operating region could be used but in this study a better experimental design called central composite design was selected. This type of design was first proposed by Box and Wilson [9], and was further improved by Box and Hunter [10].

Table 12: Central Composite Design

Coded variables are:

x_1 = [(%by wt. silica)-30]/14.1421
x_2 = [(%by wt. zeolite)-25]/10.6066

Centre composite design points and compositions:

Comp. No.	x_1	x_2	No. of Runs	%by wt. Silica	%by wt. Zeolite	%by wt. Alumina
1	0.0	0.0	8	30.0	25.0	45.0
2	1.0	-1.0	1	44.1421	14.3934	41.4645
3	1.0	1.0	1	44.1421	35.6066	20.2513
4	-1.0	-1.0	1	15.8579	14.3934	69.7487
5	-1.0	1.0	1	15.8579	35.6066	48.5355
6	0.0	-1.4142	1	30.0	10.0	60.0
7	0.0	1.4142	1	30.0	40.0	30.0
8	-1.4142	0.0	1	10.0	25.0	65.0
9	1.4142	0.0	1	50.0	25.0	25.0

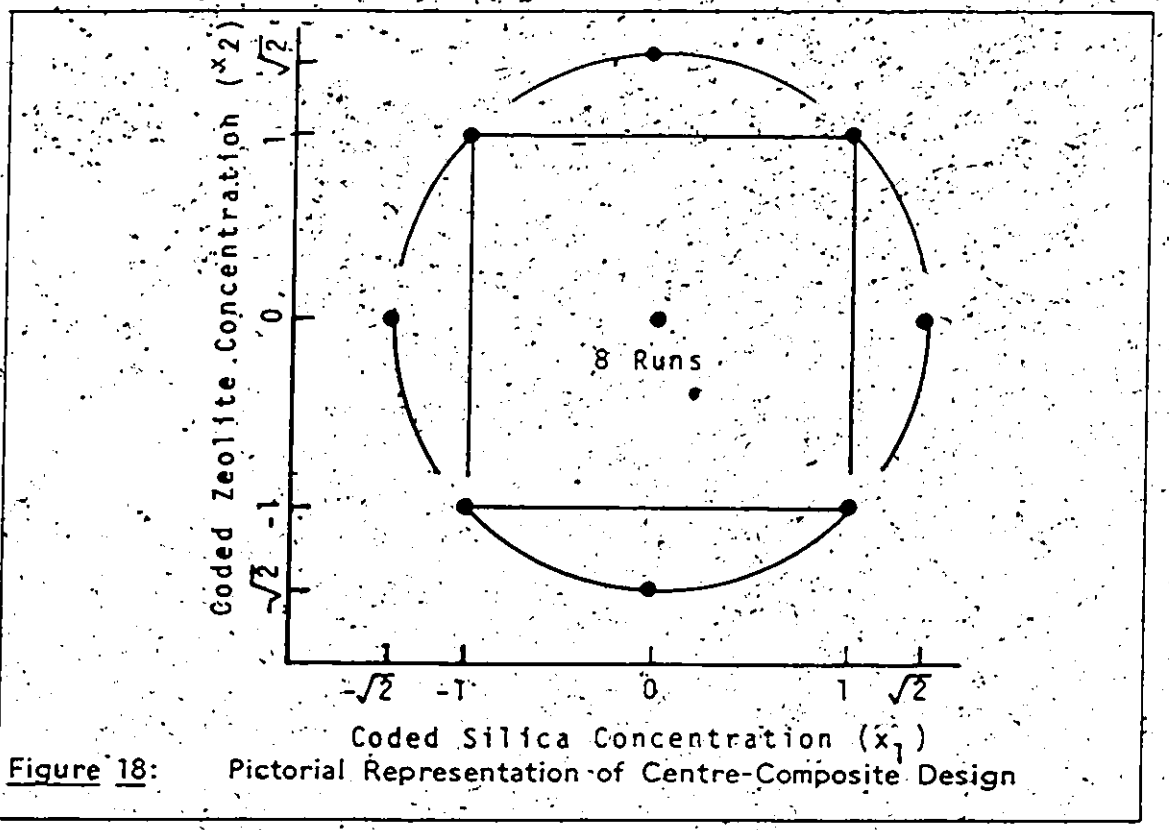

Figure 18: Pictorial Representation of Centre-Composite Design

Various setting of the compositions of silica and zeolite and the coded values of these compositions (i.e. x_1 and x_2) are shown in Table 12. The composition of alumina is given by difference. This design requires a total of 16 runs, out of which 8 runs are replicates at the centre point. 4 runs correspond to the two level factorial design and the other four runs are along the axis passing through the centre point. These eight points are equidistance from the centre. In this way these eight points actually lie on a circle as shown in Figure 18.

This design has the following advantages:

1. It is a second degree design which allows for the second degree terms in the predicted model.
2. It has a uniform precision throughout the region.

3. The parameter estimates are uncorrelated because of orthogonality of design.

4. Design is rotateable around its centre point.

Eight runs are required in the above experimental design at the centre point composition. Eight repeated runs for the same composition were judged sufficient to prove the reproducibility of the entire catalyst preparation, catalyst testing as well as the analytical schemes. The order of catalyst preparation was randomized in order to spread the effect of any extraneous source of variation equally over all the results to avoid the confounding of the variable of interest with these extraneous sources of error.

7.2.2 Results of Catalyst Physical and Chemical Testing

As described earlier, the prepared catalysts were tested for their physical properties as well as chemical composition before actual hydrotreatment tests. The order of catalyst preparation was randomized by drawing lots. The catalyst number in the following presentation refers to this randomized order of catalyst preparation.

Physical properties of the prepared catalyst and their chemical composition are shown in Table 13 and Table 14. The first table shows the results of the eight replicate runs. The average values and the standard deviations for each column are shown at the bottom. From these values it can be concluded that, within the limits of the experimental errors, the catalyst preparation method was reproducible

Table 13: Physical Properties and Chemical Composition of Catalysts (For 8 Replicate Runs)

Cat No	No	x_1	x_2	Bulk Density g/ml	Pore Vol. ml/g	BET Surface Area m^2/g	Chemical Composition (wt.%) SiO_2	Al_2O_3	NiO	MoO_3
4	1	0	0	0.6213	0.602	283	44.23	51.03	1.02	3.13
5	1	0	0	0.6078	0.613	279	46.19	50.79	1.63	3.59
6	1	0	0	0.6139	0.643	263	48.30	51.32	1.74	3.40
10	1	0	0	0.6205	0.631	269	45.76	49.05	1.59	4.09
12	1	0	0	0.6300	0.618	260	46.09	49.93	1.43	3.81
14	1	0	0	0.6050	0.593	257	46.66	50.05	1.89	3.77
15	1	0	0	0.6100	0.619	264	45.32	50.95	1.31	2.98
16	1	0	0	0.6193	0.623	262	44.95	49.94	1.65	3.18
Average				0.6160	0.618	267	45.94	50.38	1.53	3.49
Standard Deviation				0.0008	0.016	9.3	1.22	0.76	0.27	0.39

as far as the chemical composition and the physical properties were concerned. Table 14 shows the results of the physical properties and chemical composition of the remaining eight catalysts prepared as per the central-composite design. Columns 3 and 4 of these tables indicate the values of the coded variables x_1, and x_2. Comparing the values of standard deviations for bulk-density, pore volume and BET surface area, it is seen that these values show more variation in Table 14. This is due to the change in compositions indicating that inspite of keeping all other factors in catalyst preparation uniform, the properties of these catalysts are affected by their composition.

Table 14: Physical Properties and Chemical Composition of Catalysts (For 8 Design Runs)

Cat No	No	x_1	x_2	Bulk Density g/ml	Pore Vol. ml/g	BET Surface Area m^2/g	Chemical Composition (wt.%) SiO_2	Al_2O_3	NiO	MoO_3
1	2	1	-1	0.5750	0.639	249	52.13	45.14	1.88	3.11
8	3	1	1	0.6011	0.613	294	67.82	29.01	1.91	4.01
13	4	-1	-1	0.7934	0.598	266	23.11	72.83	1.33	4.31
9	5	-1	1	0.7023	0.576	289	38.07	56.11	1.62	3.89
7	6	0	2	0.6726	0.601	253	34.91	63.30	1.13	3.71
2	7	0	2	0.5786	0.642	241	55.80	39.95	1.45	3.49
11	8	2	0	0.7911	0.601	288	25.14	71.01	1.69	3.88
3	9	2	0	0.5886	0.633	240	63.81	31.85	1.49	3.33
Average				0.6628	0.613	265			1.56	3.72
Standard Deviation				0.0920	0.023	23			0.27	0.39

The active metal loading (i.e. Ni, Mo) was kept to low levels of 5% by wt. for this part of study, as the excessive loading would have made the comparison of the catalysts on the basis of support material impossible. The catalyst supports were impregnated with these active metals so as to get a $NiO:MoO_3$ ratio of 0.3.

From Table 13 and Table 14, it can be concluded that the impregnation technique too was quite adequate and gave the desired results. The amounts of active metal components actually found on the catalysts by analysis compare closely with the intended compositions. Also, it can be concluded from the standard deviation values that the

amounts of scatter in the results of impregnated active metals, is independent of composition of the support material. This also confirmed the reproducibility of the entire catalyst preparation scheme.

7.3 Hydrotreatment Results

Sixteen catalysts prepared as per the central composite design were then tested in the hydrotreatment trickle-bed reactor for their performance. Once again the order of the catalyst testing was randomized for the same reasons as explained earlier. In the following discussion the order of catalysts testing is referred to as "Run-number". The required procedure has already been described earlier. For the present study, HDS and HDN were the main criteria for comparing the activity of different catalysts. Therefore, in this study main emphasis was on these activities. However, to augment the data other properties like density, viscosity, aniline point and mid-boiling point were also determined.

7.3.1 Study of Catalyst Initial Activity Decay

It is generally known that the initial activity of such catalysts is much higher than the average activity these catalyst show later. It is hard to define a steady-state activity as the activity decay is an ongoing process for such systems. However, the initial high activity decays to lower levels within first 5 to 20 hours of run and the further decrease in activity takes place at a much smaller rate. It is this second level of catalyst activity which may be considered as a 'pseudo-steady-state', in

the catalyst is small (e.g. generally not more than 5%). The time when this pseudo steady-state may be reached in a particular situation depends upon the properties of catalyst, the liquid being processed and the operating conditions, and this could only be determined experimentally.

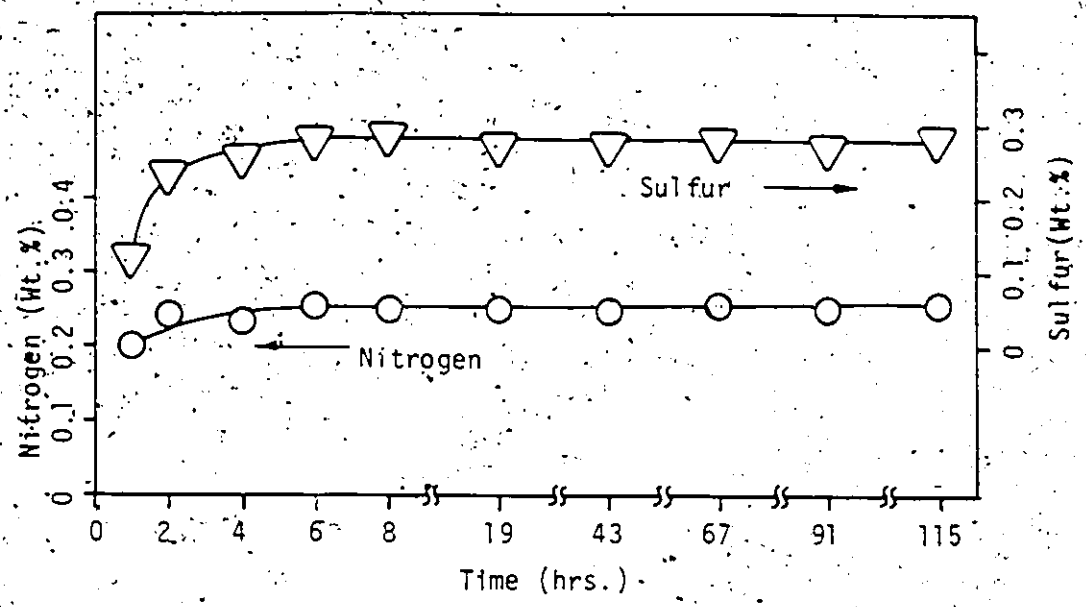

Figure 19: Initial Activity Decay. Catalyst No:30; Temperature = 375°C Pressure = 1000 psig; LHSV = 1.5; and Gas Flow Rate = 0.89 st.l/ml of oil.

Samples were drawn at different time intervals after the start of the hydrotreatment reaction. These samples were analyzed mainly for the sulfur concentrations. Results obtained with a typical catalyst are shown in Figure 19. It can be seen from this figure that the initial high

activity of the catalyst decays very fast and within first six hours the catalyst activity reached the level where further decay in activity takes place at a much slower rate. This pseudo-steady-state is reached approximately within the same time interva as was observed with two more catalysts. Therefore it was decided to withdraw oil samples after a catalyst was on stream for about 20 hours for comparison of activities of different catalysts.

7.3.2 Results

The results of analysis of oil samples withdrawn at the standard test condition (i.e. Temperature= 375°C pressure= 1000psig; LHSV= 1.5; and Gas Flow Rate= 5000 scf/bbl) after each catalyst was on stream for at least 20 to 22 hours, are shown in Table 15.

Values of nitrogen and sulfur concentrations, density, viscosity, aniline point and the mid-boiling point are given for all the sixteen design catalysts. For ease of comparison, the results of eight design runs (i.e. 4 corner points and 4 axial points) are tabulated first followed by the results of 8 replicate runs. While first two columns indicate the catalyst and run numbers, the third and the fourth columns indicate the values of the coded design variables x_1, and x_2 respectively. The average values, standard deviation and the 95% confidence interval for the eight replicate runs are given at the bottom of each column.

Table 15: Results Obtained With Sixteen Design Catalysts

Cat No.	Run No.	x_1	x_2	N ppm	S wt.%	Density g/cc	Viscosity cp	Aniline point °C	Mid-B-pt °C
1	10	1	-1	4155	0.37	0.9508	103.3	50.4	399.5
8	15	1	1	4027	0.89	0.9521	96.6	50.4	414.6
13	1	-1	-1	2638	0.32	0.9352	65.5	53.4	402.5
9	2	-1	1	3029	0.48	0.9384	70.8	52.2	405.0
3	14	$\sqrt{2}$	0	3864	0.77	0.9508	97.4	50.4	410.7
11	9	$-\sqrt{2}$	0	2659	0.26	0.9337	61.1	52.9	390.8
2	13	0	$\sqrt{2}$	3905	0.72	0.9489	91.6	50.9	411.6
7	5	0	$-\sqrt{2}$	2618	0.31	0.9345	63.0	52.8	391.6
4	8	0	0	3333	0.44	0.9398	74.1	52.0	402.7
5	6	0	0	3445	0.52	0.9409	73.6	52.3	389.1
6	11	0	0	3374	0.47	0.9404	74.6	51.7	408.1
10	16	0	0	3487	0.54	0.9450	78.5	51.6	407.5
12	7	0	0	3654	0.70	0.9467	86.0	51.1	398.9
14	12	0	0	3610	0.58	0.9441	83.5	51.3	409.7
15	3	0	0	3532	0.57	0.9428	82.9	51.5	412.9
16	4	0	0	3385	0.48	0.9416	75.4	52.3	403.8
Average :				3478	0.54	0.9427	78.6	51.7	404.1
Standard Deviation :				115	0.08	0.0024	4.9	0.5	7.5
95% Conf. Interval :				±96	±0.07	±0.002	±4.1	±0.4	±6.2

The results of the 8 replicate runs did indicate a fairly good reproduciblity of the catalyst performance within the limits of experimental errors. The values of aniline point again indicated more scatter. The same was observed previously in the study of operating region. Therefore, this performance criterion was not considered appropriate for further analysis.

7.3:2.1 Model Fitting

The data in Table 15 indicated that, out of the sixteen catalysts tested, catalysts 11, 7 and 13 gave the best performance. The values of nitrogen concentrations in the product oils obtained with these catalysts are quite comparable whereas, the performance of catalyst number 11 was best for sulfur removal. A similar conclusion was also reached looking the other properties. However, this did not ascertain the expected performance at points other than the ones selected for catalyst preparation. Therefore, a detailed mathematical analysis of the data was done to get a better picture of the entire response surface within the operating region.

The data values were scaled between -1 and +1 for the sake of better comparison between the different performance criteria as was done earlier in the analysis of results obtained for the operating region. The resulting scaled values of each performance criteria were fitted to the second degree polynomial type of model equation (Eqn. (20)) using the linear regression technique. The values of the parameter estimates are listed in Table 16. The 95% confidence intervals for each parameter estimate are given below each estimated value. At the bottom of each column, the pure error variance σ_{pe}^2 which was obtained from the 8 replicate runs, the R-ratio test value and corresponding F-values are listed for each fitted model.

Table 16: The Estimated Parameters of Fitted Model

The model equation is

$$E(y_i) = \beta_0 + \beta_1 x_1 + \beta_2 x_2 + \beta_{11} x_1^2 + \beta_{22} x_2^2 + \beta_{12} x_1 x_2$$

The values of the estimated parameter:-

coefficient	N	S	Density	Viscosity	Mid-BP
β_0	0.118	-0.119	-0.026	-0.172	0.175
	±0.125	±0.217	±0.221	±0.195	±0.490
β_1	0.686	0.469	0.727	0.681	0.341
	±0.125	±0.217	±0.221	±0.195	±0.490
β_2	0.339	0.500	0.338	0.231	0.450
	±0.125	±0.217	±0.221	±0.195	±0.490
β_{11}	-0.075	-0.036	0.036	0.084	-0.480
	±0.125	±0.217	±0.221	±0.195	±0.490
β_{22}	-0.075	-0.036	0.006	0.038	-0.147
	±0.125	±0.217	±0.221	±0.195	±0.490
β_{12}	-0.169	0.286	-0.052	-0.142	0.247
	±0.177	±0.307	±0.313	±0.275	±0.693
σ_{pe}^2	0.022	0.068	0.070	0.054	0.343
R	11.7	0.5	2.48	4.21	0.65
F-value	3.64	3.64	3.64	3.64	3.64

7.3.2.2 Model Interpretation

It can be seen from the Table 16 that except for the values of the coefficients β_1 and β_2, the values of all other coefficients are less than their 95% confidence intervals. Dropping out these terms leaves just a first degree model which in three dimensions is represented by a plane passing through the origin. Such a model would not yield any useful conclusion as far as finding an optimum is concerned. Therefore, such an exercise was considered futile.

The reason for wider confidence intervals was identified to be the higher values of the pure error variance which was a result of higher degree of spread in the values of properties of the oil samples from eight replicate runs. At this stage of catalyst testing such a spread was expected as this indicated the total error accumulated in the entire sequence of catalyst preparation and testing. Considering this limitation, it was decided to analyze the resulting models as obtained without any attempts to drop the insignificant terms.

7.3.2.3 Canonical Transformation

As explained earlier, the model interpretation is simplified by canonical transformations. This transformation converts the model equation into a simple two parameter form and the interpretation of the response surface is easy. The values of the new parameters for the transformed model and the coordinates of the stationary point are given in Table 17.

Table 17: Canonical Transformation Parameters

The canonical model form is:

$$E(y_i) = \gamma_0 + \gamma_1 z_1^2 + \gamma_2 z_2^2$$

where

$$z_1 = A(x_1 - x_1^*) + B(x_2 - x_2^*), \text{ and}$$

$$z_2 = B(x_1 - x_1^*) + A(x_2 - x_2^*).$$

and (x_1^*, x_2^*) is the stationary point coordinates.

	N	S	Density	Viscosity	Mid-BP
x_1^*	-7.847	-2.304	14.750	11.614	-2.081
x_2^*	11.057	-2.217	34.648	18.581	-2.188
A	-0.709	0.576	-0.711	-0.723	0.642
B	0.705	-0.817	-0.703	-0.691	-0.766
γ_0	0.118	-0.119	-0.026	-0.172	-0.175
γ_1	-0.971	-0.212	-1.405	-1.205	-0.341
γ_2	0.811	0.319	1.385	1.172	0.449

From Table 17 it can be seen that all the stationary points lie very much outside the region. The opposite signs of the coefficients of γ_1, and γ_2 indicate that all the response surfaces are 'saddle' type. The estimated value of each performance criteria increase in z_1 direction and decrease in the z_2 direction. The minimum value of all the performance criteria are desireable in the present case.

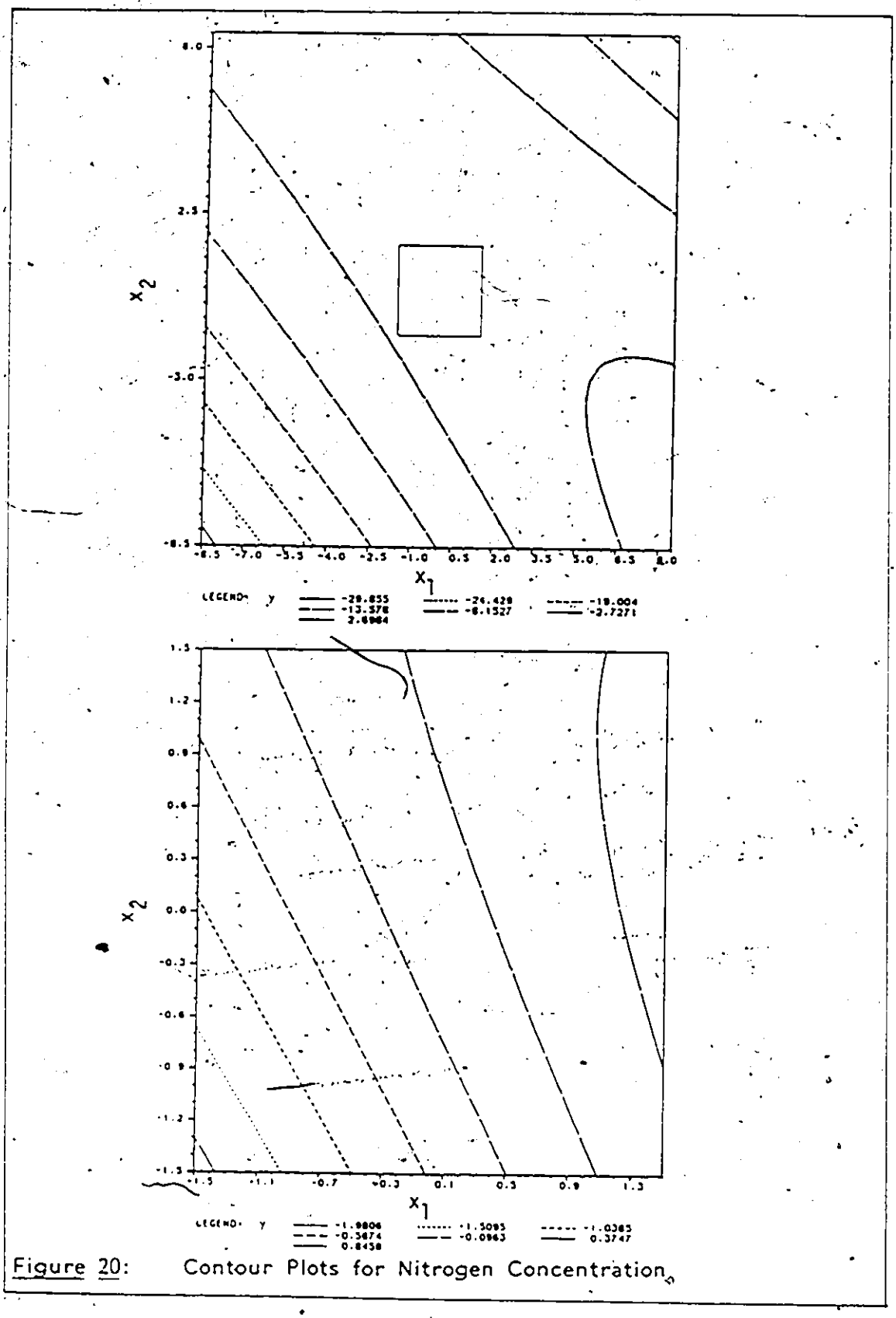

Figure 20: Contour Plots for Nitrogen Concentration

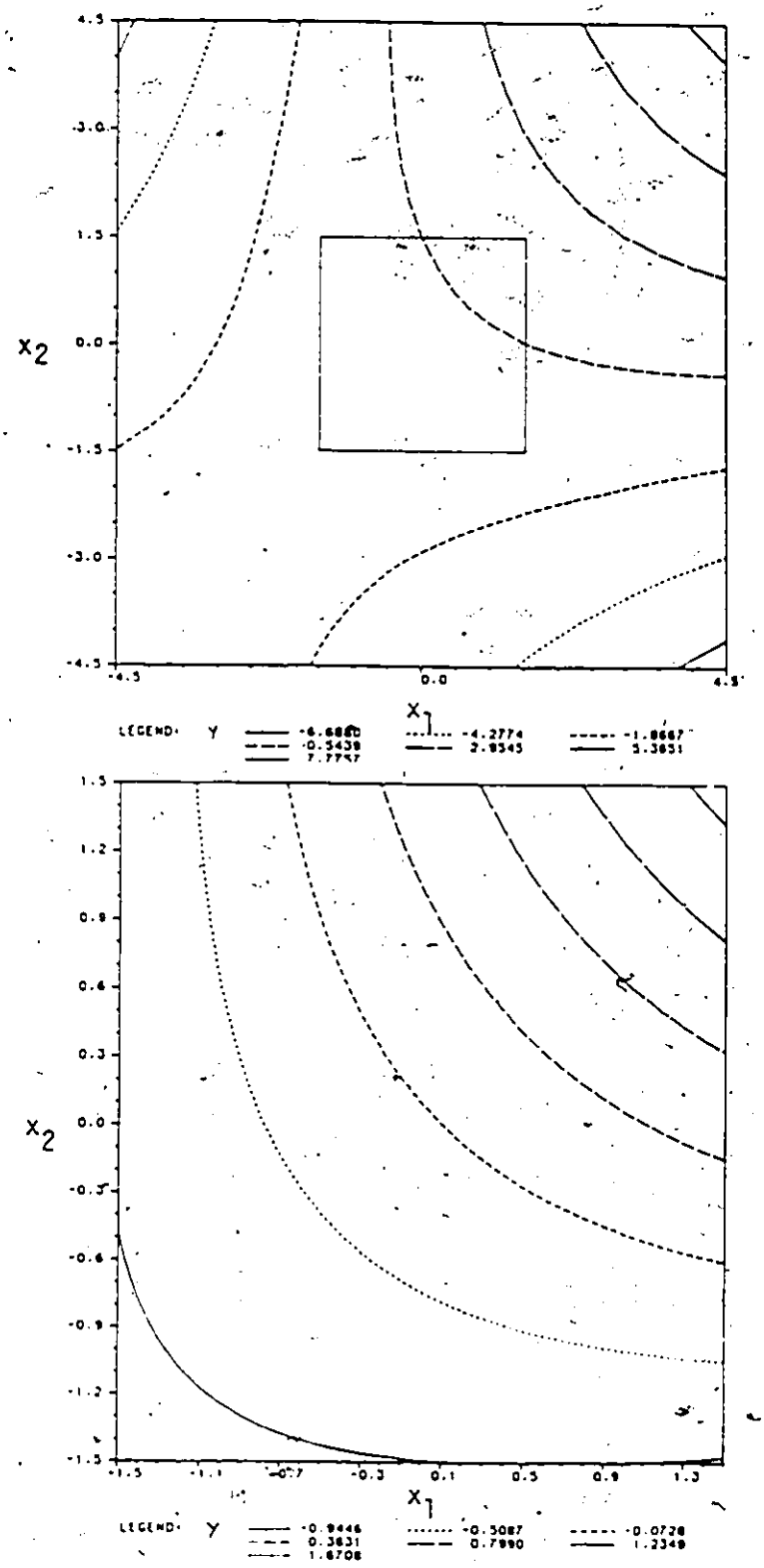

Figure 21: Contour Plots for Sulfur Concentration

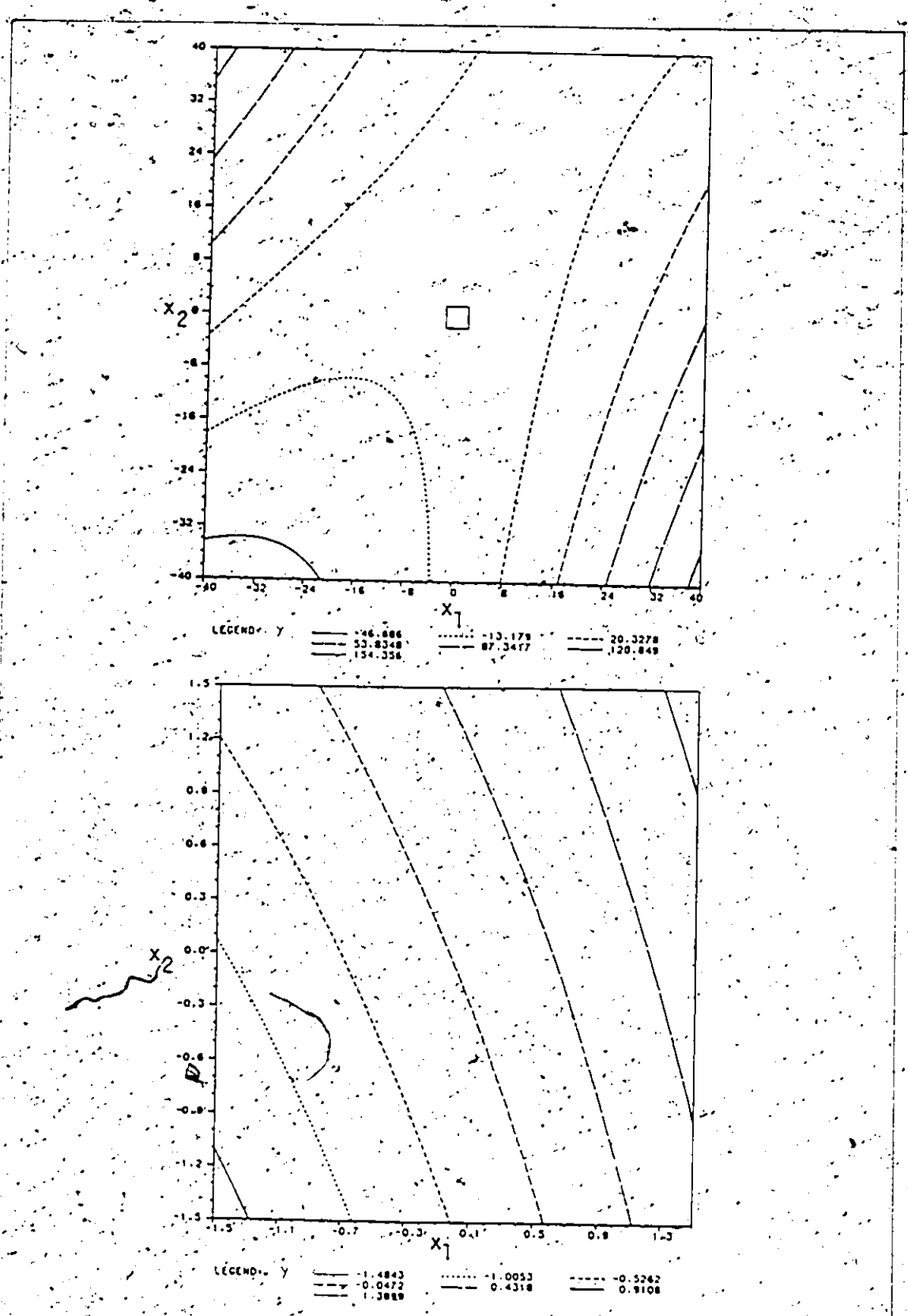

Figure 22: Contour Plots for Density

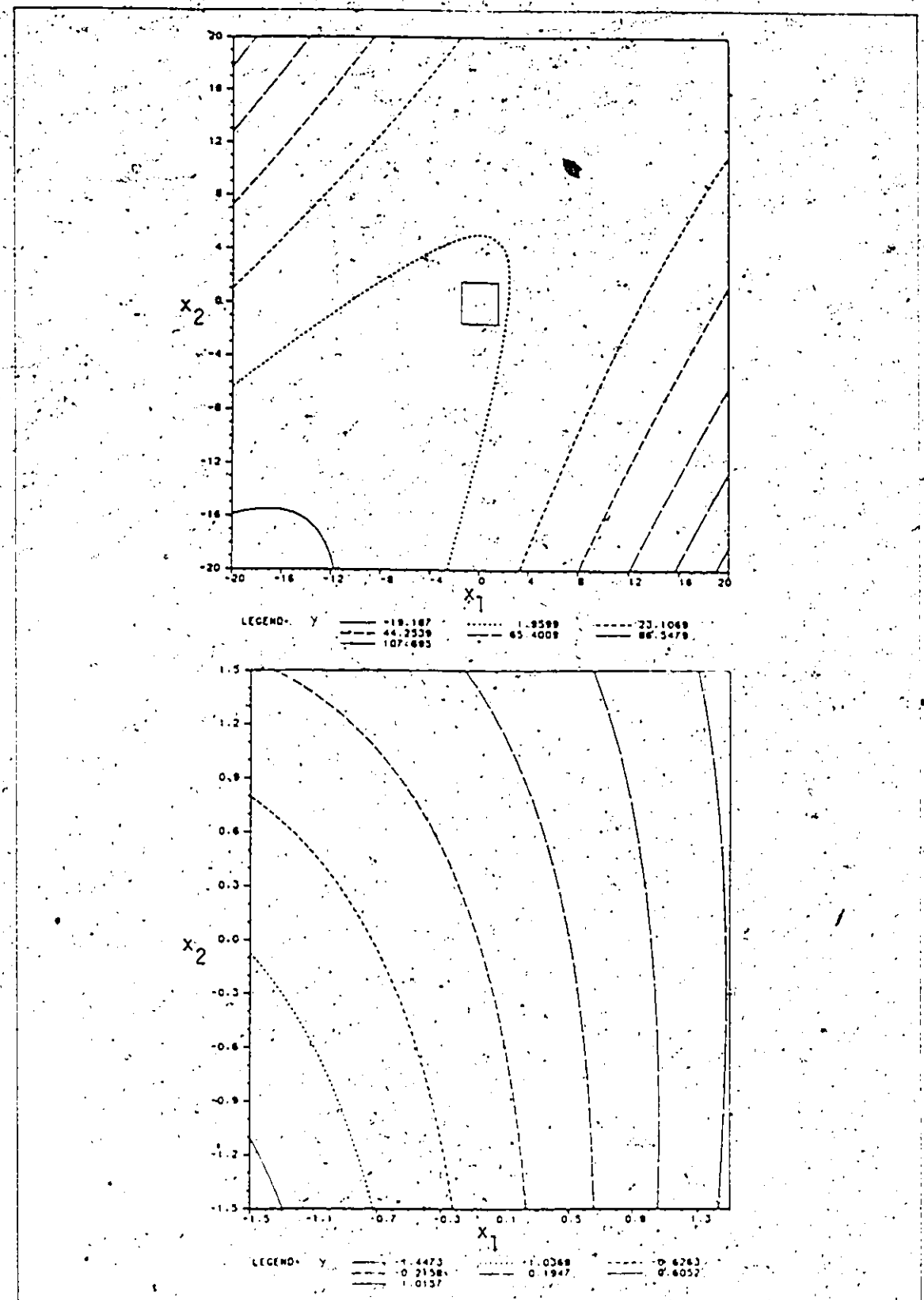

Figure 23: Contour Plots for Viscosity

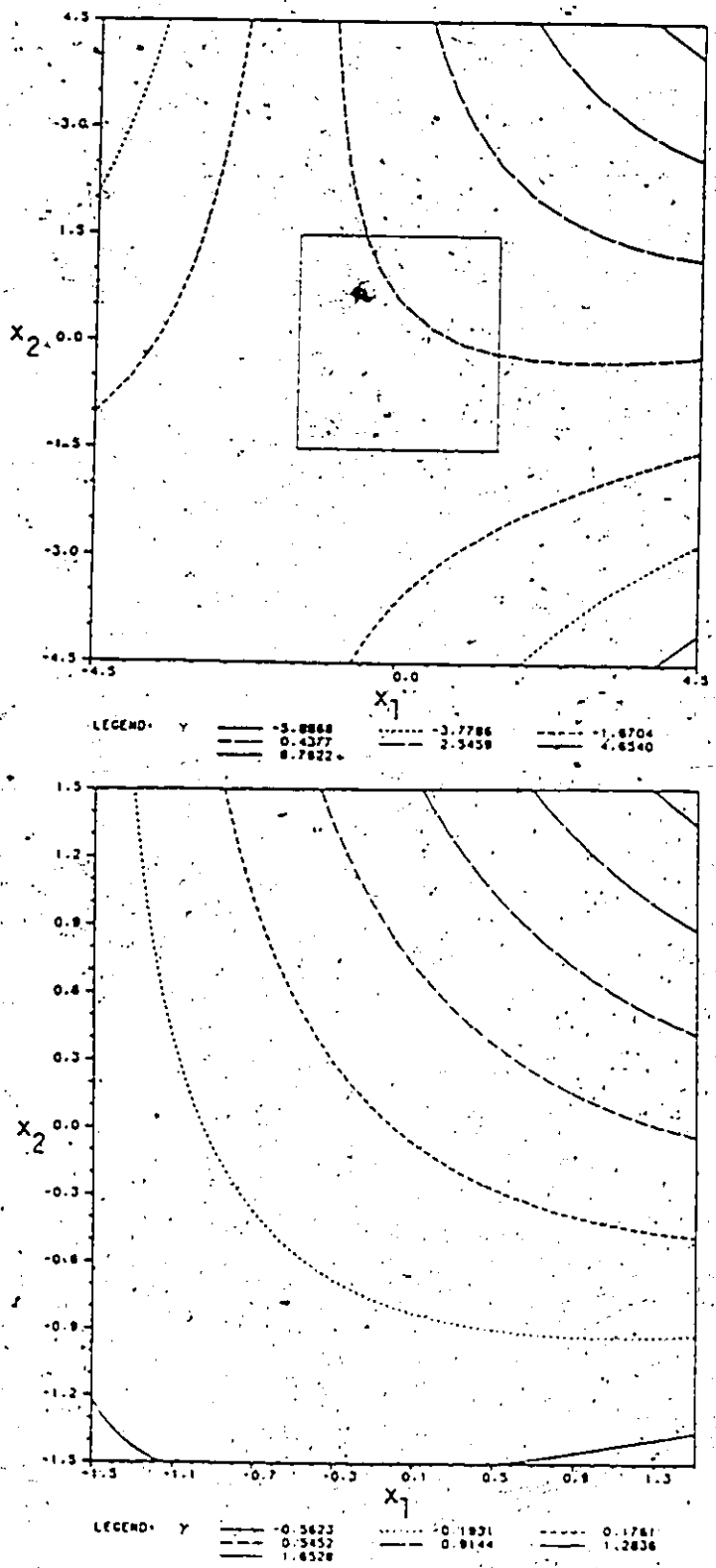

Figure 24: Contour Plots for Mid-Boiling-Point

7.3.2.4 Contour-Plots

The response surface can be better visualized with the help of contour-plots. These are shown in Figure 20 to Figure 24. In each of these figures the plot at the top shows the overall response surface including the stationary point for an expanded region, whereas the plot at the bottom focuses on only the selected range of the design region.

All these plots indicate that within the design region the minimum expected value of each of the five performance criteria will be obtained at the point (-1,-1). This is the catalyst number 13. The above conclusion was not in complete agreement with the actual results. Both catalysts (7 and 11) at the neighboring points $(0,-\sqrt{2})$ and $(-\sqrt{2},0)$ respectively gave better performance than the catalyst number 13 at point (-1,-1). To resolve this conflict it was thought best to repeat these three catalysts and evaluate their performance again.

7.3.2.5 Results of Three Repeat Runs

Catalysts 17, 18 and 19 were prepared with the compositions corresponding to points $(-\sqrt{2},0)$, (-1,-1) and $(0,-\sqrt{2})$ of the central-composity design. Their preparation and testing was done in exactly the same manner as was done for the previous catalysts. They were each run in the hydrotreatment tests and the oil samples were drawn at the standard test conditions. The results of the catalyst testing as well as the results obtained from the analysis of the oil samples are shown in Table 18. The results obtained with the previous three catalysts are also listed in this table for comparison.

Table 18: Results of Three Repeat Catalysts

	Design Designations					
	$(-\sqrt{2},0)$		$(-1,-1)$		$(0,-\sqrt{2})$	
Cat. No:	11	17	13	18	7	19
Run No:	9	17	1	18	5	19
CATALYST TESTING						
Density (bulk)(g/ml)	0.7911	0.7623	0.7934	0.7659	0.6726	0.6831
BET Surface Area(m^2/g)	288	293	266	251	253	261
Chemical Composition						
SiO_2	25.14	25.33	23.11	22.89	34.91	35.01
Al_2O_3	71.01	69.83	72.83	71.99	63.30	64.18
NiO	1.69	1.53	1.33	1.54	1.13	1.33
MoO_3	3.88	3.67	4.31	4.09	3.71	4.09
OIL SAMPLES ANALYSIS						
N(wt.%)	0.2659	0.2431	0.2638	0.2719	0.2618	0.2655
S(wt.%)	0.26	0.23	0.32	0.33	0.31	0.33
Density (g/ml)	0.9337	0.9313	0.9352	0.9381	0.9345	0.9351
Visc.(cp)	61.1	62.3	65.5	64.3	63.0	64.1
An.Pt.(°C)	52.9	51.5	53.4	55.1	52.8	51.8
Mid-BP(°C)	390.8	388.9	402.5	401.0	391.6	398.1

The results obtained with the repeat runs were close to the ones obtained earlier. Catalyst number 17 gave the best performance out of the three repeated catalysts. Therefore, this was considered the optimum point within the design region. The explanation for the little discrepancy between the conclusions based on the mathematical analysis of the central-composite design and physical observations was the fact that the model fitting for a given data always smoothes out the small variations in a particular region. Because of this nature of the model

fitting procedure, although the point (-1,-1) gave slightly higher values of nearly all performance criteria than the two neighboring points $(-\sqrt{2},0)$ and $(0,-\sqrt{2})$, the model averaged out the values and pointed towards point (-1,-1) as an optimum. The results of the sixteen design runs are shown on the pictorial presentation of the design model in Figure 28 to Figure 32.

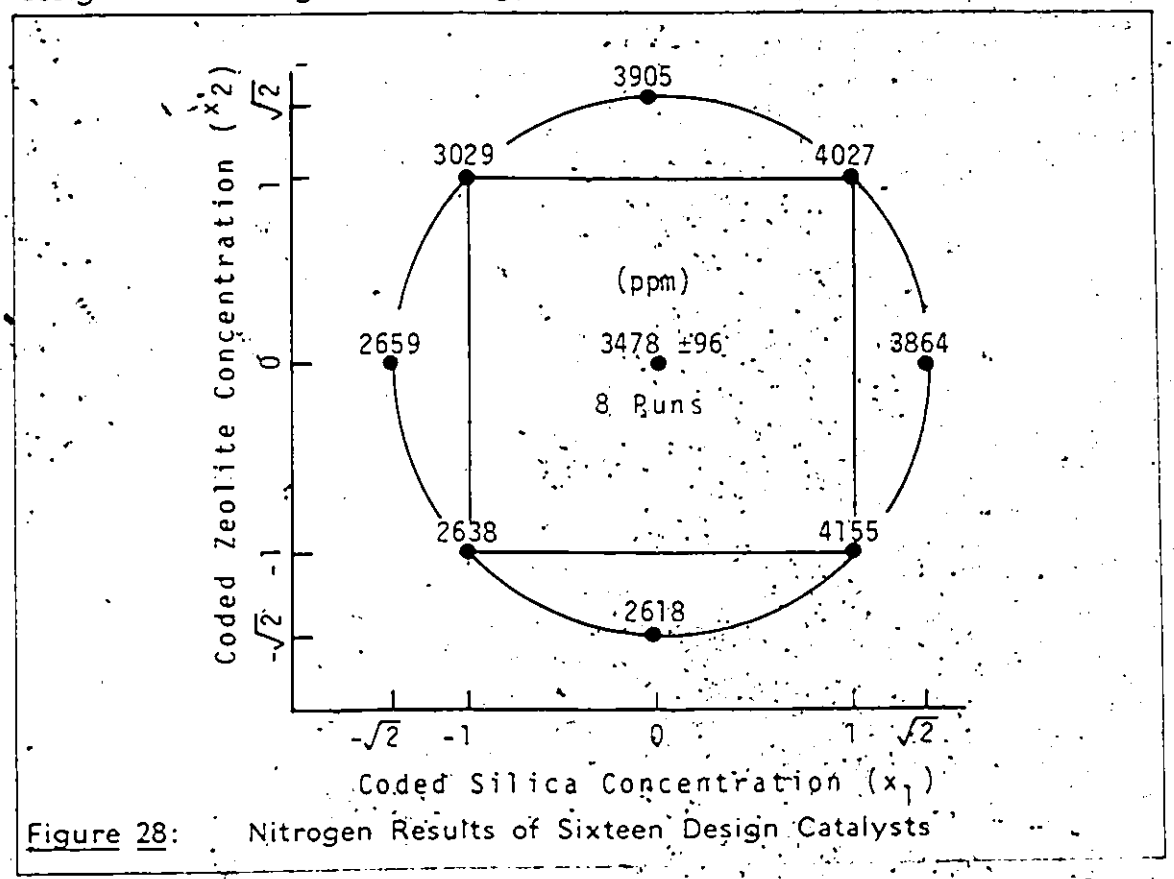

Figure 28: Nitrogen Results of Sixteen Design Catalysts

These figures support the above explanation. Looking at these figures, it can be seen that nearly at all levels of zeolite concentrations, the values of the these properties decrease with decrease in the concentration of silica. This indicated that a catalyst with no silica would probably perform the best. However, our

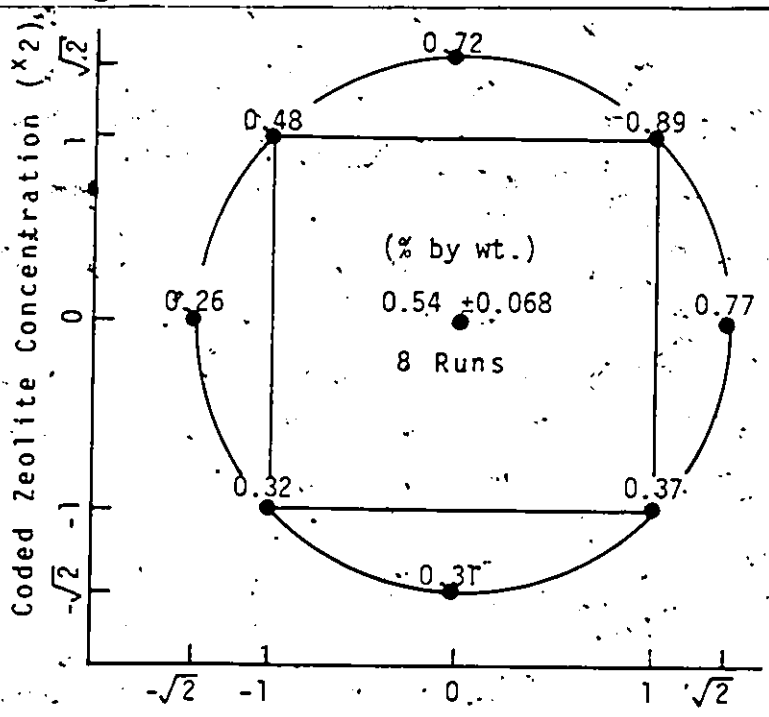

Figure 29: Sulfur Results of Sixteen Design Catalysts

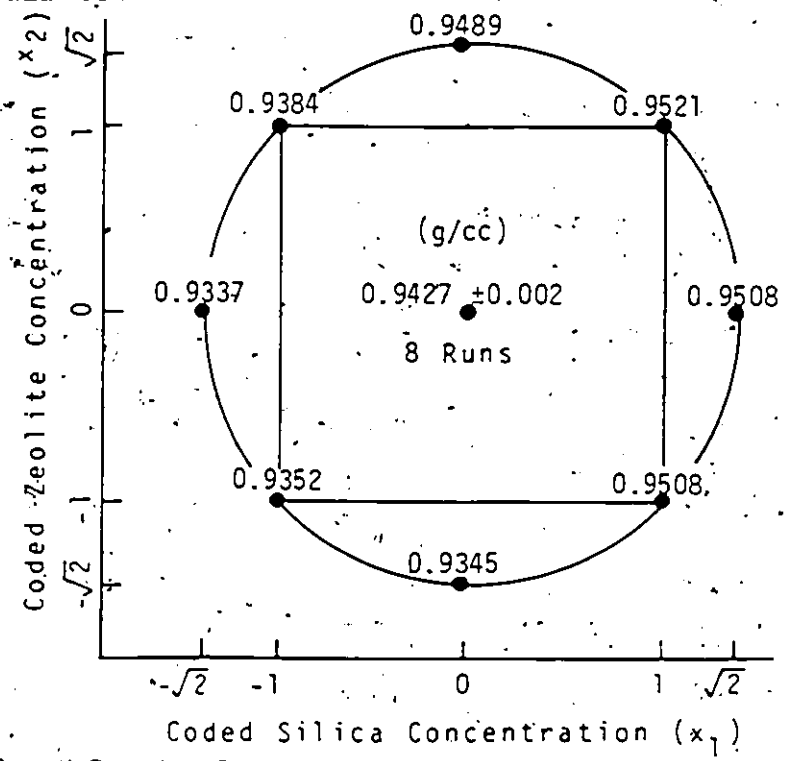

Figure 30: Density Results of Sixteen Design Catalysts

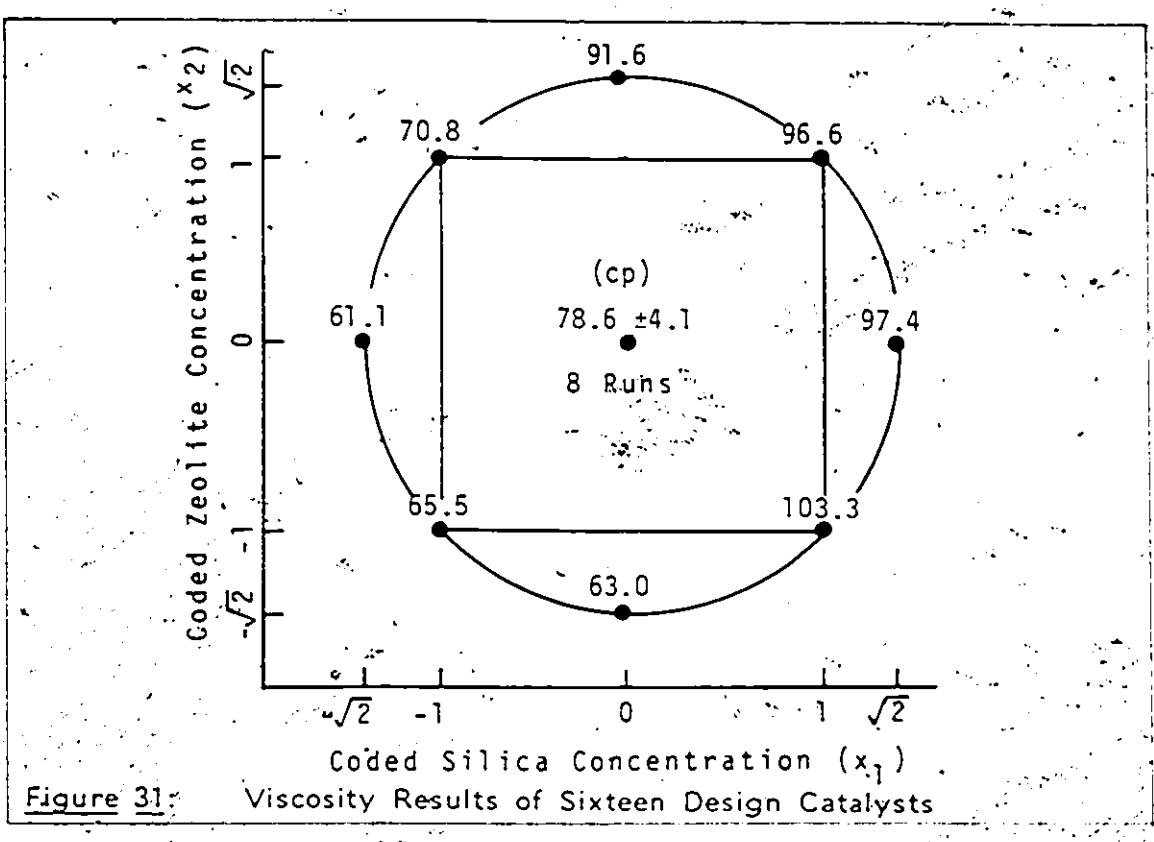

Figure 31: Viscosity Results of Sixteen Design Catalysts

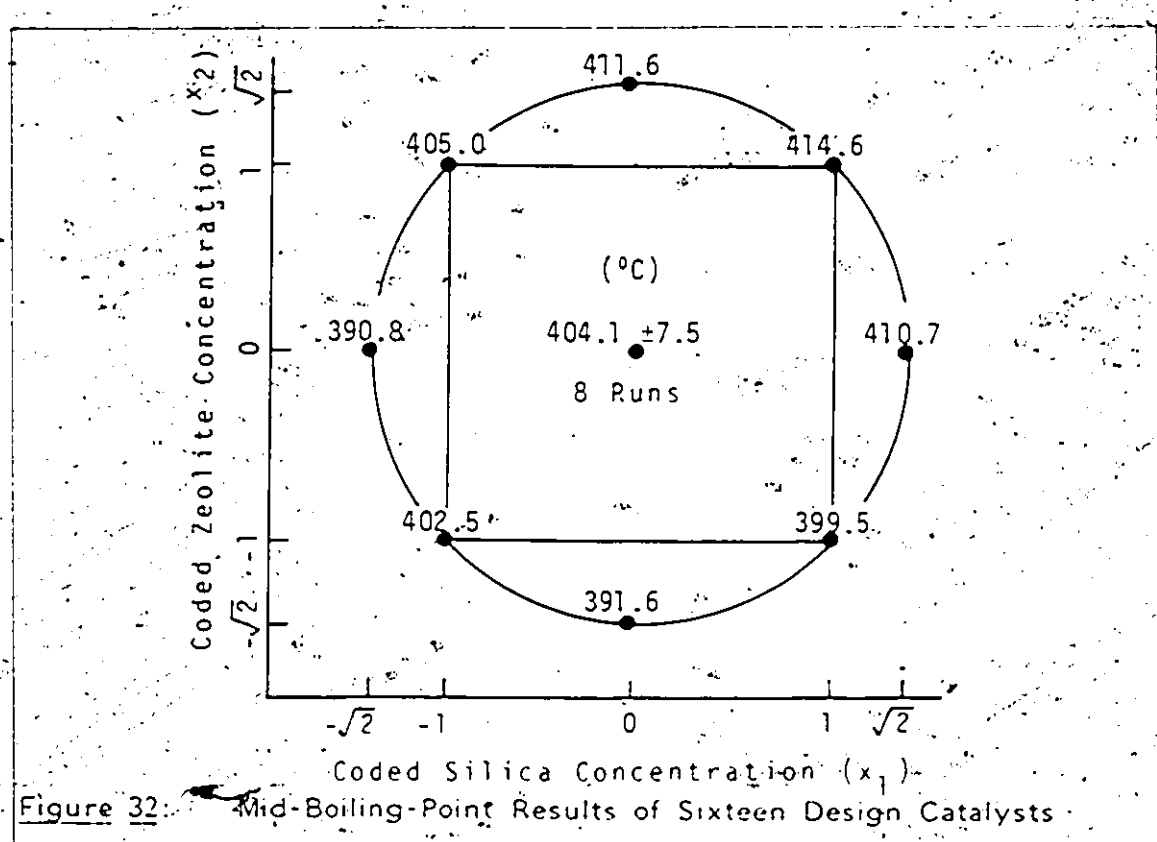

Figure 32: Mid-Boiling-Point Results of Sixteen Design Catalysts

preliminary study supported the addition of silica for improving catalyst properties. To further substantiate the earlier findings, catalyst 20 was prepared with same zeolite concentration as that of the above optimum point (-/2,0), with no silica added. The performance of this catalyst was tested in the same way as earlier. The results are tabulated in Table 19. From this table it was seen that the catalyst containing no silica gave worse performance than the optimum point catalyst.

Table 19: Results Obtained With Catalyst No. 20

Cat No.	Run No.	x_1	x_2	N- ppm	S wt.%	Density g/cc	Viscosity cp	Aniline point °C	Mid-B-pt °C
20	20	*	*	2853	0.42	0.9498	90.8	51.6	407.8

* * :- The catalyst support was 25% zeolite and rest alumina.

7.3.3 Conclusion

In conclusion of this part of study, it was found that the catalyst support material containing 25% by wt. zeolite material, 10% by wt. silica and the rest alumina gave the best performance for sulfur and nitrogen removal, and also gave the product oil with lowest density, viscosity and the mid-boiling point, out of the catalyst tested as per the central-composite design. This design was useful in defining the response surfaces for different criteria with the minimum number of runs and was useful in pointing towards the direction of optimum.

The second major outcome of this part of study was the confirmation of the good reproducibility of the entire catalyst preparation and testing scheme.

7.4 KINETIC STUDY

This part of the present study mainly deals with a single catalyst and, the results obtained from the hydrotreatment of the heavy gas oil in the trickle-bed reactor are presented here. The data obtained for hydrodesulfurization (HDS) and hydrodenitrogenation (HDN) was fitted to the kinetic models and the resulting rate constants were evaluated. Data are obtained at different temperatures to get estimates of the activations energies for these reactions. The performance of the trickle-bed reactor, heat and mass transfer effects and the effectiveness factor considerations are also discussed.

7.4.1 Catalyst Used for Kinetic Study

The catalyst used in this part of the study was prepared with the optimum composition found in the previous section. The catalyst preparation and testing schemes were exactly the same as were used earlier. These have been discussed in the experimental sections. The properties of the prepared catalyst and the results of the analysis of its physical properties and the chemical composition are listed in Table 20.

Table 20: Physical Properties and Chemical Composition of Catalyst Used for Kinetic Study

Cat No.	Bulk Density g/ml	Pore Vol. ml/g	BET Surface Area m^2/g	Chemical Composition SiO_2	Al_2O_3	NiO	MoO_3
30	0.7956	0.597	293	25.53	70.94	2.24	5.37

7.4.2 SEM Imaging and Energy-Dispersive X-Ray Analysis

The catalyst used for this study was tested for distribution of its constituent atoms mainly Ni, Mo, Si, Al and the rare-earth atoms La and Nd by scanning-electron microscope x-ray dot maps. These are shown in Figure 33 to Figure 37.

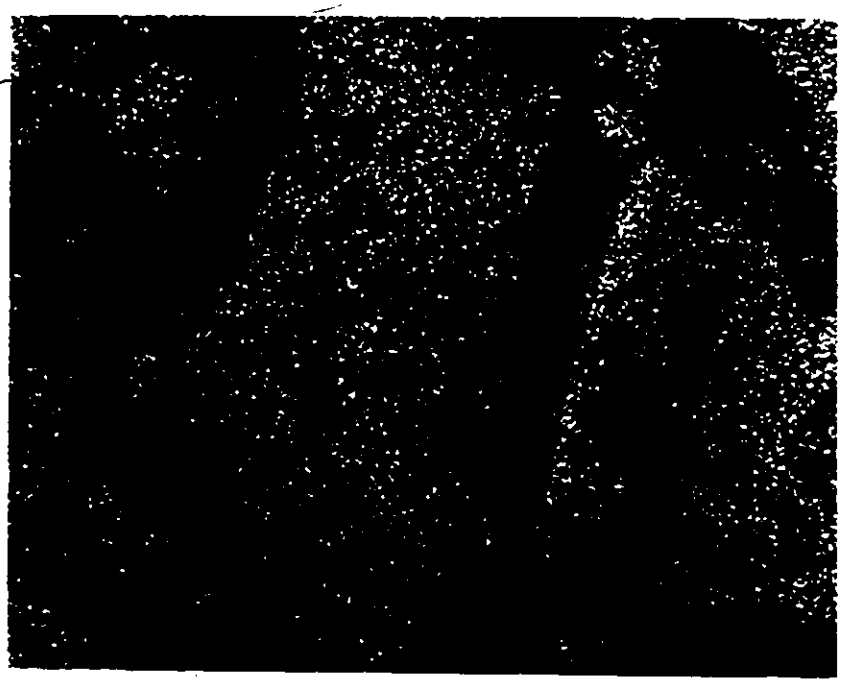

Figure 33: SEM Image for Aluminium. The bright dots represent aluminium distribution.

Figure 34: SEM Image for Silicon. The bright dots represent silicon distribution.

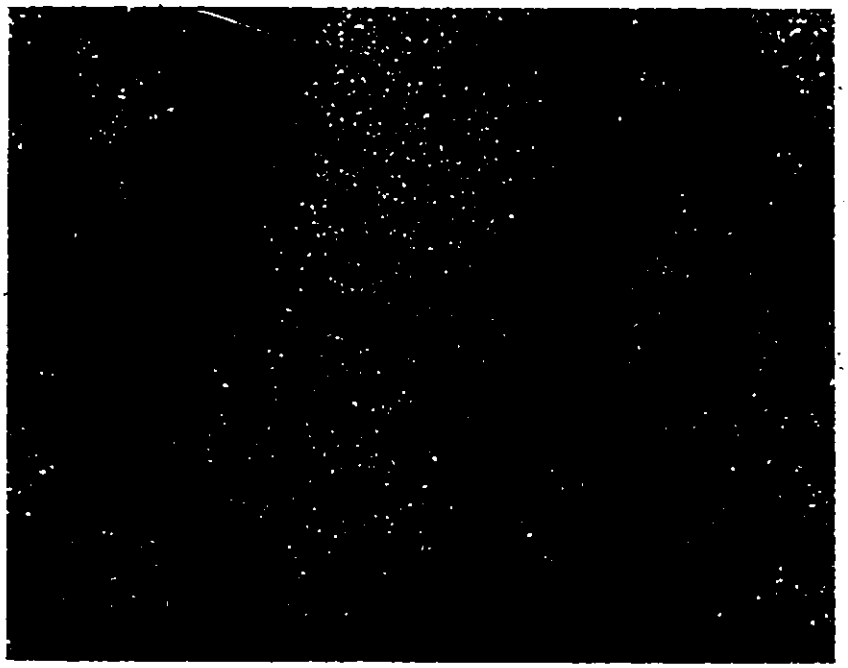

Figure 35: SEM Image for Nickel. The bright dots represent nickel distribution.

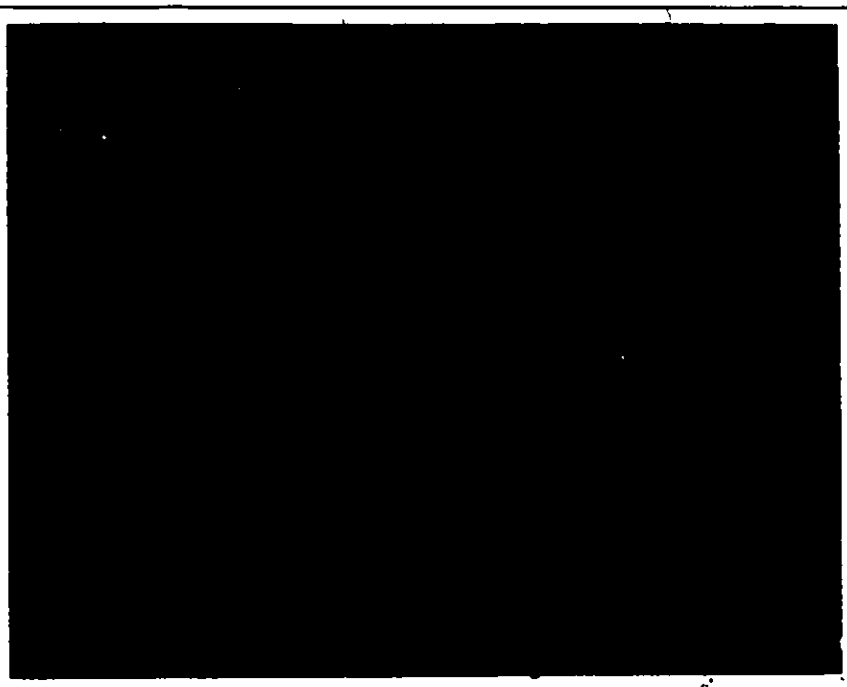

Figure 36: SEM Image for Molybdenum. The bright dots represent molybdenum distribution.

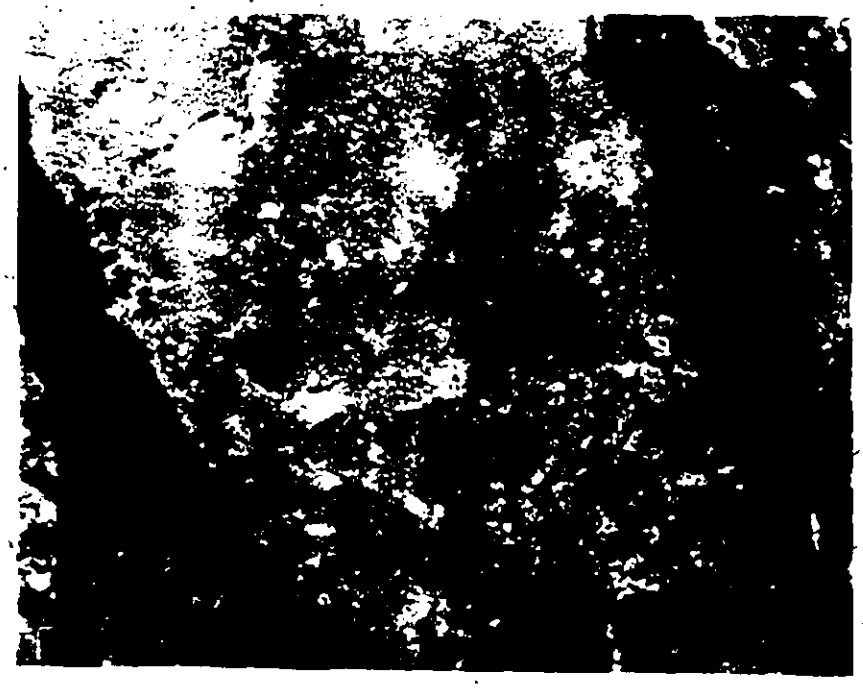

Figure 37: SEM Image for Lanthanum. The bright spots represent lanthanum distribution.

These figures indicate a uniform distribution of Si, Al, Ni, and Mo atoms throughout the catalyst matrix. Figure 37 indicates the distribution of the zeolite material in the catalyst support as depicted by the bright spots showing the agglomerates of La(Nd) rare-earth atoms of the zeolite material. This figure too indicated quite a good mixing of the zeolite material in the prepared catalyst. Since the zeolite material was added in the form of a powder, the uniformity of mixing can not be as good as the other atoms indicated in the remaining four figures.

7.4.3 X-Ray Diffraction Studies

X-ray diffraction patterns were taken for the catalyst as well as the original zeolite powder. This study confirmed the zeolite type. The x-ray diffraction spectrogram showed the characteristic peaks typical of the type of zeolite (faujasite) used in the preparation of catalyst. However, the actual amount of crystallinity in the catalyst matrix could not be accurately estimated. This study confirmed that the final catalyst consisted of crystalline particles well mixed in the amorphous support material.

7.4.4 Operating Conditions Used

The trickle-bed reactor was used to collect the kinetic data for mainly HDS and HDN reactions. The reactor was operated at a constant pressure of 1000 psig and a gas flow rate equivalent of 5000 scf/bbl of oil was maintained. 350°C, 375°C, 400°C, and 425°C were the four

temperatures selected. The high temperature of 425°C was selected mainly to see the catalyst performance at higher temperature. The liquid flow rates were varied to get liquid-hourly-space-velocity (LHSV) of 1.0, 1.333, 2.0 and 4.0. These values of LHSV were selected to get (1/LHSV) factors as 1.0, 0.75, 0.5, and 0.25. Although some of the literature indicated using much lower values of LHSV to get (1/LHSV) factors as high as high as 4.0, it was considered quite undesireable. Our experience with the present heavy gas oil had shown that operating a trickle-bed reactor with such low liquid flow rates gives excessive coke formation on the catalyst. The present catalyst had quite enhanced hydrogenolysis activity due to addition of highly acidic material, and this would only have resulted in very fast catalyst deactivation at low liquid flow rates.

7.4.5 Kinetic Study Results

The results obtained with the hydrotreatment of heavy gas oil using the above mentioned catalyst 30 are presented in this section. 8 ml of catalyst was used and it was diluted with equal volume of inert material (α-alumina). The operating procedure has already been described in the experimental section. The catalyst was first conditioned for a period of 20 hours at the standard operating conditions (i.e. 375°C 1000 psig; LHSV of 1.5 and gas flow rate of 5000 scf/bbl).

After the initial running-in (stabilization) period of twenty hours, the kinetic study runs were started with the lowest temperature of 350°C, followed by the higher temperatures in increasing order. Liquid

Table 21: Results of Kinetic Runs (1)

Pressure = 1000 psig
Gas Flow Rate = 5000 scf/bbl

Temperature (°C)	LHSV	Sulfur (wt.%)	Nitrogen ppm	Formation of gas (wt.%)
Original Oil		3.05	4831	
350	4.0	1.04	3650	0.0864
350	2.0	0.70	3341	0.1734
350	4/3	0.53	3094	0.2553
350	1.0	0.40	2946	0.3379
375	4.0	0.72	3214	0.1929
375	2.0	0.39	2757	0.2984
375	4/3	0.25	2235	0.4198
375	1.0	0.13	2063	0.5585
400	4.0	0.34	2280	0.5837
400	2.0	0.13	1765	0.9576
400	4/3	0.08	1403	1.2815
400	1.0	0.04	1226	1.4651
425	4.0	0.16	1927	1.5824
425	2.0	0.04	987	1.9669
425	4/3	0.03	760	2.1747
425	1.0	0.03	738	2.6051

flow rates were changed from the maximum flow of 32 ml/hr (LHSV=4.0) to the lowest selected flow of 8 ml/hr (LHSV=1.0) for each temperature. In the begining and the end as well as in-between the two different temperature runs the operating conditions were changed to the standard operating conditions and samples were drawn. This was done to check the catalyst activity during the kinetic study.

Table 22: Results of Kinetic Runs (II)

Pressure = 1000 psig
Gas Flow Rate = 5000 scf/bbl

Temperature (°C)	LHSV	Density (g/ml)	Viscosity cp	Aniline Point (°C)	Mid-B-Pt. (°C)
Original Oil		0.9803	241.5	52.7	429.1
350	4.0	0.9575	123.0	50.4	411.8
350	2.0	0.9517	118.1	51.2	393.8
350	4/3	0.9470	94.6	51.7	396.8
350	1.0	0.9437	95.7	52.4	402.1
375	4.0	0.9490	95.7	51.6	402.1
375	2.0	0.9431	78.7	52.5	403.0
375	4/3	0.9396	68.6	54.0	389.9
375	1.0	0.9379	61.1	53.8	389.8
400	4.0	0.9428	61.5	52.6	389.6
400	2.0	0.9349	41.7	52.0	385.8
400	4/3	0.9376	31.7	53.8	382.8
400	1.0	0.9256	26.2	51.3	378.3
425	4.0	0.9343	33.9	48.9	378.0
425	2.0	0.9247	20.5	47.2	370.4
425	4/3	0.9214	17.2	46.5	368.1
425	1.0	0.9216	16.9	46.0	388.5

It was very important to make sure that each oil sample was drawn at the steady state condition. To ensure this, a waiting period of at least one hour was allowed after the setting of a new temperature. This one hour was counted from the time when the temperature inside the sand bath had reached the new set steady-state temperature. It was found sufficient to get a uniform sample. Similarly, for every new liquid flow rate setting a suitable time period depending upon the new set flow rate was allowed. It was one hour for the high flow rate setting of 32

ml/hr and longer periods were used for the lower flow rates. A time period of more than three hours was used for the flow of 8 ml/hr.

The inlet flow of the oil was measured using the 50 ml burette attached to the pump inlet. The steady state out-flow of liquid was measured by weighing the mass of sample collected in a given time period. The exit gases were analyzed with the help of an on-line gas chromatograph. The concentration of each gas in the exit stream was calculated using the calibration charts. The exit gas flow rate was measured with the wet-test meter. These data were used to calculate the total gas formation for each of the hydrotreatment runs. The overall material balance on the oil was performed for each run. The results of analysis of the samples obtained from this kinetic study are given in Table 21 and Table 22.

Table 21 gives the concentrations of sulfur in wt % and nitrogen in ppm (by wt.). The gas formation values are given in % by weight of the oil feed. It can be seen that the gas formation increases as the hydrotreatment temperature increases. These results are discussed shortly in comparison to the gas formation rates obtained from hydrotreatment without catalyst.

7.4.6 Kinetic Models

The data for the sulfur and nitrogen concentrations in the oil samples taken at various temperatures and the flow rates was fitted into the power law rate equations of the type shown below:

$$r = \frac{dC}{dt} = -k_m [C]^m \qquad (21)$$

where, C is the concentration of sulfur or nitrogen in wt. %, and m is the order of the rate equation. Using the ideal plug-flow model equation (7) and combining the effectiveness factor with the rate constant, the model equation can be integrated to yield equations (8) and (9). These are :

$$\ln \frac{C_i}{C_o} = \frac{k_1}{(LHSV)} \qquad (8)$$

$$\frac{1}{C_o} - \frac{1}{C_i} = \frac{k_2}{(LHSV)} \qquad (9)$$

where k_1 and k_2 are the first and second order rate constants, and subscripts i and o indicate the inlet and outlet concentrations of sulfur or nitrogen. The same equation can be integrated for a general case of mth order and the following equation results :

$$[C_o]^{1-m} - [C_i]^{1-m} = (m-1) \frac{k_m}{(LHSV)} \qquad (22)$$

If the left-hand-sides of the above equations are plotted against the factor(1/LHSV), then a straight line should result if that equation holds true. A SAS [58] procedure called 'PROC REG' was used for fitting the best possible straight line through the data points. This program uses a least-squares regression technique to fit a linear model into a given set of data points. In the present case, the model was nothing but a straight line passing through origin. To supress the intercept 'NOINT' was used as an option in the 'PROC REG' procedure.

Table 23: Rate constants, COD and Prob>F for Sulfur Data (Order 1 to 1.4)

Pressure = 1000 psig
Gas Flow Rate = 5000 scf/bbl

Temperature (°C)		Order of Rate-Equation 1.0	1.1	1.2	1.3	1.4
350	k	2.319	2.273	2.233	2.201	2.176
	COD	0.9594	0.9654	0.9712	0.9766	0.9815
	P>F	0.0035	0.0028	0.0021	0.0015	0.0011
375	k	2.424	3.517	3.637	3.788	3.975
	COD	0.9760	0.9835	0.9895	0.9937	0.9957
	P>F	0.0016	0.0009	0.0005	0.0002	0.0001
400	k	4.902	5.337	5.889	6.587	7.465
	COD	0.9624	0.9744	0.9846	0.9822	0.9966
	P>F	0.0037	0.0018	0.0008	0.0003	0.0001
425	k	5.862	6.608	7.576	8.832	10.463
	COD	0.9180	0.9284	0.9379	0.9463	0.9533
	P>F	0.0102	0.0083	0.0067	0.0054	0.0043

This procedure gives analysis of regression which includes among other parameters, a coefficient of determination (COD). This is a ratio of Sum of Squares (model) and Sum of Squares (total). This value represents the quality of fit of a given model to the given data.

The data for the nitrogen fitted quite well to the pseudo second order model but the sulfur results did not give a good fit for either first or the second order models. Therefore it was decided to try orders between 1.0 and 2.0. Orders 1.1, 1.2 ... up to 1.9 were then tried for both nitrogen and sulfur. The results of the linear-regression are shown in Table 23 to Table 26.

Table 24: Rate Constants, COD and Prob>F for Sulfur Data (Order 1.5 to 2)

Pressure = 1000 psig
Gas Flow Rate = 5000 scf/bbl

Temperature (°C)		Order of Rate-Equation 1.5	1.6	1.7	1.8	1.9	2.0
350	k	2.158	2.146	2.140	2.140	2.147	2.160
	COD	0.9860	0.9898	0.9931	0.9956	0.9975	0.9985
	P>F	0.0007	0.0004	0.0002	0.0001	0.0001	0.0001
375	k	4.200	4.469	4.789	5.168	5.612	6.134
	COD	0.9953	0.9923	0.9867	0.9786	0.9681	0.9555
	P>F	0.0001	0.0003	0.0006	0.0013	0.0024	0.0040
400	k	8.571	9.964	11.722	13.944	16.760	20.340
	COD	0.9973	0.9943	0.9875	0.9773	0.9640	0.9483
	P>F	0.0001	0.0002	0.0006	0.0015	0.0029	0.0051
425	k	12.584	15.348	18.963	23.703	29.940	38.174
	COD	0.9588	0.9628	0.9656	0.9672	0.9680	0.9681
	P>F	0.0036	0.0031	0.0027	0.0025	0.0025	0.0024

In these tables the values of the rate constants (which were nothing but the values of slopes of the fitted straight lines), the coefficient of determination (COD) and the Prob>F are listed for each order for all temperatures. The values of COD close to the value 1.0 indicate a better fit of a model. Also a low value of the factor P>F is indicative of a good fit of data to a given model. This value indicates the probability of getting a greater F-sfatistic than observed if the estimated value of the model parameter (the k-value in the present case) is zero.

Table 25: Rate Constants, COD and Prob>F for Nitrogen Data (Order 1 to 1.4)

Pressure = 1000 psig
Gas Flow Rate = 5000 scf/bbl

Temperature (°C)		Order of Rate-Equation 1.0	1.1	1.2	1.3	1.4
350	k	0.578	0.635	0.699	0.769	0.846
	COD	0.9515	0.9530	0.9545	0.9560	0.9575
	P>F	0.0046	0.0044	0.0042	0.0040	0.0038
375	k	0.966	1.079	1.206	1.349	1.510
	COD	0.9727	0.9749	0.9770	0.9790	0.9810
	P>F	0.0019	0.0017	0.0015	0.0013	0.0011
400	k	1.595	1.825	2.091	2.400	2.758
	COD	0.9560	0.9601	0.9641	0.9680	0.9718
	P>F	0.0040	0.0034	0.0029	0.0025	0.0020
425	k	2.288	2.691	3.174	3.755	4.454
	COD	0.9513	0.9554	0.9593	0.9630	0.9664
	P>F	0.0046	0.0041	0.0035	0.0031	0.0026

It can be seen from these tables that for nitrogen data, a 2nd order model fits the data values at all temperatures. This is indicated by values of COD close to 1.0 and low values of the P>F factors for all temperatures for the order 2.0. Therefore it was concluded that with this catalyst the nitrogen removal (HDN) followed a pseudo-second order kinetics.

In the case of the sulfur removal (HDS) data, the choice of the order of reaction was not that straight forward. As can be seen from Table 23 and Table 24, the data at 350°C and 425°C gives a better fit

Table 26: Rate Constants, COD and Prob>F for Nitrogen Data (Order 1.5 to 2)

Pressure = 1000 psig
Gas Flow Rate = 5000 scf/bbl

Temperature (°C)		Order of Rate-Equation 1.5	1.6	1.7	1.8	1.9	2.0
350	k	0.931	1.025	1.128	1.242	1.368	1.507
	COD	0.9590	0.9605	0.9619	0.9634	0.9648	0.9662
	P>F	0.0036	0.0034	0.0032	0.0030	0.0028	0.0027
375	k	1.690	1.893	2.122	2.380	2.670	2.997
	COD	0.9828	0.9846	0.9862	0.9877	0.9892	0.9905
	P>F	0.0010	0.0008	0.0007	0.0006	0.0005	0.0004
400	k	3.174	3.657	4.220	4.876	5.642	6.537
	COD	0.9853	0.9787	0.9819	0.9849	0.9877	0.9901
	P>F	0.0017	0.0013	0.0010	0.0008	0.0006	0.0004
425	k	5.297	6.317	7.554	9.058	10.889	13.124
	COD	0.9695	0.9723	0.9748	0.9769	0.9787	0.9802
	P>F	0.0020	0.0020	0.0017	0.0015	0.0013	0.0012

Table 27: Final Rate Constants for HDS and HDN

Pressure = 1000 psig
Gas Flow Rate = 5000 scf/bbl

Temperature (°C)	HDN 2nd Order Rate Constant ($hr^{-1}(wt.\%)^{-1}$)	HDS 1.5th Order Rate Constant ($hr^{-1}(wt.\%)^{-0.5}$)
350	1.5067	2.158
375	2.9971	4.200
400	6.5369	8.571
425	13.1237	12.584

for a 2nd order model, whereas, the data at 375°C and 400°C fitted more appropriately to the 1.5th order kinetics. To resolve this conflict, the values of the COD and P>F were compared for all four temperatures for 2nd and 1.5th order kinetic. It was found that the degree of fit did not deteriorate very much if we go from 2nd order to 1.5th order model in case of the data at temperatures 350°C and 425°C. However, for the data at 375°C and 400°C, shifting the order of reaction from 1.5 to 2.0, the degree of fit as indicated by the COD and P>F values, declines by a much greater value. Therefore, 1.5th order power low model was found to be more appropriate at all temperatures to represent the sulfur (HDS) data for the present catalyst.

Table 28: Activation Energies for HDN and HDS

Arrhenius Equation:

$$k = A \exp(-E/RT)$$

where, k is the rate constant,
A is the coefficient,
E is the activation Energy,
T is absolute temperature, and
R is the gas constant.

	HDN 2nd Order	HDS 1.5th Order
Slope	-12.6447	-10.4741
Intercept	20.6640	17.6040
COD	0.9980	0.9910
P>F	0.0010	0.0045
E (K Cal/g mole)	25.12	20.81
A (Units of k)	9.4248×10^8	4.4188×10^7

The values of the rate constants obtained from the above analysis are listed in Table 27 for both sulfur removal and the nitrogen removal at the four temperatures. Standard Arrhenius type of correlation was used for evaluating the respective activation energies. The values of ln(k) are plotted against (1000/T°K). Again to get the best fit, SAS subroutine mentioned above was used. The corresponding values of the slope and intercepts, COD and P>F as well as the activation energies (E = -slope*1000*R) and the coefficient A (A = Exp(intercept)) obtained for both nitrogen and sulfur data are listed in Table 28.

7.4.7 : Material Balance

Mass balance was done on the oil feed and the exit stream. Inlet flow was measured by volume. The steady state out-flow of oil was determined by weighing the oil collected in a known time period. Amount of hydrocarbons in the exit gas stream were calcululated from the exit gas flow rates and compostions as determined by the gas chromatographic analysis.

Amount of total coke formation on the catalysts was determined by removing the used catalyst from the reactor after washing it with a mixture of 25% by volume benzene in acetone. It was then weighed and calcined at 700°C for a period of 12 hours in air. This was found sufficient to oxidize all the deposit on the catalyst. Constant weight of catalyst resulted within about eight hours. The difference in weight was the measure of the weight of coke deposited on the catalyst.

Table 29: Material Balance

Basis: One Hour
All units in g

Oil In	$+H_2$	-S	-N	-Gas	Oil Out	Balance
31.3696	0.0872	0.6305	0.0371	0.0271	30.7319	0.0403
15.6848	0.0894	0.3686	0.0234	0.0272	15.3769	-0.0219
10.4566	0.0941	0.2635	0.0182	0.0267	10.4381	-0.1958
7.8424	0.0729	0.2078	0.0148	0.0265	7.5995	0.0667
31.3696	0.1412	0.7309	0.0507	0.0605	30.7185	-0.0499
15.6848	0.1082	0.4172	0.0325	0.0468	15.0801	0.2164
10.4566	0.1014	0.2928	0.0271	0.0439	10.1836	0.0106
7.8424	0.0800	0.2290	0.0217	0.0438	7.4978	0.1301
31.3696	0.2698	0.8501	0.0800	0.1831	30.3251	0.2010
15.6848	0.1474	0.4580	0.0480	0.1502	14.9991	0.1769
10.4566	0.0920	0.3106	0.0358	0.1340	10.0000	0.1942
7.8424	0.0737	0.2361	0.0283	0.1149	7.3057	0.2312
31.3696	0.1694	0.9066	0.0911	0.4964	29.8918	0.1731
15.6848	0.1427	0.4721	0.0603	0.3085	14.7398	0.2468
10.4566	0.0774	0.3158	0.0426	0.2274	9.6924	0.2558
7.8424	0.0784	0.2368	0.0321	0.0204	7.1334	0.3142

The coke formation rate is a function of the operating conditions as well as the age of the catalyst. It was very difficult to know exactly how much of coke was formed on the catalyst within a given period of time for the material balance calculations. Therefore, it was excluded from this analysis.

Table 29 shows the results of material balance for the sixteen kinetic runs. The results are listed for the kinetic runs at 350°C first,

followed by other temperatures in increasing order. This table is prepared taking one hour period as a basis for all calculations. The first column of this table gives the mass feed rate of oil and the second column gives the mass of hydrogen addition to oil. Column three and four give the loss of mass because of sulfur and nitrogen removal, and column five is the loss of hydrocarbons in the exit gas stream. Column six gives the weight of oil sample collected in one hour and the the last column is the net material balance.

The positive balance indicates the loss of oil which is most likely used up in the coke formation. In general, it can be concluded from the values of the material balance that for the present study, a good overall material balance of the liquid feed is achieved and most of the liquid feed as well as the product could be accounted for.

7.4.7.1 - Hydrogen Consumption

Material balance on hydrogen was not performed since the inlet flow of hydrogen could not be measured. Only the exit gas flow and the composition was determined. hydrogen is consumed for conversion of S to H_2S and N to NH_3, and for hydrogenation of unsaturated and cracked hydrocarbons. Consumption of hydrogen for S and N conversions was directly determined from the amounts of S and N removed. Hydrogen used for hydrogenation was calculated from the hydrogen analysis of the feed and the product oil.

Table 30: Hydrogen Consumption

Pressure = 1000 psig
Gas Flow Rate = 5000 scf/bbl

Temperature (°C)	LHSV	Hydrogen Consumption (Scf/bbl)
350	4.0	565
350	2.0	918
350	4/3	1341
350	1.0	1392
375	4.0	773
375	2.0	1104
375	4/3	1471
375	1.0	1546
400	4.0	1328
400	2.0	1456
400	4/3	1396
400	1.0	1477
425	4.0	960
425	2.0	1447
425	4/3	1245
425	1.0	1564

A small amount of hydrogen was consumed in hydrogenating the cracked gaseous products and hence could not be considered in these calculations. This is expected to be only a small fraction of the total hydrogen consumption, and thus would not have changed the total consumption figures significantly. Total hydrogen consumption calculated as described above is given in Table 30.

The values of the hydrogen consumption are very sensitive to the concentrations of S, N and H in the oil, and due to the errors in the

analysis of oil samples, no clear correlation could be observed between the hydrogen consumption and the operating conditions. However, the results indicate that the hydrogen consumption is more at higher temperatures and low liquid flow rates.

7.4.8 Reactor Performance

In the kinetic study, the basic assumption was that the reactor operation was essentially isothermal and plug-flow. Some of the important factors which make the performance of a laboratory trickle-bed reactor deviate from the ideal plug-flow have been discussed in the 'Literature Review'. These fundamentals were applied to the present reactor system to check its performance. This discussion is presented in the following sections.

7.4.8.1 Axial Dispersion

Axial dispersion is one of the major factors which make the reactor performance deviate from the ideal plug-flow. The most widely used criterion to assess the magnitude of this problem is given by Mears [40]. This has been described in the 'Literature Review'. According to this criterion, for the axial dispersion effect on reactor performance to be less than 5%, the reactor length to the particle diameter ratio (L/d_p) should be more than 350. In the present case, 100 cm long reactor was used and the particle size was 0.02 cm. This gives a the L/d_p ratio of 5000. Therefore, it can be concluded that as per this criterion, there was no possibility of significant axial dispersion or back-mixing effects and the assumption of ideal plug-flow was valid.

7.4.8.2 Effective Catalyst Utilization

It is important for the catalyst to be wetted by the process fluids to really be effective as a catalyst. Inefficient catalyst wetting or the channeling of the liquid in the packed bed could adversely affect the utilization of the catalyst. The literature on the hydrodynamics of trickle-bed reactors indicated that for a tube diameter to particle size ratio (d_t/d_p) greater than 20, there is minimal or no channeling of liquid in a trickle-bed reactor. For this study the tube diameter was 0.52 cm and particle size of the catalyst was 0.02 cm, a ratio of d_t/d_p of 26. Therefore with this size of catalyst particles in this study, the liquid distribution was good and no adverse channeling effects could be anticipated.

The wetting efficiencies in the laboratory trickle-bed reactors are generally low as predicted by the most commonly used correlation given by Satterfield [64]. This problem was circumvented by diluting the catalyst bed with equal volumes of an inert material (α-alumina). Studies of de Bruijn [15], and van Klinken and van Dongen [77] indicated the enormous advantage of catalyst bed dilution in case of laboratory scale reactors.

de Bruijn indicated that in diluted catalyst beds, the effect of catalyst size on the activity was much smaller as compared to the same effect in undiluted beds. Also he concluded that in the diluted beds the space time (=1/LHSV) was a realistic reaction time parameter rather than $1/LHSV^{\alpha}$ factor as proposed by the effective catalyst wetting model or the axial dispersion model.

van Klinken and van Dongen observed a six-fold increase in the value of Peclet number in the diluted bed which strongly supports the assumption of plug-flow in the trickle-bed reactor with diluted bed. Also in the static-holdup studies, they observed a two fold increase in the pore volume utilization in case of a diluted catalyst bed. This increase actually indicated a much bigger increase in catalyst utilization since they used rather big molecules of $C_{32}H_{66}$ for their RTD studies. Both these studies were carried out for actual hydrotreatment systems at the usual operating conditions. Thus, their results formed a more sound basis of prediction of reactor performance in the present study.

Considering the predictions of the above mentioned studies, it can be concluded that in the present study, by dilution of the catalyst bed, the effective catalyst utilization was very good.

7.4.9 Mass-Transfer Effects and Effectiveness Factor

Hydrotreating reactions occur on active catalyst sites. For this reason it is very important for the reactants to reach these active sites. Most of the active sites in the porous catalysts are inside the catalyst pores. This makes the following five steps important for such catalytic reaction:

1. Diffusion of reactants into the pores of the catalyst.
2. Adsorption of the reactant species on the active catalyst sites.
3. The chemical reaction on the catalyst site.

4. Desorption of the products from the catalyst site.

5. Diffusion of the products out of the catalyst pores.

The overall rate of a reaction will be determined by the slowest of above mentioned steps. For doing the kinetic study of a catalyst, it is very important to have the experimental set-up designed in such a way that the chemical reaction step becomes the rate controlling step and all other steps have a faster rate. To do this for the studies like hydrotreating, normally the particle size of the catalyst is reduced sufficiently to achieve an effectiveness factor of close to one. The same technique was employed in the present study.

Table 31: Effectiveness Factors

Catalyst Used	Reaction	Size	Effectiveness Factor	Reference
Co-Mo on Alumina	HDS	5mm X 5mm	0.36	van Deemter [75]
"	"	3.6mm X 3.6mm	0.6	Adlington [1]
"	"	3mm X3mm	0.5 to 0.8	van Zoonen [78]
"	HDS and HDN	8/10 mesh to 48/50 mesh	0.8 to 1.0	Sooter and Satchell, [58]

The available data on the effectiveness factors of the catalysts used in similar studies was very useful in determining the size of the catalyst used in the present study. Some of these data is shown in Table 31.

It was predicted from the listed values of effectiveness factors in the above table, that for a particle size of 0.2mm, the effectiveness factor would be very close to one. This prediction was tested by using a catalyst of smaller size but the same composition as catalyst 30 used in the kinetic study. This catalyst (number 31) had a particle size between 100 and 120 mesh (0.124mm to 0.147mm). This was tested in the trickle-bed reactor in the same manner as the other catalysts. This catalyst too, was first run at standard conditions for a period of 20 hours and then the samples were drawn at LHSV of 2 at all the four temperatures used for the kinetic study. The samples were tested and the results are indicated in Table 32.

The results obtained with this catalyst were close to the results obtained with catalyst number 30 within the limits of the experimental errors. Therefore, it was concluded with the help of these results as well as the previous data available on the effectiveness factors, that for all practical reasons, the effectiveness factors of the catalysts used in this study were close to unity.

Table 32: Results Obtained With Catalyst Number 31

Pressure = 1000 psig
Gas Flow Rate = 5000 scf/bbl
LHSV = 2.0

Temperature	Nitrogen ppm		Sulfur (wt.%)	
(°C)	No.30	No.31	No.30	No.31
350	3341	3363	0.70	0.72
375	2757	2713	0.39	0.39
400	1765	1689	0.13	0.14
425	987	1003	0.04	0.03

7.4.10 Heat Transfer Effects

Another assumption involved in the kinetic analysis was the isothermal operation of the trickle-bed reactor. Non-isothermal conditions can occur because of two main factors:

1. inefficient physical temperature control around the reactor and/or,
2. excessive heat effects involved in chemical reactions occurring in the reactor.

The temperature control around the reactor was very efficient in the present case. A sand bath was used to maintain the reactor at a constant temperature. Temperature inside the sand bath was checked several times during the course of this investigation and was found to

be within 2°C at all points inside the sand bath. Therefore, there was a good physical temperature control around the reactor and there was no possibility of temperature differences due to this factor.

The heats of reactions involved in hydrotreatment are generally very low (of the order of 25 to 30 Kcal/g mole) and the concentrations of the reaction species are also very low. Secondly, the catalyst is always wetted by the process liquid. This helps the intra-particle as well as inter-particle heat transfer. Also the reactor used in the present study had an internal diameter of only 0.52 cm. Therefore, it was not expected to have any significant temperature gradient in the radial direction of the catalyst bed.

However, to check the temperature difference between inside the reactor and outside, a thermocouple was placed at the middle of the catalyst bed length inside the reactor. The thermocouple size was was 1/32 of an inch (0.8mm) and was inserted from top of the reactor. Another thermocouple of the same type and size was attached outside the reactor tube with a small spot weld at approximately the same length where the inner thermocouple was placed. The experiment was run at all the four temperatures and the temperatures from both the thermocouples were read with a digital thermometer. Under steady state conditions no temperature difference could be noticed between the two temperature readings. The thermometer used was only capable of reading the temperature within ±1 °C. Therefore it was concluded that even if there was any temperature difference between inside and outside of the reactor, it was less than 1°C.

7.4.11 Hydrotreatment Without Catalyst.

Miki et.al. [43] reported their study on hydrocracking of atmospheric residue without using any catalyst in an autoclave type of reactor. They observed some hydrodesulfurization and hydrodenitrogenation. Some other investigators also have reported similar findings. The proportions of HDS and HDN occurring without catalyst is dependent upon the feed type and the operating conditions. To evaluate the extent of thermal HDS and HDN for the present catalyst system, hydrotreatment study was carried out without using the catalyst.

The inert material α-alumina was used in this study to dilute the catalyst. The size of this inert material was same as that of the catalyst (70 to 80 mesh). α-Alumina was packed into the trickle-bed reactor. The same operating procedure was followed as was done in the case of the catalyst no. 30 used in the kinetic-study.

The hydrotreatment was carried out at the standard conditions for a period of 20 hours. Samples were drawn at all the four temperatures in the same way as was done for the kinetic-runs. The exit gas analysis was also performed for all the runs. After the completion of these runs the inert material packed in the reactor was taken out and amount of coke formation was determined. There was very little coke formation on this inert material (1.98%) whereas the catalyst number 30 was found to have a 13.3% coke deposition. The results of the sample analysis and the gas formation are given in Table 33 and Table 34.

Table 33: Results of Hydrotreatment Without Catalyst (I)

Pressure = 1000 psig
Gas Flow Rate = 5000 scf/bbl

Temperature (°C)	LHSV	Sulfur (wt.%)	Nitrogen ppm	Formation of gas (wt.%)
Original Oil		3.05	4831	
350	4.0	2.92	3948	0.0708
350	2.0	2.88	3952	0.1230
350	4/3	2.87	3991	0.1435
350	1.0	2.78	3950	0.1785
375	4.0	2.82	4115	0.0583
375	2.0	2.76	3983	0.1511
375	4/3	2.82	4051	0.2276
375	1.0	2.72	4113	0.2627
400	4.0	2.80	4082	0.0864
400	2.0	2.77	4057	0.1779
400	4/3	2.74	4116	0.2974
400	1.0	2.78	4165	0.3379
425	4.0	2.79	4059	0.1909
425	2.0	2.68	3938	0.3558
425	4/3	2.61	4022	0.5279
425	1.0	2.63	3973	0.7013

Table 33 gives the sulfur and nitrogen concentrations and the gas formation rates. From these values it can be seen that a maximum of 18.3% HDN and 13.8% HDS occurred without catalyst as compared to 84.7% HDN and 99.0% HDS achieved with the catalyst. The gas formation rates were also lower in case of α-alumina at all temperatures. The gas formed without the use of catalyst had small amounts of unsaturated gases like acetylene and butylene whereas no unsaturated gases were observed with the catalyst.

Table 34: Results of Hydrotreatment Without Catalyst (II)

Pressure = 1000 psig
Gas Flow Rate = 5000 scf/bbl

Temperature (°C)	LHSV	Density (g/ml)	Viscosity cp	Aniline Point (°C)	Mid-B-Pt. (°C)
Original Oil		0.9803	241.5	52.7	429.1
350	4.0	0.9828	216.0	46.8	424.6
350	2.0	0.9819	205.6	47.2	425.3
350	4/3	0.9822	202.4	46.7	423.3
350	1.0	0.9798	193.0	46.8	414.5
375	4.0	0.9793	201.4	47.0	421.5
375	2.0	0.9792	193.8	46.5	416.9
375	4/3	0.9801	195.2	46.4	419.6
375	1.0	0.9799	186.8	46.8	418.2
400	4.0	0.9809	187.9	46.7	421.4
400	2.0	0.9790	174.1	46.8	416.3
400	4/3	0.9797	163.0	46.4	417.9
400	1.0	0.9766	157.3	46.1	413.1
425	4.0	0.9806	168.9	45.8	414.1
425	2.0	0.9776	133.8	44.8	411.8
425	4/3	0.9747	130.4	44.0	407.7
425	1.0	0.9765	131.6	45.7	412.2

Gas formation rate increased with increasing temperature and decreasing liquid flow rate for both catalyst and α-alumina. It could be concluded form this observation that the gas formation was mainly because of thermal cracking. Higher gas formation rates were obtained with the catalyst than the α-alumina alone because of the higher cracking activity of the catalyst.

Table 34 gives the values of the physical properties, aniline point and the mid-boiling point values of the samples obtained with α-alumina. Density values at all temperatures were very close to the density of the original oil and in fact at 350°C, values higher than the density of original oil were also obtained. This observation along with the higher gas formation at this temperature suggests that with α-alumina, mostly the smaller molecules of oil cracked to produce the gases and the bigger molecules were not affected.

Mid-boiling point values were also not very much affected in case of the hydrotreatment with α-alumina. Aniline point values are all in a small range between 44 and 47°C. Viscosity values reduced with increase in temperature. Lower values of the aniline point than the original oil indicate lesser paraffinicity of the products. From these values it can be concluded that with the α-alumina alone, the paraffins were converted into the aliphatics and aromatics and that is why, although the mid-boiling point values showed little change, the viscosity was substantially reduced.

The above comparison showed that most of the cracking activity of the big molecules as well as most of the sulfur and nitrogen removal was by virtue of the catalyst and not because of the thermal effects alone.

Chapter VIII

CONCLUSIONS

Most of the conclusions have been elaborated in the previous chapter at the end of the discussions on each part of the present study. Some of the important conclusions are summarized as follow:

1. There was no single optimum point for operating a hydrotreatment reaction within the nominal operating range which could satisfy all hydrotreatment criteria. However, the experimental technique used was good to point out individual optimums as well as optimum for any joint criteria if desired.
2. Study of the operating region indicated a strong interaction of pressure and temperature for mid-boiling point as well as HDN, whereby increase in pressure enhanced the %HDN but increased the mid-boiling point.
3. There was not any significant effect of gas flow rate on hydrotreatment and no high-interaction or low-interaction flow regimes could be observed within the selected range for the gas flow rates.
4. The catalyst preparation and testing scheme demonstrated in this study showed very good reproducibility.
5. A catalyst support material having 10% by wt. silica, 25% by wt. of type Y zeolite material rare-earth exchanged, and the rest

alumina was found to be the best for both sulfur and nitrogen removal.

6. The catalyst with the optimum composition was able to remove up to 99% of the sulfur and 85% of the nitrogen present in the heavy gas oil as compared to a maximum of 86.2% HDS and 61.4% HDN obtained at a 25°C higher hydrotreatment temperature with a best commercial catalyst (NI-Mo on alumina) tested in the previous study.

7. The kinetic study of the optimum catalyst suggested a 1.5th order power law model for sulfur removal and a 2nd order model for nitrogen removal.

8. The values of activation energies for the HDS and HDN were 20.8 and 25.1 Kcal/g mole respectively.

9. There was very little HDS (≤ 14%) and HDN (≤ 18%) by virtue of thermal effect alone as indicated by the results obtained without using catalyst.

10. Reactor performance as per the available literature was close to isothermal plug-flow.

11. A good material balance of oil feed was achieved for all the runs.

12. The analysis of the exit gases did not indicate any unsaturated gases present in the exit gas stream which points to a good hydrogenation capability of the catalyst developed in this study.

13. A maximum gas formation of about 0.7% by wt. of feed oil was observed at 425°C and LHSV of 1.0.

14. The gas formation decreased with increase in liquid flow rate or decrease in temperature.

15. Hydrogen consumption was found to be between 565 scf/bbl at 350°C and LHSV of 4.0 and a maximum of 1564 scf/bbl at 425°C and LHSV of 1.0.

BIBLIOGRAPHY

1. Adlington D., Thompson E., 3rd European Symp. Chem. Reaction Eng., Pergamon, (New York), 1965.

2. Ahuja S. P., Derrien M. L. and LePage J. F., Ind. Eng. Chem., (Prod. Res. & Dev.), Vol.9, No.3, 1970.

3. Bacon D.W., Ind. Eng. Chem., Vol 62, No. 7, P27, 1970.

4. Baldi G. and Specchia V., Chem. Eng. Sci., Vol. 32, P-515, 1977.

5. Benesi H.A., Bounar R.U. and Lee C.F., 'Determination of Pore Volume of Solid Catalysts', Anal. Chem., Vol.27, P1963-1965; 1955.

6. Brunauer S., Emmett P.H. and Teller E., J. Am. Chem. Soc., Vol.60, P309, 1938.

7. Bolton A. P., 'Zeolite Chemistry and Catalysis', in 'Zeolite Chemistry and Catalysis', Edited by Jule A. Rabo, ACS Monograph 171, P714, 1976.

8. Bolton A. P., 'Molecular Sieve Zeolites', in 'Experimental Methods in Catalytic Research', Edited by Anderson R. B., Academic Press, New York, P33, 1976.

9. Box G.E.P. and Behnken D.W., Technometrics, Vol. 2, P455, 1960.

10. Box G.E.P. and Wilson K.B., J. of Royal Statistical Society, Vol. 13, P1, 1951.

11. Box G.E.P. and Hunter J.S., Annals of Mathematical Statistics, Vol. 28, P 95, 1957.

12. Charpentier J.C. and Favier M., 'Some Liquid Holdup Experimental Data in Trickle-bed Reactors for Foaming and Nonfoaming hydrocarbons', AIChE J., Vol. 21, P1213, 1975.

13. Charpentier J.C., 'Recent progress in Two-Phase Gas-Liquid Mass Transfer in Packed Beds', Chem. Eng. J., Vol. 1, P-161, 1976.

14. Charpentier J.C., Morsi B.I. and Midoux N., 'Flow Patterns and Some Holdup Data in Trickle-Bed Reactors for Foaming,

Nonfoaming and Viscous Organic Liquids', AIChE Journal, Vol 24, No. 2, March, 1978.

15. de Bruijn A., 'Testing of hds Catalyst in Small Trickle Phase Reactors', Sixth International Congress on Catalysis, The Chemical Society, London, P 951-964, 1976.

16. Draper N.R. and Smith H., 'Applied Regression Analysis', 2nd Edn., Wiley, New York., 1981.

17. Dudukovic M.P. and Mills P.L., 'Catalyst Effectiveness Factor in Trickle-Bed Reactors', ACS Preprints, 5th Int. Symp. on Chem. Reaction Eng., Houston, P 387-399.

18. Eberline C. R., Wilson R. T. and Larson L.G., Ind. Eng. Chem., 49(4), P661-663, April 1957.

19. Elenkov D., and Kolev n., Chem. Eng. Technol., Vol. 44, P 845, 1972.

20. Faeth P.A. and Willingham C.B., 'The Assembly, Calibration and Operation of a Gas Adsorption Apparatus for Measurement of Surface Area, Pore Volume Distribution and Density of Finely Divided Solids', A Technical Bulletin of Dept. of Physical Chemistry, Mellon Institute of Ind. Research, Pittsburough, Pennsylvania, September 1953.

21. Fraissard J., 'Why Are HY Zeolites So Much More Active Than Amorphous Silica-Alumina', Catalysis by Zeolites, B. Imelik et.al. Editors, Elsevier, Netherlands, P 343-350, 1980.

22. Frost C. M. and Cottingham P. L., "Hydrodesulfurization of Venezuelan Residual Fuel Oils", Report no. 7557, U.S. Department of Interior, Bureau of Mines.

23. Furimsky Edward , A.I.Ch.E.,J.,25(2),P306-311, March 1981.

24. Gary H.James, and Glenn E. Handwerk, "Petroleum Refining Technology and Economics", A textbook by marcel Dekker, Inc., New York, 1975.

25. Green D. C. and Broderick D. H., CEP, Dec. 1981, P33-39.

26. Guray Tosum, 'A Study of Cocurrent Downflow of Non-foaming Gas-Liquid Systems in a Packed Bed. 1. Flow Regimes: Search for a Generalized Flow Map', Ind. Eng. Chem. Process Des. Dev., Vol. 23, P29-35, 1984.

27. Hass R. G., Ph.D. Thesis, Montana state University, USA, 1978.

28. Haynes H.W., Parcher J.F. and Helmer N.E., 'Hydrocracking Polycyclic Hydrocarbons over a Dual-functional Zeolite (Faujasite)-Based Catalyst', Ind. Eng. Chem. Process Des. Dev., Vol. 22, P401-409, 1983.

29. Heinz Heinemann, Catalyst Review, Science and Engineering, 23(182), P315-328, 1981.

30. Henry H.C., and Gilbert J.B., Ind. Eng. Chem. Process Des. Dev., Vol. 12, P 328, 1973.

31. Herskowitz M., and Smith J.M., 'Liquid Distribution in Trickle-Bed Reactors, Part I: Flow Measurement', AIChE J., Vol. 24, P 439, 1978.

32. Herskowitz M., and Smith J.M., 'Liquid Distribution in Trickle-Bed Reactors, Part II: Tracer Studies', AIChE J., Vol. 24, P 450, 1978.

33. Hochman J.M. and Effron E., 'Two Phase Co-Current Down Flow in Packed Beds', Ind. & Eng. Chem., Fundam., Vol. 8, No. 1, Feb. 1969.

34. Hydroprocessing Catalysts for Heavy Oil and Coal, Edited by M.J.Satriana, Noyes Data Corporation, New Jersey, 1982.

35. Jacobs Peter A., "Carboniogenic Activity of Zeolites", Elsevier Scientific Publishing Co., New York, 1977.

36. Khulbe C.P., Pruden B.B., Denis J.M. and Merrill W.M., 'Pilot Plant Thermal Cracking of GCOS (Great Canadian Oil Sands) Bitumen', CANMET Report No.76-28, June 1976.

37. Kobayashi S., Kushiyama S., Ida Y., and Wakao N., 'Flow Characteristics and Axial Dispersion in Two-Phase Downflow in Packed Coulmns', Kagaku Kogaku Ronbunshu, Vol. 5, P 256, 1979.

38. Krauze R. and Serwinski M., Inzynteria Chemizna, Vol. 1, P 415, 1971.

39. Magee J.S. and Blazek J.J., 'Preparation and Performance of Zeolite Cracking Catalyst', in 'Zeolite Chemistry and Catalysis', Edited by Jule A. Rabo, ACS Monograph 171, 1976.

40. Mears D.E., 'The Role of Liquid Holdup and Effective Wetting in the Performance of Trickle-bed Reactors', ACS Monograph Ser., No. 133, Chem. Reaction Engg-II, P218, 1974.

41. Mears D.E., Chem. Eng. Sci., Vol. 26, P 1361, 1971.

42. Miale J.N., Chen N.Y. and Weisz P.B., J. Catal., Vol. 6, P276, 1966.

44. Michell R.W., and Furzer I.A., Chem. Eng. J., Vol. 4, P 53, 1972.

43. Miki Y., Yamadaya S., Oba M. and Sugimoto Y., 'Role of Catalyst in Hydrocracking of Heavy Oil', J. of Catalysis, Vol. 83, P371-383, 1983.

45. Mills P.L., Erk E.F., Evans J., and Dudukovic M.P., 'Some Comments on Evaluation of Catalyst Effectiveness Factors in Trickle-Bed Reactors', Chem. Eng. Sci., Vol. 36, P 947, 1981.

46. Mirza Aziz, Massood M. A., Mallikarajunan M. M. and Vaidyeswaran R., Petroleum and Hydrocarbons, Vol.3, No.1, April 1968.

47. Montagna A.A., and Shah Y.T., Ind. Eng. Chem. Process Des. Dev., Vol. 14, P 479, 1975.

48. Montagna A.A., and Shah Y.T., and Paraskos J.A., Ind. Eng. Chem. Process Des. Dev., Vol. 16, P 152, 1977.

49. Mordechay Herskowitz and Sheiomo Mosseri, 'Global Rates of Reaction in Trickle-Bed Reactors: Effects of Gas and Liquid Flow Rates', Ind. Eng. Chem. Fundam., Vol. 22, No. 1, 1983.

50. Onda K., Sada E., and Mursae Y., AIChE J., Vol. 5, P 235, 1959.

51. Onda K., Takeuchi H., and Koyama H., Kagaku kogaku., vol. 31, P 121, 1976.

52. Paraskos J.A., Frayer J.F. and Shah Y.T., Ind. Eng. Chem. Process Des. Dev., Vol. 14, P 315, 1975.

53. Parsons Basil I. and Ternan M., Proceedings of VI International Congr. on Catalysis, Vol.2, P965, 1975.

54. Prchlik J., Soukup J., Zapletal V. and Ruzicka V., 'Liquid Distribution in Reactors With Randomly Porous Beds', Coll. Czech. Chem. Commun., Vol. 40, P 845, 1975.

55. Puranik S.S., and Vogelpohl A., Chem. Eng. Sci., Vol. 29, P 501, 1974.

56. Ray W.H. and Szekely J., 'Process Optimization', Wiley, New York, N.Y., 1973.

57. Sambi I. S., "Catalytic Hydrotreatment of Heavy Gas Oil", M.A.Sc. thesis, University of Ottawa, Canada, 1982.

58. Statistical Analysis System, SAS Institute Inc., Box 8000, Cary, North Carolina, USA, 27511.

59. Satchell D.P., Ph.D. Thesis, Oklahoma Stata University, Stillwater, Oklahoma, USA, 1974.

60. Sato Y., Hirose T., Takahashi F., Toda M., and Hashigughi Y., J. of Chem. Eng. (Japan), Vol. 6, No. 4, P315, 1973.

61. Satterfield G.N., Pelossof A.A., and Sherwood T.K., AIChE J., Vol. 15, No. 2, P 226, 1969.

62. Satterfield Chrles N. and Yang Shan Hsl, Ind. Eng. Chem. Process Des. Dev., Vol.23, P 11-19, 1984.

63. Satterfield C.N., Heterogeneous Catalysis in Practice, McGraw Hill, New York, P174, 1980.

64. Satterfield C.N., AIChE J., Vol. 21, P 209, 1975.

65. Schulman k.L., Ulbrich G.F., Proulx A.Z., and Zimmerman J.O., AIChE J., Vol. 1, P 253, 1955.

66. Shah Y.T., Paraskos J.A., and Frayer J.A., 'Effect of Holdup, Incomplete Catalyst Wetting and Backmixing during Hydroprocessing in Trickle-Bed Reactors', Ind. Eng. Chem. Process Des. Dev., Vol. 14, No. 3, P315-322, 1975.

67. Shah Y.T., 'Gas-Liquid-Solid Reactor Design', McGraw Hill, USA, 1979.

68. Smith J.V., 'Origin and Structure of Zeolites', in 'Zeolite Chemistry and Catalysis', Edited by Jule A. Rabo, ACS Monograph 171, 1976.

69. Smith J. M., "Chemical Engineering Kinetics", 2nd Edition, McGraw Hill, New York,

70. Smith and Mordechay Herskowitz, AIChE Journal, Vol.29, No.1, P1-18, Jan.1983.

71. Sooter M.C., Ph.D. Thesis, Oklahoma Stata University, Stillwater, Oklahoma, USA, 1974.

72. Sosvowski J., Florham N.J. and Turner D.W., CEP, Vol 77, No.2, P51-55, Feb. 1981.

73. Specchia V., Rossini A. and Baldi G., 'Distribution and Radial Spread of Liquid in Two-Phase concurrent Flows in a Packed Bed', Ing. Chim. Ital., Vol. 10, P171, 1974

74. Specchia V., and Baldi G., Chem. Eng. Sci., Vol. 32, P 515, 1977.

75. Sylvester N.D., and Pitayagulsarn P., 'Radial Liquid Distribution in Concurrent Two-Phase Downflow in Packed Beds', Can. J. of Chemical Eng., Vol. 53, P 599, 1975.

76. van Deemter J.J., 3rd European Symp. Chem. Reaction Engg., Pergamon (New York), 1965.

77. van Klinken J., and van Dogen R.H., 'Catalyst Dilution For Improved Performance of Laboratory Trickle-Flow Rectors', Chem. Eng. Sci., Vol. 35, P 59, 1980.

78. Van Swaaij W.M.P., Charpentier J.C., and Villermoux J., Chem. Eng. Sci., Vol. 24, P 1083, 1969.

79. van Zoonen D. and Douwes C.T., J. Inst. Petrol., Vol. 49, P383, 1963.

80. Vogel's, 'Text Book of Quantitative Inorganic Analysis', 4th Edition, Longman, London, 1978.

81. Wittington E. L., Pierce V. E., and Bansal B. B., CEP Feb. 1981, P45-50.

82. Zeolite Technology and Applications, Recent advances, Edited by Jeanette Scott, Noyes Data Corporation, New Jersey, 1980.

Appendix A

COMPUTER PROGRAMS

1. PROGRAM FOR BET.SURFACE AREA

```
C     THIS PROGRAM WILL CALCULATE THE VALUES IN THE WORK SHEET FOR
C     B.E.T. SURFACE AREA .FIRST FOUR VALUES OF DATA SHOULD BE FOR
C     EMPTY SPACE FACTOR CALCULATIONS. NEXT TWO VALUES  SHOULD BE
C     FOR CALCULATING THE NITROGEN TOTAL VOLUME.
C
C
C
      REAL P,PC,PO,TB,VT,VB,VS,VA,Y,X,FV,FS,FSM,RANGE,Y1,X1,XYW,ALBP,ANO
     1VA,B,PRED,WT,S,XY
      DOUBLE PRECISION WK
      INTEGER M,N,IER,MDP,SNUM
      DIMENSION P(15),PC(15),PO(15),TB(15),VT(15),VA(15),VB(15),VS(15),Y
     1(15),X(15),FV(6,5),FS(2),M(15),N(15),RANGE(4),Y1(15,1),X1(15),XYW(
     215,3),ALBP(2),ANOVA(13),MDP(3),B(4,12),PRED(15,6),WK(60),XY(15,4)
C
C   DATA READ FOROM A FILE DEFINED AS NO.5
C
      READ(5,1)SNUM,WT,L
1     FORMAT(///,15X,I3,/,15X,F6.4,/,15X,I2,//)
      DO 2 I=1,L
      READ(5,3)M(I),N(I),P(I),TB(I),PO(I)
3     FORMAT(10X,I1,1X,I1,1X,F5.1,1X,F4.1,1X,F5.1)
      M(I)=M(I)+1
      N(I)=N(I)+1
2     CONTINUE
C
C   READ THE NITROGEN BULB FACTORS FORM A FILE:  FB FORTRAN DEFINED AS
C   NUMBER 7.
C
      READ(7,51)FV(1,1),FV(1,2),FV(1,3),FV(1,4),FV(1,5)
51    FORMAT(5(/),14X,5(F8.4,2X),/)
      DO 50 I=2,6
      READ(7,53)FV(I,1),FV(I,2),FV(I,3),FV(I,4),FV(I,5)
53    FORMAT(14X,5(F8.4,2X),/)
50    CONTINUE
C
C
C   CALCULATE EMPTY SPACE FACTOR
C
      DO 5 I=1,L
      PC(I)=P(I)*(0.9955-  (TB(I)-25.0)*1.8E-4)
```

```
5     CONTINUE
      DO 6 I=1,2
      VT(I)=PC(I)*FV(M(I),N(I))/298.13
6     CONTINUE
      VT(3)=(VT(1)+VT(2))/2
      VT(4)=VT(3)
      DO 7 I=3,4
      VB(I)=PC(I)*FV(M(I),N(I))/298.13
      VS(I)=VT(I)-VB(I)
      FS(I-2)=VS(I)/PC(I)
7     CONTINUE
      FSM=(FS(1)+FS(2))/2.
      DO 8 I=5,6
      VT(I)=PC(I)*FV(M(I),N(I))/298.13
8     CONTINUE
      DO 9 I=7,L
      VT(I)=(VT(5)+VT(6))/2.
      VB(I)=PC(I)*FV(M(I),N(I))/298.13
      VS(I)=PC(I)*FSM*(1.+PC(I)*6.65E-5)
      VA(I)=VT(I)-VB(I)-VS(I)
      Y(I)=1./(VA(I)*(PO(I)/P(I)-1.))
      XYW(I-6,2)=Y(I)
      XYW(I-6,3)=1.0
      Y1(I-6,1)=Y(I)
      X(I)=P(I)/PO(I)
      XYW(I-6,1)=X(I)
      X1(I-6)=X(I)
9     CONTINUE
      WRITE(6,20)SNUM,WT
20    FORMAT(1H1,6X,'*',41X,'**',41X,'*',10X,'I',/,'
     1          ',/,30X,21('*'),/,30X,'*   SAMPLE NO:  ',I8,' *',/,30X,2
     111('*'),//,10X,'SAMPLE  WEIGHT = ',F8.4,/,'
     1               ',/,5X,'BU-  PRES-  PC.  TEMP VAP.  VT(I)  VB(I)  VS(I)
     1  VA(I)   P/PO   Y',/,5X,'LBS SURE              PR.    CC     CC
     2  CC     CC ',//)
      DO 42 I=1,L
      M(I)=M(I)-1
      N(I)=N(I)-1
42    CONTINUE
      DO 21 I=1,2
      WRITE(6,22)M(I),N(I),P(I),PC(I),TB(I),VT(I)
22    FORMAT(5X,I1,'+',I1,1X,F5.1,1X,F5.1,1X,F4.1,7X,F6.3,/)
21    CONTINUE
      DO 23 I=3,4
      WRITE(6,24)M(I),N(I),P(I),PC(I),TB(I),VT(I),VB(I),VS(I),FS(I-2),FS
     1M
24    FORMAT(5X,I1,'+',I1,1X,F5.1,1X,F5.1,1X,F4.1,7X,F6.3,1X,F6.3,1X,F6.
     13,2X,'FS = ',F6.3,3X,'FSM = ',F6.3,/)
23    CONTINUE
      DO 25 I=5,6
      WRITE(6,26)M(I),N(I),P(I),PC(I),TB(I),VT(I)
26    FORMAT(5X,I1,'+',I1,1X,F5.1,1X,F5.1,1X,F4.1,7X,F6.3,/)
25    CONTINUE
      DO 27 I=7,L
```

```
      WRITE(6,28)M(I),N(I),P(I),PC(I),TB(I),P0(I),VT(I),VB(I),VS(I),VA(I
     1),X(I),Y(I)
28    FORMAT(5X,I1,'+',I1,1X,F5.1,1X,F5.1,1X,F4.1,1X,F5.1,1X,F6.3,1X,F6.
     13,1X,F6.3,1X,F6.3,1X,F6.4,1X,E11.5,/)
27    CONTINUE
      WRITE(6,41)
41    FORMAT(///,10X,'
     1',/,10X,'NO. OF      SLOPE          INTERCEPTPT.      SURFACE
     2',/,10X,'POINTS        S                 I             AREA',//)
      MDP(1)=1
      MDP(3)=0
      ALBP(1)=0.05
      ALBP(2)=0.05
      IK=L-6
      DO 11 I=3,IK
      DO 44 K=1,I
      DO 44 KK=1,3
      XY(K,KK)=XYW(K,KK)
44    CONTINUE
      NN=I
      CALL RLFOR(XY,15,NN,95.,MDP,ALBP,ANOVA,B,4,PRED,15,WK,IER)
      S=4.38/((B(1,2)+B(2,2))*WT)
      WRITE(6,40)I,B(1,2),B(2,2),S
40    FORMAT(12X,I2,2X,2(E13.6,4X),3X,F8.3,/)
11    CONTINUE
      RANGE(1)=0.0
      RANGE(2)=0.6
      RANGE(3)=0.0
      RANGE(4)=0.08
      CALL USPLO(X1,Y1,1,(L-6),1,1,15HADSORPTION PLOT,15,4HP/P0,4,13HP/(
     1VA/(P0-P)),13,RANGE,1H*,0,IER)
      WRITE(6,30)IER
30    FORMAT(///,10X,'THE ERROR MESSAGE = ',I3)
      STOP
      END
```

2. Programs for the Simulated-Distillation

```
C    THIS PROGRAM ACCEPTS RAW DATA AS GENERATED BY THE GC INTEGRATOR
C
C    TO RUN : FSIM EXEC
C
      INTEGER NS,NP,NT,NOFS
      REAL X,X1,X2,Y,Y1,SUM,MIDBP
      DIMENSION X(20),X1(20),X2(20),Y(20),Y1(20),NS(2)
C
C  GIVE THE VALUES OF TEMPERATURES CORRESSPONDING TO THE RETENTIONS
C  TIMES FOR EVERY 2.5 MINUTES INTERVAL TO Y1'S BELOW:-
C
C
      DO 9 I  =1,20
         Y1(I)=0.0
9        CONTINUE
      NT=8
      Y1(1)=142.0
      Y1(2)=196.00
      Y1(3)=243.00
      Y1(4)=307.00
      Y1(5)=366.00
      Y1(6)=417.00
      Y1(7)=482.00
      Y1(8)=533.00
C
C READ NUMBER OF SAMPLES AND THEN
C READ THE SAMPLE NO. AND THE VALUES OF THE AREAS FROM THE INTEGRATOR.
C
            READ(5,49)NOFS
49       FORMAT(14X,I3)
       DO 48 J=1,NOFS
       READ(5,50)(NS(I),I=1,2)
50      FORMAT(13X,4A4)
       READ(5,53)NP
53      FORMAT(19X,I2)
         DO 6 I=1,NP
           READ(5,51)X(I)
51        FORMAT(E8.4)
6          CONTINUE
C
C  CUMMULATIVE AREA (X1(I)) AND  AREA (X2(I)) ARE CALULATED.
C
      SUM=0.0
        DO 1 I=1,NP
          SUM=SUM+X(I)
          X1(I)=SUM
1           CONTINUE
      DO 2 I=1,NP
```

```
      X2(I)=(X1(I)/SUM)*100.0
        Y(I)=2.5*I
2        CONTINUE
C
C  CALCULATE THE MID-BOILING POINT BY USING A ST. LINE IN THE
C  IN-BETWEEN POINTS
C
     I=1
24     IF(X2(I+1).LT.50.0) GO TO 21
          GO TO 23
21       I=I+1
           GO TO 24
23           IF(X2(I+1).EQ.50.0) GO TO 22
      MIDBP=Y1(I+1)-(Y1(I+1)-Y1(I))*((X2(I+1)-50.0)/(X2(I+1)-X2(I)))
       GO TO 25
22     MIDBP=Y1(I+1)
C
C   WRITE THE GIVEN DATA IN AN OUT PUT FILE DEFINED AS 6.
C
25    WRITE(6,60)NS
60    FORMAT(1H1,///,15X,'SAMPLE  NUMBER :- ',2A4,/,15X,21('_'),////,17X
      1,'CUMULATIVE',2X,'RETENTION',3X,'PERCENT',2X,'TEMPERATURE',/,8X,'A
      1REA',8X,'AREA',7X,'TIME',7X,'AREA',7X,'DEG.C',/,5X,10('_'),2X,10('
      1_'),2X,9('_'),3X,7('_'),2X,11('_'),///)
       DO 3 I=1,NP
       WRITE(6,61)X(I),X1(I),Y(I),X2(I),Y1(I)
61    FORMAT(5X,E10.4,2X,F10.1,4X,F5.2,4X,F6.2,5X,F6.2,/)
3     CONTINUE
                    WRITE(6,62)MIDBP
62                 FORMAT(//,10X,'MID-BOILING-POINT = ',F6.2,' C')
C
C   WRITE VALUES IN A FILE CALLED PD FORTRAN FOR PLOTTING
C
      DO 33 I=1,NT
        WRITE(7,34)X2(I),Y1(I)
34      FORMAT(F7.3,1X,F7.2)
33        CONTINUE
48          CONTINUE
                  STOP
                    END
      REAL XARRAY,YARRAY
      DIMENSION XARRAY(11),YARRAY(11)
      CALL PLOTS(200.0,27.5)
      CALL PLOT(0.0,5.0,2)
      CALL PLOT(6.6,5.0,-3)
      XARRAY(9)=0.0
      XARRAY(10)=1.0
      YARRAY(9)=0.0
      YARRAY(10)=1.0
      DO 2 J=1,2
      DO 1 I=1,8
      READ(5,51) XARRAY(I),YARRAY(I)
51    FORMAT(F7.3,1X,F7.2)
      XARRAY(I)=XARRAY(I)/10.
```

```
      YARRAY(I)=YARRAY(I)/50.
1     CONTINUE
C     CALL SCALE(XARRAY,10.0,8,1)
C     CALL SCALE(YARRAY,12.0,8,1)
      CALL AXIS(0.0,0.0,16HPERCENTAGE ( % ),-16,10.0,0.0,0.0,10.0)
      CALL AXIS(0.0,0.0,22HTEMPERATURE ( DEG. C ),22,12.0,90.0,0.0,50.0)
      CALL FLINE(XARRAY,YARRAY,-8,1,1,1)
      CALL SYMBOL(1.7,18.0,0.7,9HSIMULATED,0.0,9)
      CALL SYMBOL(1.0,16.3,0.7,12HDISTILLATION,0.0,12)
      CALL SYMBOL(1.0,15.0,0.42,14HSAMPLE NO :   ,0.0,14)
      CALL PLOT(15.0,0.0,3)
      CALL PLOT(15.0,-5.0,2)
      CALL PLOT(21.6,00,-3)
2     CONTINUE
      CALL PLOT(0.0,0.0,999)
      STOP
      END
```

3. Program used for Operating Region Study:-

This program was used for model fitting with linear regression for different performance criteria used in the Study of Operating Region:-

```
      REAL X,Y,B,E,XTXIN,XTY,YMEAN,YHAT,PERR,YM,R,BVAR,RANGE,A,MEU,CONFI
     1N,XTX,WKAREA,MAX,MIN,Y1,COV,COR,D,Y2,B1,C1
      INTEGER I,IY,N,M,INC,IOPT,LER,L,CT,NO,OK,BST,TITLE
      DOUBLE PRECISION EMEAN,SS,SSPE,ESQ
      DIMENSION X(28,15),Y(28),XTXIN(15,15),XTY(15),B(15),E(28,1),YHAT(2
     18),BVAR(15),RANGE(4),L(28),A(28),CONFIN(15),XTX(15,15),WKAREA(20),
     1Y1(28),COV(15,15),ESQ(28),COR(15,15),BST(15),TITLE(6),D(28),Y2(28,
     19),B1(15,9),C1(15,9)
      DO 1 J=1,28
      X(J,1)=1.0
      READ(5,50)X(J,2),X(J,3),X(J,4),X(J,5)
50    FORMAT(4F4.1)
      X(J,6)=X(J,2)**2
      X(J,7)=X(J,3)**2
      X(J,8)=X(J,4)**2
      X(J,9)=X(J,5)**2
      X(J,10)=X(J,2)*X(J,3)
      X(J,11)=X(J,2)*X(J,4)
      X(J,12)=X(J,2)*X(J,5)
      X(J,13)=X(J,3)*X(J,4)
      X(J,14)=X(J,3)*X(J,5)
      X(J,15)=X(J,4)*X(J,5)
1     CONTINUE
      DO 30 I=1,15
      DO 30 J=1,15
      XTX(I,J)=0.0
      DO 30 K=1,28
      XTX(I,J)=XTX(I,J)+X(K,I)*X(K,J)
30    CONTINUE
      WRITE(6,71)
71    FORMAT(1H1,///,30X,'INPUT  DATA',//)
      DO 7 I=1,28
      WRITE(6,72)X(I,1),X(I,2),X(I,3),X(I,4),X(I,5),X(I,6),X(I,7),X(I,8)
     1,X(I,9),X(I,10),X(I,11),X(I,12),X(I,13),X(I,14),X(I,15)
72    FORMAT(2X,15(F4.1,1X))
7     CONTINUE
      WRITE(6,85)
85    FORMAT(1H1,///,25X,'XTX  MATRIX',///)
      DO 25 I= 1,15
      WRITE(6,86)XTX(I,1),XTX(I,2),XTX(I,3),XTX(I,4),XTX(I,5),XTX(I,6),X
     1TX(I,7),XTX(I,8),XTX(I,9),XTX(I,10),XTX(I,11),XTX(I,12),XTX(I,13),
     1XTX(I,14),XTX(I,15)
86    FORMAT(2X,15(1X,F7.4))
25    CONTINUE
      CALL LINV1F(XTX,15,15,XTXIN,0,WKAREA,IER)
```

```
      WRITE(6,74)
74    FORMAT(    ///,36X,'XTXIN',///)
      DO 10 I=1,15
      WRITE(6,75)XTXIN(1,I),XTXIN(2,I),XTXIN(3,I),XTXIN(4,I),XTXIN(5,I),
     1XTXIN(6,I),XTXIN(7,I),XTXIN(8,I),XTXIN(9,I),XTXIN(10,I),XTXIN(11,
     1I),XTXIN(12,I),XTXIN(13,I),XTXIN(14,I),XTXIN(15,I)
75    FORMAT(1X,15(1X,F7.4))
10    CONTINUE
      WRITE(6,90)IER
90    FORMAT( //,5X,'MATRIX INVERSION ERROR MESSAGE IS = ',I4,/)
      DO 9 I=1,28
      READ(5,51)L(I)
51    FORMAT(I2)
      D(I)=L(I)
9     CONTINUE
      READ(5,57)NO,OK
57    FORMAT(2A4)
      DO 35 CT=1,9
      READ(5,55)TITLE(1),TITLE(2),TITLE(3),TITLE(4),TITLE(5),TITLE(6)
55    FORMAT(6A4)
      DO 33 I=1,28
      READ(5,56)Y1(I)
56    FORMAT(F8.4)
      Y2(I,CT)=Y1(I)
33    CONTINUE
      MIN=10000.0
      MAX=0.0
      DO 17 I=1,28
      IF(MAX.GE.Y1(I))GO TO 18
      MAX=Y1(I)
18    IF(MIN.LE.Y1(I))GO TO 17
      MIN=Y1(I)
17    CONTINUE
      DO 19 I=1,28
      Y(I)=((Y1(I)-MIN)/(MAX-MIN))*2.0-1.0
19    CONTINUE
      DO 4 K=1,15
      XTY(K)=0.0
      DO 4 J=1,28
      XTY(K)=XTY(K)+X(J,K)*Y(J)
4     CONTINUE
      DO 5 I=1,15
      B(I)=0.0
      DO 5 J=1,15
      B(I)=B(I)+XTXIN(I,J)*XTY(J)
      B1(I,CT)=B(I)
5     CONTINUE
      YMEAN=0.0
      EMEAN=0.0
      SS=0.0D 00
      DO 6 I=1,28
      YHAT(I)=0.0
      DO 11 J=1,15
      YHAT(I)=YHAT(I)+B(J)*X(I,J)
```

```
11    CONTINUE
      E(I,1)=Y(I)-YHAT(I)
      ESQ(I)=E(I,1)**2
      SS=SS+ESQ(I)
      EMEAN=EMEAN+E(I,1)*10000.0
      YMEAN=YMEAN+Y(I)
6     CONTINUE
      EMEAN=EMEAN/280000.0
      YMEAN=YMEAN/28.0
      SSPE=0.0D 00
      DO 14 I=25,28
      SSPE=SSPE+E(I,1)**2
14    CONTINUE
      R=(SS-SSPE)*3.0/(SSPE*(28.0-15.0-3.0))
      PERR=SS/(28.0-15.0)
      DO 15 I=1,15
      BVAR(I)=PERR*XTXIN(I,I)
      CONFIN(I)=2.160*(SQRT(BVAR(I)))
      C1(I,CT)=CONFIN(I)
      BST(I)=OK
      IF(ABS(B(I)).GT.ABS(CONFIN(I)))GO TO 13
      BST(I)=NO
13    DO 15 J=1,15
      COV(I,J)=XTXIN(I,J)/(SQRT(XTXIN(I,I)*XTXIN(J,J)))
      IF(I.NE.J)GO TO 15
      COV(I,J)=BVAR(I)
15    CONTINUE
      WRITE(6,82)TITLE(1),TITLE(2),TITLE(3),TITLE(4),TITLE(5),TITLE(6)
82    FORMAT(1H1,/,45X,37('*'),/,45X,'*  ',6A4,' ANALYSIS *',/,45X,37('*'
     1),//,30X,'VARIANCE-COVARIANCE MATRIX',//)
      DO 12 I=1,15
      WRITE(6,83)COV(I,1),COV(I,2),COV(I,3),COV(I,4),COV(I,5),COV(I,6),C
     1OV(I,7),COV(I,8),COV(I,9),COV(I,10),COV(I,11),COV(I,12),COV(I,13),
     1COV(I,14),COV(I,15)
83    FORMAT(15(1X,F7.4))
12    CONTINUE
      DO 31 I=1,15
      DO 31 J=1,15
      COR(I,J)=COV(I,J)/SQRT(COV(I,I)*COV(J,J))
31    CONTINUE
      WRITE(6,88)
88    FORMAT(  ///,20X,'CORRELATION MATRIX',///)
      DO 32 I=1,15
      WRITE(6,89)COR(I,1),COR(I,2),COR(I,3),COR(I,4),COR(I,5),COR(I,6),C
     1OR(I,7),COR(I,8),COR(I,9),COR(I,10),COR(I,11),COR(I,12),COR(I,13),
     1COR(I,14),COR(I,15)
89    FORMAT(15(1X,F7.1))
32    CONTINUE
      WRITE(6,77)TITLE(1),TITLE(2),TITLE(3),TITLE(4),TITLE(5),TITLE(6)
77    FORMAT(1H1,/,1X,6A4,/,
     -1           ,/,10X,'Y1',9X,'Y',9X,'YHAT',7X,'ERROR',12X,'ERRSQ',//
     -1/)
      DO 16 I=1,28
      WRITE(6,78)Y1(I),Y(I),YHAT(I),E(I,1),ESQ(I)
```

```
78    FORMAT(6X,F8.4,3X,F8.4,4X,F8.4,4X,F9.6,4X,D13.5)
16    CONTINUE
      WRITE(6,79)YMEAN,EMEAN,MAX,MIN,SS,SSPE
79    FORMAT(//,2X,'YMEAN= ',F8.4,5X,'EMEAN= ',E14.7,/,4X,'MAX= ',F8.4,5
     1X,'MIN= ',F8.4,//,10X,'SUM O SQUARES =',E14.7,//,10X,'S. S. PURE
     1ERROR =',E14.7,/,1H1)
      WRITE(6,80)PERR,R
80    FORMAT(///,24X,'PURE ERROR VARIANCE =',E14.7,//,10X,'   MODEL A
     1DEQUACY TEST VALUE - R = ',E14.7,////)
      WRITE(6,73)
73    FORMAT(12X,'COEFFICIENT VALUES',6X,'95 % CONF INTERVAL',10X,'VARI
     1ANCE ',//)
      DO 8 I=1,15
      WRITE(6,76)B(I),BST(I),CONFIN(I),BVAR(I)
76    FORMAT(13X,E14.7,1X,A4,2X,E14.7,12X,E14.7)
8     CONTINUE
      IY=1
      N=28
      M=1
      INC=1
      RANGE(1)=-1.1
      RANGE(2)=1.1
      RANGE(3)=0.0
      RANGE(4)=0.0
      IOPT=1
      CALL USPLO(Y,E,IY,N,M,INC,30HRESIDUAL PLOT ( RESIDUE VS Y ),30,28H
     1(Y)  THE DEPENDENT  VARIABLE,28,9HRESIDUALS,9,RANGE,1H*,IOPT,IER)
      RANGE(1)=0.0
      RANGE(2)=0.0
      CALL USPLO(D,E,IY,N,M,INC,30HRESIDUAL PLOT ( RESIDUE VS N ),30,28H
     1(L)  THE SAMPLE  NUMBER     ,28,9HRESIDUALS,9,RANGE,1H*,IOPT,IER)
      DO 21 I=1,28
      A(I)=X(I,2)-0.5
21    CONTINUE
      CALL USPLO(A,E,IY,N,M,INC,30HRESIDUAL PLOT ( RESIDUE VS X1),30,28H
     1TEMPERATURE (VARIABLE X1-.5),28, 9HRESIDUALS,9,RANGE,1HX,IOPT,IER)
      DO 22 I=1,28
      A(I)=X(I,3)-0.5
22    CONTINUE
      CALL USPLO(A,E,IY,N,M,INC,30HRESIDUAL PLOT ( RESIDUE VS X2),30,28H
     1PRESSURE (VARIABLE X2-0.5)  ,28, 9HRESIDUALS,9,RANGE,1HX,IOPT,IER)
      DO 23 I=1,28
      A(I)=X(I,4)-0.5
23    CONTINUE
      CALL USPLO(A,E,IY,N,M,INC,30HRESIDUAL PLOT ( RESIDUE VS X3),30,28H
     1LIQUID FLOW (VARIABLE X3-.5),28, 9HRESIDUALS,9,RANGE,1HX,IOPT,IER)
      DO 24 I=1,28
      A(I)=X(I,5)-0.5
24    CONTINUE
      CALL USPLO(A,E,IY,N,M,INC,30HRESIDUAL PLOT ( RESIDUE VS X4),30,28H
     1GAS FLOW (VARIABLE X4-0.5) ,28, 9HRESIDUALS,9,RANGE,1HX,IOPT,IER)
35    CONTINUE
      WRITE(6,81)
81    FORMAT(1H1,///,1X,'EXPERIMENTAL',4X,'SAMPLE',2X,'DENSITY',3X,'VISC
```

```
     1OSITY',2X,'MID-BOILING',2X,'ANILINE-PT',2X,'C/H RATIO',2X,'% HDS',
     14X,'% HDN',4X,'CETANE',3X,'DIESEL',/,4X,'DESIGN',7X,'NUMBER',2X,'(
     1GM/CC)',5X,'(C.P.)',3X,'PT-(DEG.C)',4X,'(DEG.C)',33X,'INDEX',4X,'I
     1NDEX',//,1X,114('_'),//)
      DO 26 I=1,28
      WRITE(6,87)X(I,2),X(I,3),X(I,4),X(I,5),
     1          L(I),Y2(I,1),Y2(I,2),Y2(I,3),Y2(I,4),Y2(I,5),Y2(I,6),Y2
     1(I,7),Y2(I,8),Y2(I,9)
87   FORMAT(1X,4F4.1,2X,I2,5X,F6.4,4X,F6.2,6X,F6.2,8X,F4.1,6X,F6.4,4X,F
     15.2,4X,F5.2,4X,F5.2,4X,F5.2)
      IF((I.EQ.4).OR.(I.EQ.8).OR.(I.EQ.12).OR.(I.EQ.16).OR.(I.EQ.20).OR.
     1(I.EQ.24).OR.(I.EQ.28))GO TO 96
      GO TO 26
96   WRITE(6,95)
95   FORMAT(1X,114('_'),/)
26   CONTINUE
      WRITE(6,92)
92   FORMAT(1H1,////,21X,'COEFFICIENT-VALUES',52X,'CONFIDENCE INTERVALS
     1',////)
      DO 34 I=1,15
      WRITE(6,93)B1(I,1),B1(I,2),B1(I,3),B1(I,4),B1(I,5),B1(I,6),B1(I,7)
     1,B1(I,8),B1(I,9),C1(I,1),C1(I,2),C1(I,3),C1(I,4),C1(I,5),C1(I,6),C
     11(I,7),C1(I,8),C1(I,9)
93   FORMAT(2X,9(F6.3,1X),5X,9(F6.3,1X),/)
34   CONTINUE
      STOP
      END
```

4: Program used for model fitting with linear regression for Location of Optimum Catalyst Composition:-

```
C     THIS FORTRAN IS WRITTEN TO DO THE MULTIPLE LINEAR REGERSSION
C     ANALYSIS.
C
C     THIS WAS FIRST WRITTEN FOR THE SIXTEEN RUN CENTRE COMPOSIT
C     USED FOR THE CATALYST SCREENING. DATA READ FROM FILE 5.
C
C     AT THE END IT CAN GIVE DATA IN FILE 7 FOR EIGNVALUES.
C
      REAL X,XTX,XTXIN,Y,B  ,YMEAN,YHAT,PERR,YM,R,BVAR,RANGE,A,MEU,CONFI
     1N,XTY,WKAREA,MAX,MIN,Y1,COV,COR,D,Y2,B1,C1,PERV,P,XS,C,CIN,W,Z,ZN,
     2F,T,Y2,Y3,YO
      INTEGER I,IY,N,M,INC,IOPT,IER,L,CT,NO,OK,BST,TITLE,KR1,KR2,R1
      DOUBLE PRECISION EMEAN,SS,SSPE,ESQ,E
      DIMENSION X(16,6),XTX(6,6),XTXIN(6,6),Y(16),B(6),E(16,1),YHAT(16),
     1BVAR(6),RANGE(4),L(16),A(16),CONFIN(6),XTY(6),WKAREA(20),Y1(16),CO
     2V(6,6),ESQ(16),COR(6,6),BST(6),TITLE(6),D(16),Y2(16),B1(16,6),C1(1
     36,6),XS(2),C(2,2),CIN(2,2),W(2),Z(2,2),      Y3(16)
C
C       THE DESIGN DATA IS GENERATED
C          NUMBER OF DATA POINTS
      M=16
C          NUMBER OF CO-EFFICIENTS TO BE ESTIMATED
      N=6
C          NUMBER OF REPLICATE RUNS
      R1=8
C               REPLICATES BEGIN AT SERIAL NUMBER
      KR1=5
C               REPLICATES END AT SERIAL NUMBER
      KR2=12
      DO 1 I=1,M
        X(I,1)=1
        IF(I .GT. 4) GO TO 2
        X(I,3)=(-1.)**I
        IF(I .GT. 2)GO TO 3
        X(I,2)=1
        GO TO 1
3     X(I,2)=-1
      GO TO 1
2     X(I,2)=0
      X(I,3)=0
1     CONTINUE
      X(13,2)=SQRT(2.)
      X(14,2)=-X(13,2)
      X(15,3)=X(13,2)
      X(16,3)=-X(13,2)
      WRITE(6,60)M,N
```

```
60    FORMAT(1H1,///,30X,'INPUT MATRIX X(',I2,',',I2,')',//)
      DO 4 I=1,M
      X(I,4)=X(I,2)**2
      X(I,5)=X(I,3)**2
      X(I,6)=X(I,2)*X(I,3)
      WRITE(6,71)X(I,1),X(I,2),X(I,3),X(I,4),X(I,5),X(I,6)
71    FORMAT(10X,6(F7.4,2X),/)
4     CONTINUE
C
C         CALCULATE XTX,XTXIN, AND XTY
C
      DO 5 I=1,N
       DO 5 J=1,N
        XTX(I,J)=0
         DO 5 K=1,M
          XTX(I,J)=XTX(I,J)+X(K,I)*X(K,J)
5        CONTINUE
      WRITE(6,72)
72    FORMAT(1H1,///,30X,'MATRIX  XTX',///)
       DO 6 I=1,N
       WRITE(6,73)XTX(I,1),XTX(I,2),XTX(I,3),XTX(I,4),XTX(I,5),XTX(I,6)
73     FORMAT(5X,6(F10.5,2X),/)
6     CONTINUE
      CALL LINV1F(XTX,N,N,XTXIN,0,WKAREA,IER)
            WRITE(6,74)
74     FORMAT(1H1,///,30X,'MATRIX  XTXIN',///)
      DO 7 I=1,N
      WRITE(6,75)XTXIN(I,1),XTXIN(I,2),XTXIN(I,3),XTXIN(I,4),XTXIN(I,5),
     1  XTXIN(I,6)
75       FORMAT(5X,6(F10.5,2X),/)
7         CONTINUE
C
C     READ THE VALUES OF THE DEPENDENT VARIABLE FROM FILE DEFINED AS
C     5. FIRST LINE GIVES THE Y0 VALUE.
C
C     DATA IS WRITTEN GIVING THE ORDER OF RUN FIRST AND THEN THE
C     VALUE OF DEPENDENT VARIABLE.
C
C
      READ (5,50)Y0
50    FORMAT(//,34X,F6.4,////)
C
C
      DO 9 I=1,M
       READ(5,51)L(I),Y2(I)
51      FORMAT(5X,I2,3X,F6.4)
            D(I)=L(I)
              Y1(I)=(Y0-Y2(I))*100.0/Y0
9           CONTINUE
      MIN=1000.0
      MAX=0.0
             DO 17 I=1,M
            IF(MAX.GE.Y1(I))GO TO 18
          MAX=Y1(I)
```

```
18      IF(MIN.LE.Y1(I))GO TO 17
        MIN=Y1(I)
17    CONTINUE
C
C      NORMALIZE THE VARIABLE Y ,CALCULATE XTY, AND B VALUES
C
      DO 19 I=1,M
           Y(I)=((Y1(I)-MIN)/(MAX-MIN))*2.0-1.0
19           CONTINUE
      DO 24 K=1,N
          XTY(K)=0.0
              DO 24 J=1,M
                 XTY(K)=XTY(K)+X(J,K)*Y(J)
24             CONTINUE
      DO 25 I=1,N
         B(I)=0.0
              DO 25 J=1,N
                 B(I)=B(I)+XTXIN(I,J)*XTY(J)
25               CONTINUE
C
C     ERROR ESTIMATIONS
C
C
                     YMEAN=0.0
                   EMEAN=0.0
                  SS=0.0D 00
      DO 26 I=1,M
          YHAT(I)=0.0
         DO 11 J=1,N
            YHAT(I)=YHAT(I)+B(J)*X(I,J)
11        CONTINUE
            Y3(I)=Y0-(0.5*(YHAT(I)*(MAX-MIN))+MIN)*(Y0/100.0)
                E(I,1)=Y(I)-YHAT(I)
                 ESQ(I)=E(I,1)*E(I,1)
                    SS=SS+ESQ(I)
                      EMEAN=EMEAN+E(I,1)*1000.0
                       YMEAN=YMEAN+Y(I)
26                   CONTINUE
      YMEAN=YMEAN/M
C
C       PURE ERROR ESTIMATION FROM REPLICATES
C
      SSPE=0.0D 00
        DO 14 I=KR1,KR2
          SSPE=SSPE+E(I,1)*E(I,1)
14        CONTINUE
                  PERV=SSPE/(R1-1)
C
C      R- RATIO TEST AND THE CORRESPONDING VALUE OF F FUNCTION
C
C
      P=M-N
        R=(SS-SSPE)*(R1-1)/(SSPE*(P-R1+1))
          BVAR(1)=M-N
```

```
      BVAR(2)=R1-1
      CALL MDFI(0.95,BVAR(1),BVAR(2),F,IER)
      PERR=SS/(M-N)
C
C     CONFIDENCE INTERVALS AND VARIANCE -CORRELATION MATRIX.
C
      BVAR(1)=R1-1
      CALL MDSTI(0.05,BVAR(1),T,IER)
C                VALUE OF T-FUNCTION IS EVALUATED ABOVE.
      DO 15 I=1,N
      BVAR(I)=PERV*XTXIN(I,I)
      CONFIN(I)=T*(SQRT(BVAR(I)))
        DO 15 J=1,N
        COV(I,J)=XTXIN(I,J)/(SQRT(XTXIN(I,I)*XTXIN(J,J)))
          IF(I .NE. J) GO TO 15
          COV(I,J)=BVAR(I)
15        CONTINUE
C
C     WRITE STATEMENTS
C     ----------------
                  WRITE(6,82)
82    FORMAT(1H1,///,19X,'XTY    VARIANCE --  CORRELATION   MATRIX',///)
      DO 12 I=1,N
      WRITE(6,83)XTY(I),COV(I,1),COV(I,2),COV(I,3),COV(I,4),COV(I,5),COV
     1(I,6)
83    FORMAT(10X,7(F7.4,3X),/)
12    CONTINUE
      WRITE(6,77)
77    FORMAT(1H1,///,2X,'SR.  RUN',4X,'Y1',9X,'Y',3X,'DATA',5X,'PRED',
     1  11X,'YHAT',7X,'ERROR',12X,'ERRSQ',/,2X,'NO.  NO.',//)
      DO 16 I=1,M
      WRITE(6,78)I,L(I),Y1(I),Y(I),Y2(I),Y3(I),YHAT(I),E(I,1),ESQ(I)
78    FORMAT(1X,I3,1X,I3,1X,F8.4,3X,F8.4,2X,F6.4,2X,F6.4,2X,E14.5,1X
     1,E14.7,4X,D13.5,/)
16    CONTINUE
      WRITE(6,79)YMEAN,EMEAN,MAX,MIN,SS,SSPE
79    FORMAT(//,2X,'YMEAN= ',F8.4,5X,'EMEAN= ',E14.7,/4X,'MAX= ',F8.4,5X
     1,'MIN= ',F8.4,//,10X,'SUM OF SQUARES= ',E14.7,//,10X,'S. S. PURE E
     2RROR= ',E14.7,/,1H1)
      WRITE(6,80)PERR,R,PERV,F,T
80    FORMAT(///24X,'TOTAL S. S.VARIANCE= ',E14.7,//,10X,'       MODEL A
     1DEQUACY TEST VALUE - R = ',E14.7,//,24X,'PURE ERROR VARIANCE= ',E1
     24.7,//,10X,'VALUE OF FUNCTION F = ',F7.3,//,10X,'VALUE OF T-FUNCTI
     3ON = ',F7.3,/,
     2    ',///,11X,'CO-EFFICIENT VALUES',6X,'95%  CON. INTERVAL',10X,'VA
     3RIANCE',//)
      DO 28 I=1,N
      WRITE(6,76)B(I),CONFIN(I),BVAR(I)
76    FORMAT(13X,E14.7,7X,E14.7,12X,E14.7,/)
28    CONTINUE
      IY=1
      J=M
      I=1
        INC=1
```

```
      RANGE(1)=-1.1
                        RANGE(2)=1.1
                                          RANGE(3)=0.0
                                                            RANGE(4)=0.0
      IOPT=1
      CALL USPLO(Y,E,IY,J,I,INC,30HRESIDUAL PLOT ( RESIDUE VS Y ),30,28H
     1(Y)  THE DEPENDENT VARIABLE ,28,9HRESIDUALS,9,RANGE,1H#,IOPT,IER)
      RANGE(1)=0.0
                     RANGE(2)=0.0
      CALL USPLO(D,E,IY,J,I,INC,30HRESIDUAL PLOT ( RESIDUE VS N ),30,28H
     1(N)  THE SAMPLE  NUMBER     ,28,9HRESIDUALS,9,RANGE,1H#,IOPT,IER)
      DO 21 K=1,M
      A(K)=X(K,2)-0.5
21    CONTINUE
      CALL USPLO(A,E,IY,J,I,INC,30HRESIDUAL PLOT ( RESIDUE VS X1),30,28H
     1(X1)THE SILICON CONCENTRATIN,28,9HRESIDUALS,9,RANGE,1H#,IOPT,IER)
      DO 22 K=1,M
      A(K)=X(K,3)-0.5
22    CONTINUE
      CALL USPLO(A,E,IY,J,I,INC,30HRESIDUAL PLOT ( RESIDUE VS X2),30,28H
     1(X2)THE ZEOLITE CONCENTRATIN,28,9HRESIDUALS,9,RANGE,1H#,IOPT,IER)
C
C     DATA WRITTEN IN FILE 7 FOR EIGN VALUES.
C
C
      WRITE(7,95)B(4),B(6),B(6),B(5),B(2),B(3),B(1)
95    FORMAT(4(2E14.7,/))
      STOP
      END
```

Appendix B

IMPREGNATION SOLUTION CALCUALTIONS

The water soluble salts of nickel and molybdenum were nickel(ous) nitrate - $Ni(NO_3)_2 \cdot 6H_2O$ (F. Wt. 290.8) and ammonium molybdate - $(NH_4)_6Mo_7O_{24} \cdot 4H_2O$ (F. Wt. 1235.86). The impregnation solutions were prepared keeping a NiO/MoO_3 ratio of 0.3 and a concentration sufficient to give a total of 5% loading of both the active metal oxides combined. Formula weight of NiO is 74.71 and that of MoO_3 is 143.94.

The amounts of the salts required for a given support of known pore volume were calculated as follow:

Total volume of the solution = 100 ml

Pore volume of the support = v ml/g

Amount of the nickel nitrate required =

$$\frac{(0.05)1}{v} \times 100 \times \frac{(0.3)}{(1.3)} \times \frac{(290.81)}{(74.71)} = 4.4914/v \text{ g}$$

Amount of the amm. molybdate required =

$$\frac{(0.05)1}{v} \times 100 \times \frac{(1.0)}{(1.3)} \times \frac{(1235.86/7)}{(143.94)} = 4.7175/v \text{ g}$$